Dynamic regulation of R7BP (*R7 Binding Protein*) containing R7 RGS (*R7 Regulators of G protein Signaling*) protein complexes: Role in controlling neuronal dopamine and opioid signaling in the striatum

A DISSERTATION
SUBMITTED TO THE FACULTY OF THE GRADUATE SCHOOL
OF THE UNIVERSITY OF MINNESOTA
BY

Garret R. Anderson

IN PARTIAL FULFILLMENT OF THE REQUIREMENTS
FOR THE DEGREE OF
DOCTOR OF PHILOSOPHY

Adviser: Dr. Kirill A. Martemyanov

February, 2010

Acknowledgements

I would like to acknowledge my advisor Dr. Kirill Martemyanov first and foremost, for his efforts put toward the work presented in this thesis. He has been instrumental at every level of my graduate school training, including the development of experimental strategy, his expertise on biochemical techniques, and perhaps most importantly for emphasizing the stylistic art of scientific presentation and writing.

I would also like to mention the great collection of scientists from the Martemyanov lab that have both directly and indirectly contributed to this research, including Joseph Song, Dr. Artur Semenov, Ekaterina Posokhova, Dr. Yan Cao, Dr. Keqiang Xie, Dr. Ikuo Masuho, Hideko Masuho, and Natalia Martemyanov. Their direct contributions and scientific discussions have pushed the evolution of our thinking of R7 RGS proteins.

Direct contributions from other groups have also been fantastic, and have moved us closer to our research goals more efficiently. Specifically I want to mention the following individuals: Dr. Rafael Lujan from the Universidad de Castilla-La Mancha for his electron microscopy images demonstrating the subcellular localization of R7BP, RGS9-2, and RGS7; Vladimir Uversky from Indiana University School of Medicine for his work on predictive modeling of RGS9-2 intrinsic disorders domains; Ching-Kang Chen from the Virginia Commonwealth University for supplying us with RGS9-2 and Gβ5 knockout mice; Dr. Kevin Wickman and Dr. Marco Pravetoni from the University of Minnesota for their assistance in stereotaxic injections of lentiviruses in adult mice, and setting up behavioral experiments; Dr. Glenn Giesler, Dr. Steve Davidson, and Hai Truong from the University of Minnesota for their assistance in developing a lentivirus delivery strategy into P05 mice; Dr. Mark Thomas and Dr. Saïd Kourrich from the University of Minnesota for behavioral experiments and electrophysiology recordings; Dr. Stanley Thayer and Dr. Alan Roloff from the University of Minnesota for their electrophysiology recordings, sharing of reagents, advice on research directions, and assistance in the development of microscopy techniques.

During the course of the preparation of this thesis, financial contributions from multiple sources have permitted this work to occur. Dr. Martemyanov is supported by the NIH grant R01 DA021743. I have been supported by the NIH Ruth L. Kirschstein NRSA F31 DA024944, the NIH NRSA Training Grant T32 DA007097, and the 3M Corporation.

I lastly would like to thank my graduate committee members Dr. Stanley Thayer (chair), Dr. Jonathan Marchant, and Dr. Anja Bielinsky. Their insight into the refinement of my F31 NRSA fellowship proposal to the NIH resulted in its funding.

For these individuals mentioned, I am grateful for working with all of you. It is because of you that science has been so enjoyable for me here at the University of Minnesota, and I thank you for that.

Abstract

G protein-coupled receptor (GPCR) signaling pathways mediate the transmission of signals from the extracellular environment to the generation of cellular responses, a process that is critically important for neurons and neurotransmitter action. The ability to promptly respond to rapidly changing stimulation requires timely inactivation of G proteins, a process controlled by a family of specialized proteins known as regulators of G protein signaling (RGS). The R7 group of RGS proteins (R7 RGS) has received special attention due to their pivotal roles in the regulation of a range of crucial neuronal processes such as vision, motor control, reward behavior and nociception in mammals. One member of the R7 RGS family, RGS9-2 has been previously implicated as an essential modulator of signaling through neuronal dopamine and opioid G protein coupled receptors. RGS9-2 is specifically expressed in striatal neurons where it forms complexes with R7BP (R7 RGS Binding Protein), which we have found to ultimately affect several critical properties of RGS9-2. First, it is this interaction with R7BP which is necessary for determining the subcellular targeting of RGS9-2 to the plasma membrane and to the specialized neuronal compartment of excitatory synapses, the postsynaptic density. Secondly, R7BP plays a selective role amongst the R7 RGS family in determining the proteolytic stability of RGS9-2.

Further characterization of R7 RGS complexes in the striatum revealed that two equally abundant R7 RGS proteins, RGS9-2 and RGS7, are unequally coupled to the R7BP subunit which is present in complex predominantly with RGS9-2 rather than with RGS7. However, upon changes in neuronal activity the subunit composition of these complexes in the striatum undergoes rapid and extensive remodeling. Changes in the neuronal excitability or oxygenation status result in extracellular calcium entry, uncoupling RGS9-2 from R7BP, triggering its selective degradation. Concurrently, released R7BP binds to cytoplasmic RGS7 and recruits it to the plasma membrane and the postsynaptic density. These observations introduce activity dependent remodeling of R7 RGS complexes as a new molecular plasticity mechanism in striatal neurons and suggest a general model for achieving rapid posttranslational subunit rearrangement in multi-subunit complexes.

The physiological consequence of this remodeling process appears to play a role in determining the signaling sensitivity to dopamine stimulation. Considering that upon the genetic elimination of RGS9, all available R7BP is funneled towards complex formation with RGS7, not only are RGS9 controlled GPCR signaling pathways affected, but those controlled by RGS7 as

well. RGS9 knockout mice have an increased sensitivity to dopamine and opioid receptor stimulation and consequently display altered motor and reward behavior. The question arises as to the role of modulation of RGS7 function in controlling these behaviors. Since the function of RGS9-2 is controlled by its association with R7BP, we would predict that the elimination of R7BP would lead to similar alterations in striatal physiology for RGS9 controlled pathways. While at the same time, RGS7 would be largely unaffected by the elimination of R7BP, thus RGS7 controlled pathways would predictably remain unaltered. Using this rationale, we report that elimination of R7BP in mice results in motor coordination deficits and greater locomotor response to morphine administration consistent with the essential role of RGS9 in controlling these behaviors and the critical role played by R7BP in maintaining RGS9-2 expression in the striatum. However, in contrast to previously reported observations with RGS9-2 knockouts, mice lacking R7BP do not exhibit higher sensitivity to locomotor-stimulating effects of cocaine, suggesting a role for RGS7 in controlling dopamine sensitivity. Using a striatum-specific knockdown approach, we demonstrate that the sensitivity of motor stimulation to cocaine is indeed dependent on RGS7 function. These results indicate that dopamine signaling in the striatum is controlled by concerted interplay between two RGS proteins, RGS7 and RGS9-2, which are balanced by a common subunit, R7BP.

Table of contents

List of Figures and Tables

Abbreviations

ACSF – Artificial cerebral spinal fluid

AMPA – α-amino-3-hydroxyl-5-methylisoxazole-4-propionic acid

CT – C-terminus

DAPI – 4',6-diamidino-2-phenylindole dihydrochloride

DARPP – Dopamine and cAMP regulated phosphoprotein

DEP – Disheveled, EGL-10, Pleckstrin

DHEX – DEP Helical Extension

DMEM – Dulbecco's modified Eagle's media

DNA – Deoxynucleic acid

ECL – Enhanced chemiluminescence

EDTA – Ethylenediaminetetraacetic acid

GABA – γ-aminobutyric acid

GAP – GTPase activating protein

Gβ5 – G-protein beta subunit 5

GDP – Guanosine diphosphate

GFP – Green fluorescent protein

GGL – G-protein gamma like

GIRK – G-protein gated inward rectifying potassium channel

GluR – AMPA glutamate receptor

GPCR – G protein-coupled receptor

GST – Glutathione S-transferase

GTP – Guanosine triphosphate

HBS – HEPES buffered saline

HEK – Human embryonic kidney

HRP – Horse radish peroxidase

IP – Immunoprecipitation

mRNA – Messenger ribonucleic acid

Ni-NTA – Nickel-nitrilotriacetic acid

NMDA – N-methyl-D-aspartic acid

NR – NMDA receptor

NT – N-terminus

PBS – phosphate buffered saline;

PCR – polymerase chain reaction

PDE – Phosphodiesterase

PKC – Protein kinase C

PSD – Post synaptic density

PVDF – Polyvinylidene fluoride

RT-PCR – Reverse transcriptase polymerase chain reaction

R7BP – R7 RGS binding protein

R9AP – RGS9 anchor protein

RGS – Regulator of G-protein signaling

SDS-PAGE – Sodium dodecyl sulfate polyacrylamide gel electrophoresis

SNARE – SNAP (Soluble N-ethylmaleimide-sensitive factor attachment protein) receptors

VGCC – Voltage gated calcium channels

List of Published Manuscripts

1. **Anderson G.R.**, Semenov A., Song J.H., Martemyanov K.A. The membrane anchor R7BP controls the proteolytic stability of the striatal specific RGS protein, RGS9-2. *Journal of Biological Chemistry*, 2007. 282(7):4772-81.
2. **Anderson G.R.**, Lujan R., Semenov A., Pravetoni M., Posokhova E.N., Song J.H., Uversky V., Chen C.K., Wickman K., Martemyanov K.A. Expression and localization of RGS9-2/Gβ5/R7BP complex in vivo is set by dynamic control of its constitutive degradation by cellular cysteine proteases. *Journal of Neuroscience*, 2007. Dec 19, 27(51):14117-27.
3. **Anderson G.R.**, Lujan R., Martemyanov K.A. Changes in striatal signaling induce remodeling of RGS complexes containing Gβ5 and R7BP subunits. *Molecular and Cellular Biology*, 2009. Jun 29, (11):3033-44.
4. **Anderson G.R.**, Posokhova E.N., Martemyanov K.A. The R7 RGS Protein Family: Multi-subunit regulators of neuronal G protein signaling. *Cell Biochemistry and Biophysics*, 2009. 54(1-3):33-46.
5. **Anderson, G.R.**, Cao Y., Davidson S., Pravetoni M., Truong H.V., Thomas M., Wickman, K., Giesler G.J., Martemyanov K.A. R7BP complexes with RGS9-2 and RGS7 in the striatum differentially control motor learning and locomotor responses to cocaine. *Neuropsychopharmacology*, *In Press.*

Chapter 1 - Introduction of the R7 RGS protein family: multi-subunit regulators of neuronal G protein signaling

Garret R. Anderson, Ekaterina Posokhova and Kirill A. Martemyanov*

From the Department of Pharmacology, University of Minnesota, Minneapolis, MN 55455 USA

Content taken from the published manuscript:

Anderson G.R., Posokhova E.N., Martemyanov K.A. The R7 RGS Protein Family: Multi-subunit regulators of neuronal G protein signaling. *Cell Biochemistry and Biophysics*, 2009. 54(1-3):33-46.

G protein-coupled receptor (GPCR) signaling pathways mediate the transmission of signals from the extracellular environment to the generation of cellular responses, a process that is critically important for neurons and neurotransmitter action. The ability to promptly respond to rapidly changing stimulation requires timely inactivation of G proteins, a process controlled by a family of specialized proteins known as regulators of G protein signaling (RGS). The R7 group of RGS proteins (R7 RGS) has received special attention due to their pivotal roles in the regulation of a range of crucial neuronal processes such as vision, motor control, reward behavior and nociception in mammals. Four proteins in this group: RGS6, RGS7, RGS9 and RGS11 share a common molecular organization of three modules: (i) the catalytic RGS domain, (ii) a GGL domain that recruits $G\beta_5$, an outlying member of the G protein beta subunit family, and (iii) a DEP/DHEX domain that mediates interactions with the membrane anchor proteins R7BP and R9AP. As heterotrimeric complexes, R7 RGS proteins not only associate with and regulate a number of G protein signaling pathway components, but have also been found to form complexes with proteins that are not traditionally associated with G protein signaling. This review summarizes our current understanding of the biology of the R7 RGS complexes including their structure/functional organization, protein-protein interactions and physiological roles.

♦ ***The role of RGS proteins in setting the timing of G protein signaling***

G protein signaling pathways are ubiquitous systems that mediate the transmission of signals from the extracellular environment to generate cellular responses. In these pathways, propagation of a signal from plasma membrane receptors to effectors is mediated by molecular switches known as heterotrimeric G proteins (1, 2). In the prototypical sequence of events, G protein-coupled receptors (GPCRs) are activated by ligand binding, which catalyzes GDP/GTP exchange on many Gα protein molecules. Upon GTP binding, Gα-GTP and Gβγ subunits dissociate from one another, and both proceed to activate or inhibit a variety of downstream signaling molecules (ranging from enzymes that regulate second messenger homeostasis to ion channels and protein kinases) that are collectively referred to as effectors (reviewed in 3, 4). Thus, a cellular response is elicited by modulation of the activity of an effector molecule by G protein subunits. The extent of effector activity regulation, and consequently the magnitude and duration of the response, depends on how long the G proteins stay in the activated state. Processes that inactivate G proteins therefore play critical roles in shaping the kinetics of the response. The first recognized molecular events that contribute to the inactivation of G protein signaling were those that lead to GPCR desensitization, including phosphorylation by receptor kinases, binding of arrestin molecules and internalization via endocytosis (reviewed in 5). Currently well accepted, these reactions represent powerful mechanisms for limiting G protein activation during sustained stimulation of GPCRs. Controlling G protein activation can be further modulated by controlling the inactivation of G protein subunits, which occurs when the Gα subunit hydrolyzes GTP and its inactive GDP-bound state re-associates with Gβγ subunits (6). Although Gα subunits can hydrolyze GTP and self-inactivate, this process is rather slow and does not account for the fast deactivation kinetics observed under physiological conditions (discussed in 7). Timely inactivation of G proteins is controlled by a specialized family of proteins classified as regulators of G protein signaling (RGSs). Comprising more than 30 members, RGS proteins act to accelerate the rate of GTP hydrolysis of G protein α subunits (8-10). This activity makes RGS proteins key elements that determine the lifetime of the activated G proteins in the cell, thus determining the overall duration of the response to GPCR activation. The importance of RGS proteins in regulating the magnitude of cellular reactions within an organism is underscored by a number of studies with genetic mouse models either deficient in genes encoding individual RGS proteins (11-18) or carrying G proteins insensitive to RGS action (19). These mouse models often suffer from a range of dysfunctions that severely affect most systems in the organism.

Furthermore, recent evidence suggests that the activity of RGS proteins may in fact be a rate-limiting step in the termination of G protein-mediated responses in a similar way to that of the visual signal transduction pathway in retinal photoreceptors (20). In this context, understanding the mechanisms that regulate RGS protein function will provide critical insight into how the timing of G protein-mediated cellular reactions is achieved.

- ***Regulation of G protein signaling in the nervous system and the R7 group of the RGS family***

Perhaps one of the most impressive features of G protein signaling in neuronal cells is the exquisite timing of signaling events. Neurons heavily rely on GPCR pathways for mediating neurotransmitter action, requiring simultaneous processing of multiple incoming signals in a rapid timeframe and in a constantly changing environment (reviewed in 21). In many cases, changes in the precise timing of these signaling events lead to a range of grave dysfunctions of the nervous systems (22, 23). Thus, it is perhaps not surprising that regulation of neuronal G protein signal termination mediated by RGS proteins has raised considerable interest. Neuronal RGS proteins have been implicated in many neurological conditions such as anxiety, schizophrenia, drug dependence and visual problems (See 23-25 for reviews).

Although the expression of several RGS proteins has been detected in the nervous system, the R7 group of RGS proteins has received special attention due to their pivotal roles in the regulation of a range of crucial neuronal processes such as vision, motor control, reward behavior and nociception in animals from *C. elegans* to humans (10, 26). Additionally, R7 RGS proteins are key modulators of the pharmacological effects of drugs involved in the development of tolerance and addiction (27-29). In mammals, the R7 subfamily consists of four highly homologous proteins, RGS6, RGS7, RGS9 and RGS11, all of which are expressed predominantly in the nervous system (30). Despite the important role that R7 RGS proteins play in controlling neuronal G protein signaling, relatively little was known about their operational principles. Over the last few years, significant progress has been achieved in elucidating many exciting principles underlying the function of R7 RGS proteins, essentially making them one of the best understood subfamilies of the RGS family. The purpose of this review is to summarize our understanding of this important protein family and its role in regulating neuronal processes. We hope that the lessons learned from the studies on R7 RGS proteins may lead to better understanding of the general principles underlying G protein signaling in neurons and help spur the progress in studying other members of the RGS protein family with less understood roles.

♦ ***R7 RGS proteins are multi-domain protein complexes***

A major characteristic feature of R7 RGS proteins is their modular organization. These RGS proteins contain four distinct structural domains and form tight stoichiometric complexes with two binding partners. In fact, due to the obligatory nature of the association between three constituent components, R7 RGS proteins are increasingly viewed as heterotrimeric complexes composed of three subunits (Figure 1.1).

The central element of this complex is formed by the RGS molecule itself that shares a common domain organization across all R7 RGS members. The defining feature of all RGS proteins, the catalytic RGS domain, is located at the C-terminus of the molecule and constitutes the only enzymatically active portion of the complex. The RGS domains of all R7 RGS proteins were shown to be capable of stimulating GTP hydrolysis on Gα protein subunits (31-37, 38, 39). From an enzymatic perspective, this process could be regarded as the conversion of active Gα-GTP species into inactive Gα-GDP species, accompanied by the release of the inorganic phosphate (40) commonly referred to as GAP (GTPase activating protein). Interestingly, the RGS domains of the R7 RGS proteins act as potent GAPs, even when isolated from the other, non-catalytic domains (see 31-33, 37 for examples). However, studies with RGS7 and RGS9 indicate that these other non-catalytic domains contribute to setting the maximal catalytic activity and refining Gα specificity (31-33). *In vitro* enzymatic studies have demonstrated that full-length R7 RGS proteins containing all non-catalytic domains selectively stimulate GTP hydrolysis on α subunits of the Gi/o class of G proteins but not on $G\alpha_{q/11}$, $G\alpha_z$ or $G\alpha_s$ (24, 39).

Crystal structures of isolated RGS homology domains have been solved for RGS7 (41) and RGS9 (42), both alone and, in the case of RGS9, in a complex with activated $G\alpha_t$. Analysis of these structures reveals a high degree of conformity to the all-helical bundle organization observed in a number of other RGS proteins (41, 43-45). The loops connecting the bundled helices form direct contacts with the switch region of the activated Gα subunit to stabilize it in the transition state of GTP hydrolysis, thereby providing a mechanism for the GAP activity (42). The RGS domain undergoes very little conformational change upon Gα binding, affecting mainly the α5/6 loop, which contains the catalytically critical Asn residue (42).

Upstream from the RGS domain, R7 RGS proteins carry a second conserved feature, the GGL (G protein gamma-like) domain. This domain is structurally homologous to the conventional γ subunits of G proteins (38). Like all Gγ subunits, the GGL domain binds to its

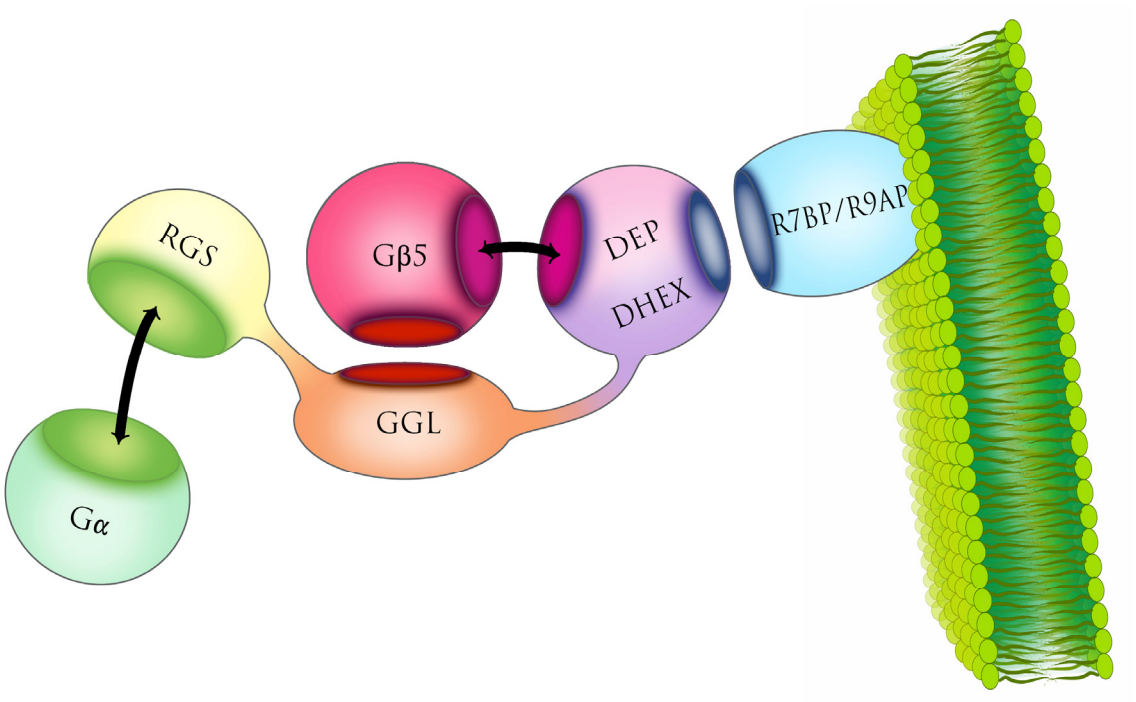

Figure 1.1: Organization of trimeric complexes between R7 RGS proteins and their subunits: R7BP/R9AP and $G\beta_5$. R7 RGS proteins consist of three functional modules. The N-terminal DEP (Disheveled, EGL-10, Pleckstrin) and DHEX (DEP helical extension) domains mediate binding to the membrane anchors R7BP and R9AP. The central GGL (G Protein gamma-like) domain forms a complex with the $G\beta_5$ (G protein β subunit, type 5). The C-terminal RGS (regulator of G protein signaling) domain mediates transient association with Gα-GTP subunits, during which GTP hydrolysis is stimulated. In addition to the GGL domain, $G\beta_5$ also associates with the DEP/DHEX module.

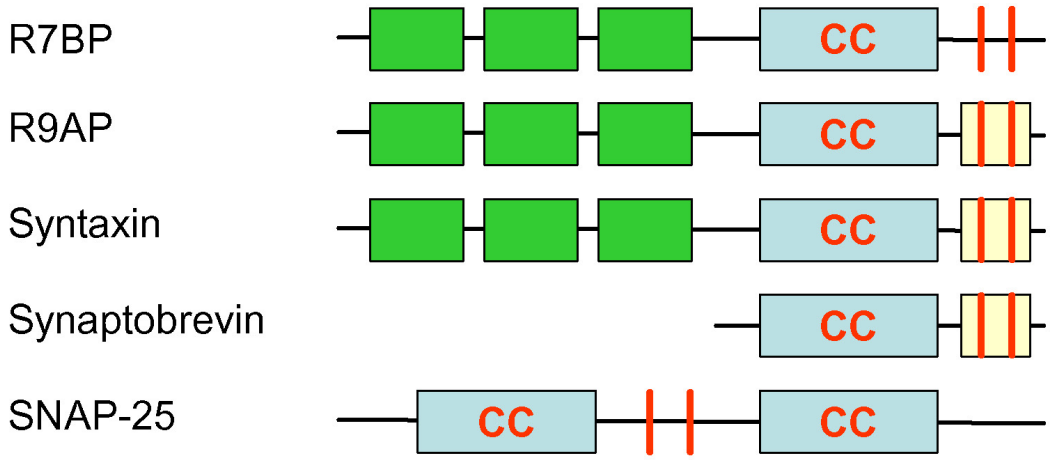

Figure 1.2: Membrane anchors R7BP and R9AP share structural similarities with SNARE proteins. Schematic representation of R7BP and R9AP domain compositions in comparison with three canonical SNARE proteins. Green boxes represent the alpha helical regions, blue boxes indicate conservative coiled-coil domains that participate in SNARE complex formation, yellow boxes indicate transmembrane regions and red lines indicate sites of membrane attachment.

obligatory partner, the Gβ subunit. However, unlike conventional Gγ subunits, this interaction of the GGL domain is incredibly specific, as it is capable of forming a coiled-coil interaction only with $G\beta_5$ (type 5 G protein β subunit), a distant member of the G protein β subunit family (35, 46, 47). A recently solved crystal structure of the RGS9-$G\beta_5$ complex reveals that the interaction between GGL and $G\beta_5$ closely follows the same orientation and association mechanisms as those observed in conventional Gβγ dimers (48).

Finally, the N-terminus of R7 RGS proteins is formed by the DEP (Disheveled, Egl-10, Pleckstrin) (49) and DHEX (DEP helical extension) (48) domains. While the DEP domain is found in many signaling proteins (49), the DHEX domain is unique to R7 RGS proteins (10). Both crystal structure (48) and chimeric mutagenesis (50) studies suggest that the DEP and DHEX domains form a single, functional domain in the molecule. Recent studies have revealed that the DEP/DHEX module of R7 RGS proteins is responsible for their interaction with two novel membrane proteins, R9AP (RGS9 anchor protein) and R7BP (R7 family binding protein), which are discussed in detail below.

Increasing evidence suggests that alternative splicing is a powerful mechanism that affects three members of the R7 RGS family: RGS6 (51), RGS9 (52-54) and RGS11(55). Combined with the modular principle of R7 RGS organization, differential splicing generates variability in domain composition, leading to the loss or gain of functions mediated by those affected domains. An extreme example of the extensive splicing patterns of R7 RGS proteins was recently provided by studies of RGS6. Alternative splicing of this protein generates 36 isoforms containing virtually all possible combinations of non-catalytic domains in addition to the RGS catalytic domain (51). Remarkably, several studied isoforms of RGS6 showed differential distribution patterns across cellular compartments (51, 56), suggesting that domain composition may regulate subcellular targeting of RGS6 in cells. The splicing pattern of RGS9 is much less complex, but nonetheless provides the best understood example of functional implications. Two splice variants of RGS9, which differ only in their composition at the C-termini, have been described (52-54). The short splice isoform, RGS9-1, contains only 18 amino acid residues at the C-terminus and is exclusively expressed in photoreceptors. In the long splice isoform, RGS9-2, the short C-terminus is replaced by a longer region of 209 amino acids. RGS9-2 is expressed in the striatum and is not present in photoreceptors (52, 57). The ability of the RGS9-1 isoform to recognize its cognate G protein target $G\alpha_t$ is regulated by the effector enzyme of the visual cascade in photoreceptors, PDEγ (58-60), which acts to dramatically enhance the affinity of

RGS9-1 for $G\alpha_t$ (61). As PDEγ is absent in the striatum, G protein recognition is enhanced by the additional C-terminal PDEγ-like domain (PGL) domain that is unique to RGS9-2 (62). It is likely that future studies on the role of alternative splicing in R7 RGS proteins will yield additional insights into the fundamental principles regulating these proteins.

In summary, R7 RGS proteins are built from the three constituent modules: (i) the catalytic RGS domain, (ii) the GGL domain that recruits the $G\beta_5$ subunit and (iii) the DEP/DHEX domain that mediates interactions with the membrane proteins R7BP and R9AP. As will be detailed in the following sections, the interplay between these functional domains determines expression level, intracellular localization and ultimately the GAP properties of the R7 family members.

- ***$G\beta_5$, an obligate subunit with an enigmatic functional role***

$G\beta_5$ was first discovered as a novel type of Gβ subunit exclusively expressed in the nervous system (63). It was shown to selectively interact with $G\gamma_2$ *in vitro*, although the existence of this interaction *in vivo* has never been demonstrated (63, 64). Despite this fact, most subsequent studies focused on analyzing the ability of the $G\beta_5\gamma_2$ complex to mediate classical G$\beta\gamma$ functions such as interactions with Gα subunits and effectors. It was found that $G\beta_5\gamma_2$ has an unusual selectivity for its effectors, as it potently regulates the activities of $PLC\beta_2$, N-type calcium channels and GIRK channels, but not $PLC\beta_3$, PI3Kγ or adenylate cyclase II (63, 65-69). Likewise, $G\beta_5\gamma_2$ was shown to interact with GDP-bound Gα subunits (70, 71). However the specificity of these interactions is more controversial. While one group reported that $G\beta_5\gamma_2$ can bind to $G\alpha_q$ but not to $G\alpha_i$ or $G\alpha_o$ (70), another group detected stable interactions with both $G\alpha_i$ and $G\alpha_o$ (71). Although no explanation for these discrepancies exists, it was noticed that the complex of $G\beta_5$ with $G\gamma_2$ is abnormally weak and prone to spontaneous dissociation, leading to loss of $G\beta_5$ activity (72, 73). Overall, these findings demonstrate that $G\beta_5$ exhibits some properties that are common to the conventional Gβ subunits, such as interaction with Gα and Gγ subunits as well as with effectors. A recently solved crystal structure supports this idea, as it indicates that most of the critical amino acids that build the protein interaction interface in $G\beta_5$ are conserved (48). However, the physiological function of $G\beta_5$ remained a mystery until the discovery that $G\beta_5$ readily forms complexes with members of the R7 family of RGS proteins instead of Gγ subunits *in vivo* (46, 47, 74). Unlike the $G\beta_5\gamma_2$ association, $G\beta_5$•RGS complex formation is very strong and resistant to dissociation in detergent solutions, allowing for its

purification by various chromatographic and immunoprecipitation strategies (46, 47, 64). It should be noted, however, that the debate on whether $G\beta_5$ can also exist and function in complex with conventional $G\gamma$ subunits continues (see 75 for most recent example), as it remains to be established whether $G\beta_5$ can be found outside of the complexes with R7 RGS proteins *in vivo*.

Two splice isoforms of $G\beta_5$ have been described (71). $G\beta_{5S}$, a 39 kDa short splice isoform, is ubiquitously expressed in the retina and brain, where it forms complexes with all R7 RGS proteins, except RGS9-1 (46, 64, 76). The 44 kDa long splice variant, $G\beta_{5L}$, containing 42 extra amino acids at the N-terminus, is exclusively present in the outer segments of photoreceptors (77), where it forms a complex with RGS9-1 (47). The longer N-terminal portion of the photoreceptor $G\beta_{5L}$ isoform has been shown to contribute to a high affinity to RGS9-1, selectively with a $G\alpha_t$-PDEγ complex, as opposed to free, activated $G\alpha_t$. However, the precise role that alternative splicing of $G\beta_5$ plays for RGS9-1 function is not fully understood.

From early studies on the functional significance of R7 RGS•$G\beta_5$ complex formation, it was unequivocally determined that $G\beta_5$ is essential for the stability and expression of all R7 RGS proteins. Co-expression with $G\beta_{5S}$ was shown to be necessary for achieving high expression levels of RGS6 and RGS7 via protecting them from proteolytic degradation (35, 74), resulting in the enhancement of RGS activity in regulating GIRK channel kinetics (78). Likewise, experiments with recombinant overexpression in heterologous systems indicate that functionally active proteins can only be obtained when R7 RGS proteins are co-expressed with $G\beta_5$ (32, 34). Finally, the ultimate proof of the importance of the interaction between R7 RGS proteins and $G\beta_5$ arose from knockout mouse studies that demonstrated that the genetic ablation of $G\beta_5$ resulted in the loss of all R7 RGS proteins (79). Conversely, deletion of RGS9, the only R7 RGS protein in photoreceptors, results in the degradation of $G\beta_5$. This indicates that, at least in this cell type, $G\beta_5$ exists only in complex with RGS proteins and becomes destabilized in the absence of its interaction with the GGL domain (13). These observations are reminiscent of the reciprocal stabilization seen in conventional $G\beta\gamma$ subunits, which are thought to form inseparable entities (see (80, 81) for examples). Overall, most of the accumulated evidence establishes R7 RGS proteins and $G\beta_5$ as obligate subunits of a complex that exists and functions *in vivo* as a single entity.

Delineation of the functional roles that $G\beta_5$ plays as a part of the heterodimeric complex with RGS proteins beyond proteolytic protection has proven to be more difficult. The regulatory

effector and Gα binding properties observed for $G\beta_5\gamma_2$ have not been found for $G\beta_5$ in complex with R7 RGS proteins. RGS6•$G\beta_5$ and RGS7•$G\beta_5$ were shown to not modulate either PLCβ or adenylate cyclase (39). Similarly, recombinant RGS6•$G\beta_5$, RGS7•$G\beta_5$ and RGS9•$G\beta_5$ were demonstrated to be incapable of interacting with GDP-bound $G\alpha_{i/o/t}$ subunits (33, 39, 62). The crystal structure of the RGS9•$G\beta_5$ complex sheds some light on the apparent discrepancy between the capability of $G\beta_5$ to interact with Gα subunits and effectors when in complex with $G\gamma_2$ but not when in complex with RGS proteins (48). Analysis of the structure indicates that although the protein interaction interface that mediates association of Gβ subunits with Gα subunits and effectors is conserved in $G\beta_5$, it is inaccessible due to its interactions with the N-terminal DEP domain. The DEP domain is intricately interwoven with the adjacent DHEX domain, with both of the domains forming a single structural domain that caps the protein interaction interface of $G\beta_5$. This cap is connected to the rest of the RGS polypeptide via an unstructured hinge region, which is postulated to bear significant conformational flexibility (48). These observations led to the idea that the complex in the crystal structure was captured in the "closed" conformation, which could be transformed into the "open" state by conformational changes that would disrupt the interactions between the DEP domain and $G\beta_5$ (48, 82). Intriguingly, it is speculated that the R7BP and R9AP proteins that bind to the DEP/DHEX domains could impact the equilibrium between "open" and "closed" conformations, thus altering access to the protein-protein interaction interface of $G\beta_5$.

An alternative possibility is that the GGL-$G\beta_5$ module could be employed by RGS complexes to play a role in setting their G protein selectivity, thus regulating the GAP activity of RGS proteins. Indeed, several similar effects of $G\beta_5$ have been reported. Deletion mutagenesis studies on RGS9-1•$G\beta_5$ complexes indicate that the GGL-$G\beta_5$ module acts to non-specifically reduce the affinity of the RGS catalytic domain to its two G protein targets: free activated $G\alpha_t$ and $G\alpha_t$-PDEγ complexes (33). In contrast, the non-catalytic domains of RGS9-1 enhance binding specifically for $G\alpha_t$-PDEγ complexes. In conjunction with the function of $G\beta_5$, this activity is thought to be required for setting the high degree of RGS9-1•$G\beta_5$ discrimination for its physiological substrate, $G\alpha_t$-PDEγ, and for preventing short-circuiting of the cascade due to deactivation of $G\alpha_t$ before it can relay the signal to the effector (32, 33). The ability of $G\beta_5$ to affect RGS interactions with Gα was also observed for RGS7, which was shown to bind to activated $G\alpha_o$ more tightly alone than when in complex with $G\beta_5$ (83). Finally, $G\beta_5$, in complex with the GGL domain of RGS9, was found to be important for sustaining the high turnover rate of

$G\alpha_t$ on the RGS domain of RGS9 (33). These results suggest that $G\beta_5$ is involved in regulating GAP properties of R7 RGS proteins. However, much of the underlying mechanisms remain to be elucidated.

- ***R7BP and R9AP: Adaptor subunits specifying expression, localization and activity of R7 RGS complexes***

The function of many signaling proteins in cells is determined to a great extent by their targeting to specific subcellular compartments. Photoreceptor neurons have served as a convenient model for delineating compartmentalization mechanisms of several signaling molecules, including that of R7 RGS proteins (84-86). In these cells, the visual signal transduction pathway is physically restricted to a specialized compartment, the outer segment, which is separated from the rest of the cellular compartments containing other G protein pathways (87). The outer segment is also the exclusive localization site for RGS9-1, which is tightly bound to the disc membranes (88, 89). Biochemical reconstitution studies and experiments with transgenic animals have indicated that the association of RGS9-1·$G\beta_5$ with the disc membranes and its specific targeting to the outer segment is mediated by the DEP domain (89, 90). Proteomic screening for the molecules that mediate this function in the photoreceptors resulted in the identification of the membrane anchor protein R9AP (91). Similar to RGS9-1, RGS9-2 also associates with membranes and is specifically targeted to the postsynaptic density site in striatal neurons (92). The absence of R9AP in the brain led to another proteomic search that identified R7BP, an R9AP homologue that binds to RGS9-2 and all other R7 RGS proteins in striatal neurons (76). At the same time, R7BP was also independently discovered as a binding partner of R7 RGS proteins via bioinformatics homology searches using R9AP as bait (93). Although the binding of both R9AP and R7BP to RGS proteins has been shown to be mediated by the DEP domain (50, 76), complex formation exhibits clear interaction specificity. Although all four R7 RGS proteins can bind to R7BP, only RGS9 and RGS11 are capable of forming complexes with R9AP (76, 93).

At the amino acid sequence level, the similarity between R9AP and R7BP is limited to only 30% (15% identity). However, both proteins share a significant homology and similarity in overall architecture with SNARE proteins (89, 94). SNAREs are membrane-associated proteins involved in the vesicular trafficking and exocytosis that underlie synaptic fusion events (for review, see (95, 96). Like the SNARE protein syntaxin, R9AP and R7BP are predicted to contain an N-terminal three-helical bundle followed by an extensive coiled-coil domain and a membrane

attachment site (Figure 1.2). This similarity invites speculation that the interaction between DEP domains and SNARE-like proteins may be a common principle underlying the targeting of DEP domain-containing proteins, which include numerous signaling proteins (9, 49). In this context, it is intriguing that in yeast, syntaxin homologues are found among the binding partners of the DEP domain-containing RGS protein, Sst2 (97).

Although both R9AP and R7BP are membrane proteins, the mechanisms of their binding to membranes differ. R9AP is anchored via a single-pass C-terminal transmembrane helix, making it an integral membrane protein (91). In contrast, association of R7BP with the plasma membrane is mediated by two palmitoyl lipids that are post-translationally attached to the C-terminal cysteine residues, acting synergistically with an upstream polybasic stretch of six amino acids (93, 98). The labile nature of palmitoylation provides R7BP with flexibility in its localization. In cultured cells, it has been shown that de-palmitoylation of R7BP not only removes it from the plasma membrane but also uncovers a nuclear localization signal, resulting in its translocation into the nucleus (93, 98). This mechanism is thought to contribute to the regulation of R7 RGS protein availability at the plasma membrane (93, 99). However, the exact functional implications of R7BP shuttling from the plasma membrane to the nucleus are unknown. Furthermore, in native neurons R7BP has been primarily found at the plasma membrane compartments (92, 98, 100) and its translocation into the nucleus has not been established despite several reports documenting nuclear localization of R7 RGS proteins *in vivo* (56, 101, 102).

What does appear to be firmly established is the role of R7BP/R9AP-mediated membrane association in the function of R7 RGS proteins. First, the membrane anchors regulate the activity of R7 RGS proteins. Studies have shown that association of RGS9-1•$G\beta_5$ with R9AP causes a dramatic potentiation of the ability of RGS9-1 to activate transducin GTPase (89, 90, 103). Under optimal conditions, the degree of this potentiation can be as large as 70-fold (40, 90). Similar to R9AP, it was found that co-expression of RGS7•$G\beta_5$ with R7BP in *Xenopus* oocytes enhances the ability of RGS7 to augment M2 receptor-elicited GIRK channel kinetics, presumably due to the stimulation of the catalytic activity of RGS7 (93, 99). Because the effects of both R7BP and R9AP require the presence of the elements that mediate their membrane attachment, it is reasonable to assume that stimulatory activity of R7BP/R9AP can be attributed to a large extent to concentrating R7 RGS proteins on the membranes and in close proximity to membrane-bound G proteins. However, direct allosteric mechanisms also appear to contribute to the effects of anchors on R7 RGS proteins, as suggested by the observation that R9AP influences not only the catalytic rate of RGS9-1•$G\beta_5$ GAP activity but also its affinity to activated $G\alpha_t$ (104). Second,

R7BP and R9AP play major roles in dictating the subcellular localization of R7 RGS proteins. In addition to translocation of R7 RGS proteins to the plasma membrane, as observed in transfected cells upon co-expression with R7BP/R9AP (91, 93, 98), membrane anchors target RGS proteins to unique subcellular compartments in neurons. In photoreceptors, R9AP mediates RGS9-1 delivery to the outer segments and excludes it from the axonal terminals (89, 105). In striatal neurons, R7BP specifies the targeting of RGS9-2 to the postsynaptic density (92). Interestingly, R7BP/R9AP activity is not universally required for targeting all R7 RGS proteins in all cells, as it was recently shown that targeting of RGS7•$G\beta_5$ in retinal bipolar neurons occurs independently from its association with R7BP (106).

Studies with mouse knockout models revealed that R9AP and R7BP also play an important role in determining the expression levels of R7 RGS•$G\beta_5$ complexes. Knockout of R9AP in mice results in nearly complete elimination of detectable RGS9-1 and RGS11 proteins in the retina (106, 107). Similarly, knockout of R7BP leads to severe down-regulation of RGS9-2 protein levels in the striatum (92). At the same time, transcription of the RGS9 and RGS11 genes is unaltered, as evidenced by similar levels of mRNA in both knockout and wild type tissues (92, 107). The protein levels of RGS9-1, RGS9-2 and RGS11 are reduced by half in the tissues of heterozygous mice carrying one R9AP- or R7BP-deficient allele, which corresponds to the extent of the reduction in R7BP or R9AP expression, respectively. Conversely, overexpression of R9AP in the photoreceptors and R7BP in the striatum led to an increase in the levels of RGS9-1 (20) and RGS9-2 (92), respectively. Examination of the mechanisms by which R7BP/R9AP confer their effects revealed that RGS9 isoforms, even when in complex with $G\beta_5$, are proteolytically unstable proteins with an estimated half life in the cell of less than one hour (50). RGS9 isoforms carry instability determinants located within their N-terminal DEP/DHEX domains that target they for degradation by cellular cysteine proteases (92). Binding of R7BP or R9AP to this region is thought to shield these determinants and thus prevent the degradation of RGS9, drastically prolonging its life time. Thus, R9AP and R7BP proteins could be viewed as subunits whose expression levels ultimately set the levels of RGS9- and RGS11-containing complexes in cells. Interestingly, RGS7 (and likely RGS6) does not possess these instability determinants and is therefore resistant to degradation when present in complex only with $G\beta_5$ (35, 50). Consistent with this observation, the levels of RGS6 and RGS7 are unaltered in R9AP or R7BP knockout tissues (92, 106). These observations suggest that RGS9 and RGS11 likely exist as obligate heterotrimeric complexes with either R9AP or R7BP, while RGS7•$G\beta_5$ and RGS6•$G\beta_5$ dimers with could associate with R7BP conditionally. In summary, current evidence indicates that R7BP

and R9AP are integral subunits of R7 RGS proteins and play critical roles in regulating the (i) catalytic activity, (ii) subcellular targeting and (iii) protein expression levels of R7 RGS complexes.

♦ ***R7 RGS proteins associate with a wide spectrum of cellular proteins***

As discussed above, R7 RGS proteins form trimeric complexes with R7BP (or R9AP) and $G\beta_5$ subunits. These interactions are intrinsic to all members of the R7 family and have been demonstrated to play critical roles in their activity. Interactions of R7 RGS complexes with their G protein substrates and the Gα subunits of the heterotrimeric G proteins of the $G_{i/o}$ family in the transition state of GTP hydrolysis are equally well established (31, 42, 61), (37, 38, 108). Interestingly, in addition to these well accepted interactions, R7 RGSs have been also reported to bind a number of other proteins, suggesting that these RGS proteins are likely integrated into larger macromolecular complexes in cells. Additional interactions were found for RGS6 and both splice isoforms of RGS9 and RGS7, but not for RGS11 (Table 1). In contrast to the conventional complexes of R7 RGS proteins with R9AP, R7BP and $G\beta_5$, most interactions reported in Table 1 were shown only for some members of the family, and their universality is unknown. Furthermore, for most of these interactions, it is unknown whether the binding occurs directly or is mediated by other proteins. Information about the binding determinants is often missing, and most of these interactions were not considered in the context of constitutive R7 RGS complexes with $G\beta_5$ and R7BP or R9AP. Despite these limitations, analysis of the patterns of these interactions may be productive, as it may suggest not only a potential involvement of R7 RGS proteins in the regulation of discrete cellular processes, but may also provide models of the regulation of RGS protein function. Interaction partners of R7 RGS proteins can be divided into three groups: (i) components of G proteins receptor complexes, (ii) signaling proteins outside of classical GPCR pathways and (iii) proteins that modulate RGS function.

The first consistent theme of R7 RGS proteins is the association with components of GPCR signaling complexes. In brain lysates, RGS9-2 was co-precipitated with the μ-opioid receptor (109, 110). Furthermore, targeting of RGS9-2 to membrane compartments required the presence of its DEP domain and co-transfection with μ-opioid (110) or D2 dopamine (111) receptors in transfected cells. Similarly, RGS7 was shown to directly interact with the intracellular loops of the muscarinic M3 receptor through its N-terminus (112). The interactions of mammalian R7 RGS proteins with GPCRs are further supported by the observation that the DEP domain of the yeast RGS protein Sst2 directly interacts with the C-terminal domain of its

Table 1. Interactions of R7 RGS proteins outside of the complexes with Gβ5 and membrane anchors R7BP/R9AP.

Interaction partner	R7 RGS	System	Method	Domain	Reference
μ-opioid receptor	RGS9-2	PC12	Co-IP	N/A	(110)
		periaqueductal gray matter	Co-IP	N/A	(109)
M3 receptor	RGS7	CHO-K1	Pull-down	DEP	(112)
β-arrestin	RGS9-2	PC12	Co-IP	N/A	(110)
α-actinin-2	RGS9-2	HEK293, brain	Y2H, Co-IP	N/A	(113)
NMDAR, subunit NR1	RGS9-2	HEK293, brain	Co-IP	N/A	(113)
14-3-3	RGS7	HEK293, brain	Co-IP, pull-down	RGS	(114)
	RGS9-2	periaqueductal gray matter	Co-IP	N/A	(109)
DMAP1, DNMT1	RGS6	COS-7, SH-SY5Y, brain	Y2H, Co-IP, pull-down	GGL	(115)
SCG10	RGS6	COS-7	Y2H, Co-IP	GGL	(116)
Snapin	RGS7	CHOK1	Co-IP, pull-down	DEP	(117)
Polycystin	RGS7	HEK293	Co-IP, pull-down	GGL	(118)
Spinophilin	RGS9-2	striatum	Co-IP	N/A	(119)
GRK2	RGS9-2	striatum	Co-IP	N/A	(119)
Guanylyl cyclase	RGS9-1	bovine ROS	Overlay	N/A	(120)

cognate receptor, Ste2 (121). Hypothetically, the RGS-GPCR pairing can serve as a powerful mechanism that provides the specificity of RGS activity and shapes the kinetics of the response. In this respect, it is important to note the discovery of the polypeptide that contains both GPCR and RGS domains, which allow it to effectively modulate cell proliferation (122). Interestingly, binding partners of R7 RGS proteins also include proteins that are normally found in complexes with GPCRs. Receptor kinase GRK2, β-arrestin and the GPCR scaffold spinophilin were found to co-immunoprecipitate with RGS9-2 in brain tissue (110, 119). Although it is unclear whether these interactions occur directly or are mediated by μ-opioid receptors, they are thought to contribute to the regulation of receptor internalization and the development of tolerance, both of which are influenced by RGS9-2 (28, 110, 119).

The second large group of R7 RGS binding partners is composed of the non-conventional interactions of R7 RGS proteins with signaling proteins outside of G protein signaling pathways. For example, a yeast two hybrid screen has revealed interactions between RGS6 and the transcriptional repressor complex DMAP1/Dnmt1 (115), an observation that is consistent with the previously reported localization of RGS6 in the nucleus (56). Nuclear localization has also been reported for other R7 RGSs (101, 102, 123) and is thought to be mediated by R7BP, which can serve as a membrane-nuclear shuttle in a palmitoylation-dependent fashion (98, 99). This raises the possibility that additional interactions of R7 RGS proteins with components of signaling pathways in the nucleus exist. The discovery of these interactions may provide significant insight into the function of these proteins in the nucleus. In the cytoplasm, RGS6 was found to be associated with the microtubule destabilizing protein SCG10. This interaction that was shown to result in the enhancement of neurite outgrowth when studied in transfected cells (116). Similarly, RGS9-2 was reported to be associated with another cytoskeletal protein, α-actinin-2 (113). In transfected cells, this interaction was demonstrated to link RGS9-2 to the regulation of NMDA receptor function (113). Finally, RGS7 was found to bind a component of the synaptic fusion complex, snapin, leading to the hypothesis that R7 RGS proteins can also regulate exocytosis (94, 117). More studies will be needed to delineate the exact roles of R7 RGS proteins in mediating these signaling processes and fully validate these novel interactions. Likewise, it remains to be established whether the non-conventional functions of R7 RGS proteins are mediated by G proteins or occur via other, yet undetermined pathways.

The last group of R7 RGS binding partners consists of the proteins that serve to regulate RGS proteins themselves. Although there are only two reported observations in this category, the number of examples is expected to grow substantially as the organization of R7 RGS proteins and

their reliance on protein-protein interactions for determining their cellular function are complex. In studies of the established interactions with R7BP/R9AP and $G\beta_5$, association with other cellular proteins was shown to affect catalytic activity and proteolytic stability of R7 RGS proteins. This is a recurring theme for the regulation of this RGS family. Indeed, the binding partner of RGS7, polycystin, was shown to protect it from rapid proteolytic degradation by the ubiquitin proteasome system (118), whereas association with the 14-3-3 protein was shown to inhibit RGS7 activity in a phosphorylation-dependent manner (114).

- ***Physiological roles of R7 RGS proteins: insights from mouse models***

Most of what we know about the physiological roles of R7 RGS proteins comes from studies on selective elimination or overexpression of R7 RGS proteins in murine models. Among the four R7 RGS proteins, the function of RGS9 is best understood due to its localized expression and the abundance of mouse genetic models. The functional role of this member can serve as a valuable example of the other R7 RGS family members, the physiological roles of which remain largely unknown.

Targeting of the RGS9 gene produced a line of knockout mice that lack the expression of both splice isoforms: RGS9-1 in the retina and RGS9-2 in the brain (13). Elimination of RGS9-1 in the retina resulted in a substantial delay in the termination of photoreceptor responses to light, a process mediated by the GPCR phototransduction cascade (13). In this pathway, the activated receptor (photoexcited rhodopsin) triggers the activation of the G protein transducin ($G\alpha_t$), which in turn stimulates the activity of the effector enzyme cGMP phosphodiesterase. This leads to transient membrane hyperpolarization, a major response of the photoreceptor to light (reviewed in (25, 124). Following extinction of light excitation, wild type rod photoreceptors quickly return to the resting state, with an average time constant of approximately 200 ms. This rapid recovery requires G protein inactivation in the cascade and is critical for the high temporal resolution of our vision (125). In contrast, rods of mice lacking RGS9-1 show recovery kinetics that are an order of magnitude slower (time constant ~ 2.5 s) (13). This phenotype is thought to result from delayed transducin inactivation, which is mediated by RGS9-1. This suggests that this regulator is the GAP in the phototransduction cascade. Similar recovery deficiencies were also described in cone cells, suggesting that this function of RGS9-1 is conserved in all photoreceptor cells (126). Consistent with its obligatory trimeric organization, the function of RGS9-1 in providing timely transducin deactivation has been shown to depend on its association with R9AP and $G\beta_5$ subunits. Elimination of these subunits in mice results in an identical slow photoreceptor

deactivation phenotype (107, 127). In line with the observations in mice, mutations disrupting RGS9-1 and R9AP were found to cause the human visual disease bradyopsia, which disrupts the ability of those affected to adapt to changes in luminance and to recognize moving objects (128-130). Conversely, overexpression of RGS9-1•$G\beta_5$•R9AP in mouse rods results in an acceleration of photoresponse inactivation, demonstrating that it serves as a key rate-limiting enzyme in the cascade of recovery reactions that bring photoreceptors to a resting state (20).

The other splice isoform, RGS9-2, was found to be enriched in the striatum, a region commonly associated with reward and motor control functions. It was also found, albeit at much lower levels, in the periaqueductal gray matter, the dorsal horns of the spinal cord and the cortex, which are structures that mediate nociception (28, 113, 131, 132). This expression pattern has prompted several groups to evaluate the contribution of RGS9-2 to specific behaviors controlled by these systems. RGS9 knockout mice had the following phenotypic properties: (i) increased sensitivity to the rewarding properties of cocaine, amphetamine and morphine (27, 133, 134), (ii) increased sensitivity to the anti-nociceptive action of morphine (110, 133) (similar observation were also made with the down-regulation of RGS9-2 expression by antisense oligonucleotides (131), (iii) delayed development of tolerance to the administration of morphine (133), (iv) enhanced severity of withdrawal symptoms following the cessation of morphine administration (133) (v) rapid development of tardive dyskinesia in response to suppression of dopaminergic signaling (111) and (vi) deficits in motor coordination and working memory (135). Conversely, viral-mediated overexpression of RGS9-2 in the rat striatum resulted in the reduction of locomotor activity potentiation in response to cocaine administration (12). Similarly, overexpression of RGS9-2 in a MPTP monkey Parkinson's model has been reported to diminish L-DOPA-induced dyskinesia symptoms (136). Despite the long list, these deficiencies are likely to arise from alterations in specific pathways, as RGS9 knockout mice are quite normal in many behavioral aspects. They exhibit unaltered basal locomotor activities, cognitive function, fear conditioning and pre-pulse inhibition (12, 133, 135).

These described phenotypical observations suggest a model in which the function of RGS9-2 in the striatum negatively regulates the sensitivity of the signaling pathways that process reward and nociceptive cues. Indeed, growing pharmacological evidence supports the idea that RGS9-2 moderates signaling via D2 dopamine and μ-opioid receptors, two prominent systems that are thought to critically regulate reward, nociception and locomotor functions (27, 111, 133, 134, 136, 137). Moreover, signaling through D2 and μ-opioid receptors appears to be connected to RGS9-2 expression through feedback mechanisms that adjust the level of this negative

regulator, thus allowing dynamic modulation of the signaling intensity (12, 133, 138, 139). Furthermore, the RGS9-2 complex physically associates with D2 and μ-opioid receptors (see previous chapter and Table 1), although it is currently unknown what mediates this interaction.

In contrast to the thorough understanding of the role of RGS9-1in the phototransduction cascade, the mechanistic picture of RGS9-2 activity and the second messengers and effector systems that are involved in this activity are far less clear. Studies that have addressed this issue have found that introduction of the catalytically active portion of the RGS9 protein into the striatal cholinergic interneurons reduced the modulation of N-type voltage gated calcium channels by dopamine, suggesting that ion channels that regulate neuronal excitability are a potential target of RGS9-2 activity (137). This observation is in line with reconstitution studies in *Xenopus* oocytes that demonstrated that full length RGS9-2, both alone and in complex with $G\beta_5$, can powerfully modulate the kinetics of GIRK channel gating (12, 78). Studies with RGS9 knockout mice also revealed enhanced D2 dopamine receptor-mediated suppression of NMDA currents in striatal medium spiny neurons lacking RGS9-2. Furthermore, RGS9-2 was found to regulate Ca^{2+}-dependent NMDA inactivation via complex formation with α-actinin-2 in transfected cells (113). Although the mechanisms by which RGS9-2 controls these reactions are unclear, these studies implicate RGS9-2 in the regulation of excitatory glutamatergic transmission and potentially synaptic plasticity. Finally, RGS9-2•$G\beta_5$ was reported to diminish ERK1/2 kinase activation in response to the activation of μ-opioid receptor in transfected cells (110). While these studies outline the range of the effector systems that can be regulated by RGS9-2, much of the underlying mechanisms remain unclear. Among key unanswered questions are whether the effects of RGS9-2 require its GAP activity (as, for example, in the regulation of calcium channels (137)) or if these effects can be explained by direct association with receptors (as, for example, in the regulation of μ-opioid receptor internalization (110)). Equally important is the question whether RGS9-2 is a specific regulator of select receptors or if it can function as a universal regulator of several GPCRs in neurons (discussed in (140)). Finally, since RGS9-2 forms a constitutive complex with $G\beta_5$ and R7BP, elucidating the contribution of these subunits to its activity and selectivity will have a significant impact on our understanding of RGS9-2 function.

Our knowledge of the physiological roles played by other R7 RGS members is substantially more limited. Knockdown studies using antisense oligonucleotides have implicated RGS6, RGS7 and RGS11 in regulating nociception mediated by μ- and δ-opioid receptors and the development of tolerance to morphine administration (29, 141). In addition, the expression levels of these R7 RGS proteins have been reported to be modulated in response to changes in signaling

via a range of pathways (for examples see (142-145)). Broad expression profiles across the nervous system (30, 38, 74) and the ability to regulate responses elicited by a variety of GPCRs that are coupled not only to Gi/o (34, 38, 39, 78) but also to Gq (146, 147) suggest that R7 RGSs may be critical regulators in a range of signaling pathways. Indeed, the development of the $G\beta_5$ knockout mouse provides a glimpse into the range of dysfunctions that are caused by the elimination of all R7 family members at once (79). Aside from the known defects associated with the loss of RGS9, $G\beta_5$ knockouts exhibit a range of developmental anomalies. Homozygous mice lacking $G\beta_5$ are smaller in size at birth, gain weight at a slower rate, do not gain body weight in the critical period prior to weaning between postnatal days 15 to 20 and exhibit a high pre-weaning mortality rate (up to ~60%) by 21 days of age (79). In addition, retinas of $G\beta_5$ knockouts are unable to relay light excitation from rod photoreceptors to downstream ON-bipolar cells, as revealed by the lack of the characteristic b-wave on electroretinograms (148). This deficiency in synaptic transmission is underlined by the failure of ON-bipolar cells to establish synaptic contacts with rod terminals during the critical developmental window (148). In light of these widespread developmental deficiencies, it is interesting to note that the expression of R7BP, a universal subunit of R7 RGS proteins, is tightly and developmentally controlled. R7BP mRNA and protein are largely undetectable at birth and exhibit a rapid and dramatic induction, peaking around the age of weaning (92, 100). Delineating the roles of R7 RGS complexes in regulating the specific pathways that shape developmental processes and the establishment of synaptic connectivity will be an exciting future direction.

Acknowledgments

We thank Mr. Perry Anderson for his help with illustrations. Studies on R7 RGS proteins in our laboratory are supported by the NIH grants EY018139 and DA 021743. Garret Anderson is a recipient of the Ruth L. Kirschstein National Research Service Award DA024944.

Chapter 2 - The membrane anchor R7BP controls the proteolytic stability of the striatal specific RGS protein, RGS9-2

Garret R. Anderson, Arthur Semenov, Joseph H. Song and Kirill A. Martemyanov

From the Department of Pharmacology, University of Minnesota, Minneapolis, MN 55455

Content taken from the published manuscript:

Anderson G.R., Semenov A., Song J.H., Martemyanov K.A. The membrane anchor R7BP controls the proteolytic stability of the striatal specific RGS protein, RGS9-2. *Journal of Biological Chemistry*, 2007. 282(7):4772-81.

Specific contributions: GRA data is presented in Figures 2.1, 2.5, 2.6, 2.7, 2.8.

A member of the Regulators of G protein Signaling (RGS) family, RGS9-2 is a critical regulator of G protein signaling pathways that control locomotion and reward signaling in the brain. RGS9-2 is specifically expressed in striatal neurons where it forms complexes with its newly discovered partner, R7BP (R7 family Binding Protein). Interaction with R7BP is important for the subcellular targeting of RGS9-2 which in native neurons is found in plasma membrane and its specializations, postsynaptic densities. Here we report that R7BP plays an additional important role in determining proteolytic stability of RGS9-2. We have found that co-expression with R7BP dramatically elevates the levels of RGS9-2 and its constitutive subunit, Gβ5. Measurement of the RGS9-2 degradation kinetics in cells indicates that R7BP markedly reduces the rate of RGS9-2•Gβ5 proteolysis. Lentiviral mediated RNA interference knockdown of the R7BP expression in native striatal neurons result in the corresponding decrease in RGS9-2 protein levels. Analysis of the molecular determinants that mediate R7BP•RGS9-2 binding to result in proteolytic protection have identified that binding site for R7BP in RGS proteins is formed by pairing of the DEP domain with the R7H, a domain of previously unknown function which interact with four putative alpha helices of the R7BP's core. These findings provide a mechanism for the regulation of the RGS9 protein stability in the striatal neurons.

♦ *Introduction*

Regulators of G Protein Signaling (RGS) comprise a large family of proteins that control the duration of signal transduction through G Protein Coupled Receptors (GPCR) (10, 149). RGS proteins act to accelerate the rate of GTP hydrolysis on G protein α subunits, thus facilitating G protein inactivation and the subsequent termination of signaling through GPCRs (reviewed in ref. (150). A mounting body of evidence from clinical studies and genetic animal models indicate that the action of RGS proteins is essential for the normal functioning of almost all systems in the organism (19, 128, 151). In the nervous system, many critical neuronal processes appear to be regulated by the R7 RGS proteins, a subfamily conserved in a variety of animals from *C.elegans* to humans (10, 26). In mammals, the R7 subfamily consists of 4 highly homologous proteins: RGS6, RGS7, RGS9 and RGS11, all of which are expressed predominantly in the nervous system (30).

Arguably the best studied member of this group is RGS9. It exists in two splice isoforms, RGS9-1 and RGS9-2, which regulate vision and reward behavior, respectively (140). While the role of RGS9-1 in vertebrate phototransduction has been well established (reviewed in 87), much

remains to be learned about the molecular mechanisms that regulate RGS9-2 function. Previous studies have found that RGS9-2 in the striatum is involved in the modulation of μ-opoid (28, 131) and D2 dopamine (27, 111, 137) receptor responses. Studies of RGS9 deficient mice revealed increased locomotor responses, elevated rewarding effects and increased physical dependence in response to the administration of abused drugs such as morphine and cocaine (27, 28). Interestingly, drug administration has been shown to modulate the protein expression levels of RGS9-2, suggesting a possible mechanism for the adaptive changes in G protein signaling observed in addiction and tolerance (27, 28).

RGS9, as well as other members of the R7 subfamily, is a multidomain modular protein that exists *in vivo* as a constitutive heterodimer with the type 5 G protein β subunit (Gβ5) (152). This association is critical as genetic ablation of Gβ5 results in almost complete elimination of RGS9 protein, as well as all other R7 RGS proteins, presumably due to their proteolytic destabilization (79). In photoreceptors, the stability of the RGS9-1•Gβ5 complex, is further dependent upon its association with the RGS9 Anchor Protein (R9AP) (91). Knockout of R9AP leads to a profound reduction in both RGS9-1 and Gβ5 protein levels (107), whereas hyper-expressing R9AP leads to an elevation in the RGS9-1 and Gβ5 protein levels (20). In mammals, R9AP is expressed only in photoreceptors but we have recently found that in striatum, RGS9-2 forms a complex with a novel R9AP homolog which we named the R7 Binding Protein (R7BP) (76). Unlike R9AP which is available for binding only to RGS9-1, R7BP interacts with all four members of the R7 RGS protein family (76, 93). Studies by us and others indicate that, depending on its palmitoylation status, R7BP can target R7 RGS proteins to the plasma membrane, nucleus and postsynaptic densities (93, 153). Furthermore, R7BP binding to RGS7 can potentiate its ability to terminate G protein signaling (93, 99).

In this study we report that an additional role for R7BP is to regulate the proteolytic stability of the RGS9-2/Gβ5 complex. We have found that co-transfection of RGS9-2•Gβ5 with R7BP increases the expression level of the complex and increases the half-time of its degradation in neuronal cell lines. Using lentiviral mediated RNAi knockdown of R7BP expression in primary striatal cultures we demonstrate that decreases in R7BP levels lead to corresponding reductions in the levels of RGS9-2. We have further employed site-directed mutagenesis and chimeric approaches to dissect the molecular determinants that mediate the binding of R7 RGS proteins to R7BP to result in the observed stabilization of the complex.

♦ ***Materials and Methods***

Recombinant Proteins, Antibodies and Reagents - Generation of sheep anti-R7BP (N-terminal epitope) (76), anti-R9AP (against full-length mouse R9AP) (94) and sheep anti-RGS9-2CT (C-terminal epitope) (76) has been described previously. Antibodies were affinity purified and stored in PBS buffer containing 50% glycerol. Rabbit anti-RGS7 (7RC1) (123) and anti-Gβ5 (SGS) were a generous gift from Dr. William Simonds, NIDDK. Rabbit anti-DARPP-32 antibodies were from Chemicon (Temecula, CA). Mouse monoclonal anti-β-actin (clone AC-15) antibodies were purchased from Sigma (St. Louis, MO). pcDNA3.1 TOPO cloning systems were obtained from Invitrogen. Recombinant GST tagged R7BP and R9AP proteins were expressed in *E.coli* and purified as described previously (76). His-tagged recombinant R7 RGS complexes with Gβ5 were obtained in Sf9/baculovirus system and purified by Ni-NTA affinity chromatography(33, 76). Protein quantification was performed using Bradford reagent (Sigma) according to manufacture specifications using BSA as a standard (Pierce). All general chemicals were purchased from Sigma Aldrich.

DNA constructs and site-directed mutagenesis - Cloning of full length R7BP, R9AP, Gβ5, RGS7, RGS9-1, RGS9-2 was described previously (76, 153). The full length coding region of R7BP was sub-cloned into the 3' end of the GST open reading frame of vector pGEX-2T (GE Healthcare), to create a GST-R7BP fusion protein, using PCR primers tagged with NdeI linker at the 5' end and an EcoRI linker at the 3' end. Similarly, R7BP deletion constructs were created with NdeI and EcoRI linkers on PCR primers generated against specific regions of R7BP: R7BPΔNT (nucleotides 139-156 and 749-774; creating a R7BP protein of amino acids 47-257), R7BPΔCT (nucleotides 1-22 and 672-693; amino acids 1-231), R7BPΔCTΔH4 (nucleotides 1-22 and 495-516; amino acids 1-172), R7BP H1-H4 (nucleotides 139-156 and 672-693; amino acids 47-231), R7BP H1-H3 (nucleotides 139-156 and 495-516; amino acids 47-172), R7BP 47-211 (nucleotides 139-156 and 611-633; amino acids 47-211), R7BP 47-199 (nucleotides 139-156 and 578-597; amino acids 47-199), R7BP H2-H4 (nucleotides 225-244 and 672-693; amino acids 76-231), and R7BP H4 (nucleotides 480-501 and 672-693; amino acids 172-231).

R7BP/R9AP chimeric constructs were generated by splicing by overlap extension PCR (SOE PCR) strategy (154) utilizing primers against the following regions: chimera #1: R7BP 496-516, R9AP 394-411, producing a fusion protein of amino acid sequences encompassing R7BP 47-172, R9AP 132-206; chimera #2: PCR primer nucleotides (R7BP 321-339, R9AP 196-215) and amino acids R7BP 47-113, R9AP 66-206; chimera #3: R7BP 340-358, R9AP 180-195 and amino acids R7BP 114-231, R9AP 1-65; chimera #4: R7BP 517-535, R9AP 376-393, amino

acids R7BP 173-231, R9AP 1-131. Flanking primers used were generated against the following nucleotides: chimera #1 and chimera #2: R7BP 139-156, R9AP 600-618; and chimera #3 and chimera #4: R9AP 1-23, R7BP 672-693.

RGS7, and RGS9-1 and their chimeric constructs were cloned into pcDNA3.1/V5-His-TOPO (Invitrogen) mammalian expression vector according to manufacture specifications. RGS7/RGS9 chimeric constructs were generated to create fusion proteins of the following amino acid compositions: R7/9 -1 (RGS9 1-115, RGS7 123-469); R7/9 -2 (RGS7 1-122, RGS9 116-484); R7/9 -3 (RGS9 1-209, RGS7 218-469); R7/9 -4 (RGS7 1-244, RGS9 210-484); R7/9 -5 (RGS9 1-297, RGS7 332-469); R7/9 -6 (RGS7 1-331, RGS9 298-484).

All constructs were propagated into E.coli Top-10 strain (Invitrogen), isolated using Maxiprep kits (Qiagen) and sequenced.

Cell culture and Transfections - NG108-15 cells were purchased from ATCC and maintained in DMEM (Dulbecco's Modified Eagle Medium; Invitrogen) supplemented with 10% Fetal Bovine Serum, 0.1 mM sodium hypoxanthine, 0.4 μM aminopterin, 16 μM, thymidine, 100 units of penicillin and 100 μg of streptomycin. 293FT cells were obtained from Invitrogen and cultured at 37°C and 5% CO_2 in DMEM supplemented with antibiotics, 10% FBS, and 4 mM L-glutamine.

NG108-15 and 293 FT cells were transfected at ~ 70% confluency, using Lipofectamine 2000 (Invitrogen) according to the manufacturer's protocol. The ratio of Lipofectamine to DNA used was 4 μl : 2.5 μg per 4 cm^2 cell surface. Cells were grown for 24-48 hours post-transfection.

Primary cultures of striatal neurons were essentially prepared as developed by Ivkovic and Ehrlich (155). Briefly, striata were dissected from Swiss Webster mice at postnatal day 1. After dissection, tissues were treated by papain (Worthington, Lakewood, NJ), triturated and plated on 12 or 6 well tissue culture plates (Nunc, Denmark) coated with poly-D-lysine (20 μg/ml; BD Bioscience, Bedford MA). Cultures were maintained in Neurobasal-A medium supplemented with B27 (both from Invitrogen) and 0.5 mM L-glutamine. Cells were plated at a density of 2000 viable cells (e.g., excluded trypan blue) per 1 mm^2 of well square for Western blot analysis and at 500-700 cells/mm^2 for immunostaining. The cultures were incubated at 37°C in a humidified 5% CO_2 incubator. One-half of media was replaced with the fresh media every 72 hrs. From day 4 to day 7, the cultures were transduced by lentiviral constructs, incubated for 7 to 10 days, washed by PBS and lysed in SDS sample buffer.

RNA interference and generation of lentiviruses - R7BP expression was down-regulated by short interfering RNA duplexes. Target regions in R7BP were identified by BLOCK-iT RNAi Designer Program (Invitrogen). Two sequences were used to generate RNAi molecules which target either

248-268 coding region of R7BP gene (RNAi#248, sequence: CTCTGCGAGCTGAAATGCACA) or to the 483-583 region (RNAi#483, sequence: AGCGAAGAATTTGGACAGCAA). These sequences were synthesized as DNA oligos and in addition contained complementary sequences joined by the GTTTTGGCCACTGACTGAC loop. Synthetic duplexes were cloned into the pcDNA6.2GW/EmGFP vector in the middle of the micro RNA 155 (miR155) sequence supplied as a part of the BLOCK-iT Lentiviral Pol II miR RNAi Expression System kit (Invitrogen). In the pcDNA6.2GW/EmGFP vector the chimeric miR155-R7BP sequence is located under the control of the CMV promoter co-cistronically with EmGFP. Upon processing in the cells by the endogenous machinery, the construct is used to produce anti-R7BP RNA duplex (miRNA-αR7BP). The control construct (miRNA-CTR) was created by cloning a scrambled sequence AAATGTACTGCGCGTGGAGAC into the miR155 environment identically as described for miRNA-αR7BP. The expression cassette was transferred to the lentiviral shuttle vector pLenti6/V5-DEST vector (Invitrogen) by Gateway recombination following kit's instructions.

For the generation of infectious lentiviral particles, pLenti6/V5-DEST vectors containing miRNA-αR7BP or miRNA-CTR cassettes were co-transfected with ViraPower^{TM} packaging plasmid mixture: pLP1, pLP2 and pLP/VSV-G (Invitrogen) into 293FT cells using Lipofectamine 2000 (Invitrogen). Ten T75 flasks were used to produce each batch of lentiviruses. Virus containing media was collected 60-65 hrs after transfection, centrifuged at 2000 *g* for 6 min and filtered through a 0.45μm filter (Millipore) and viral particles were concentrated as described by Coleman et al. (156) with some modifications. Virus containing supernatants were carefully loaded on 60% OptiPrep (Sigma) cushion (150 – 200 μl) in 30 ml conical-bottom polyallomer centrifuge tubes (Beckman) and centrifuged at 50,000*g* for 2.5 h at 4^{o}C using a swinging bucket rotor SW-28 (Beckman). The media just above the media/OptiPrep interface was carefully removed and discarded. The residual media containing OptiPrep and viruses (~500 μl in each tube) were mixed gently by shaking and pooled into 3ml conical-bottom centrifuge tubes (Beckman), centrifuged at 17,000*g* for 4.5 h at 4^{o}C using Beckman SW-50.1 swinging bucket rotor. The supernatant was discarded and remaining viral pellet was resuspended in 50-100 μl of PBS by gentle pipetting, aliquoted and stored at -80^{o}C until use.

Infectious titers of viruses were determined by blasticidine selection method. For this, 293FT cells were in 6-well plate (5 x 10^5 cells per well) were incubated with serial dilutions of the viral stock in the presence of 6 μg/mL Polybrene (Invitrogen). Infected cells were selected in media containing 5 μg/mL blasticidin. The number of transdusing units (TU) was determined by

multiplying the estimated number of colonies by dilution factor. Our preparations of concentrated lentiviral stocks consistently yielded titers of 2-10 x 10^6 TU/ml. The titers of all viral stocks were equalized by adjusting the concentration of viral particles to 2 x 10^6/ml. Primary neurons cultured in 12 well plates at approximately 3 x 10^5 cells per well were infected by 30 μl of either miRNA-αR7BP or miRNA-CTR viruses.

Immunoprecipitation - Immunoprecipiation of R7BP and R9AP was performed essentially as described previously (76).For the precipitation of proteins expressed in the 293 cells, cells were lysed in PBS (Invirogen) supplemented with 150 mM NaCl, 1% Triton X-100 and Complete protease inhibitor tablets (Roche). Cellular lysates were clarified by 30 minute centrifugation at 20,000 *g* and incubated with 5 μg anti-R7BP or anti-R9AP antibodies crosslinked to 10 μl of protein G beads (GE Healthcare) with Bis(Sulfosuccinimidyl)suberate (BS^3) (Pierce) for 1 hour at 4^0C. After 3 washes with ice-cold binding buffer proteins bound to the beads were eluted with SDS-sample buffer (62mM Tris, 10% glycerol, 2%SDS, 5% β-ME) and analyzed by 4-20% PAGE (Cambrex). Immunoprecipitation of purified recombinant RGS9-2•Gβ5 complexes with R7BP and R9AP was performed identically with the exception that the RGS9-2CT antibodies used in the assay were not covalently cross-linked to the protein G beads. The specificity of the immunoprecipitations was controlled by using equal amounts of non-immune IgG fraction.

GST Pull-down Assays – Assays were performed as previously described (76). Briefly, purified recombinant GST fusion proteins (100 pmol) were attached to 10 μl of glutathione agarose beads (GE Healthcare) by incubating in binding buffer (20 mM Tris pH 7.2, 300 mM NaCl, 0.25% n-Dodecanoylsucrose, 50 μg/ml BSA) for 1 hour on ice. Beads were washed with binding buffer twice, and incubated with 1 pmol purified RGS•Gβ5 complexes for 10 minutes, followed by three washes. Proteins were eluted in SDS sample buffer, and RGS proteins retained by the beads were detected by Western blotting with specific antibodies.

Pulse-chase Degradation Experiments – NG108-15 cells grown in T-25 flasks were co-transfected with RGS9 and Gβ5 constructs with or without R7BP or R9AP plasmids. Twenty-four hours after transfection, cells were rinsed twice with PBS and placed into 5 ml of starvation medium (10% dialyzed FBS (Invitrogen), DMEM without L-Methionine or L-Cysteine (21013-024, Invitrogen) and incubated at 37°C and 5% CO_2 for 30 minutes. After this starvation period, newly synthesizing proteins were labeled by adding 30 mCi of radio-labeled [^{35}S] methionine and cysteine (NEG772, Perkin-Elmer) per flask to the starvation medium and incubating at 37°C and 5% CO_2 for 40 minutes. After labeling, the cells were rinsed twice with 2 ml of DMEM medium and incubated with 5 ml of fully supplemented media supplemented by additional 2 mM L-

Methionine and 2 mM L-Cysteine (Sigma-Aldrich) at 37^{o}C for the indicated incubation times. At the end of the incubation the cells were scraped into 5 ml of ice-chilled PBS (phosphate buffered saline) pelleted by centrifugation at 3,200 x *g* for 1 minute and resuspended in 900 µl of RIPA buffer (50 mM Tris-HCl pH 7.8, 300 mM NaCl, 1 mM EDTA, 1% Triton X-100, 0.5% sodium deoxycholate, 0.1% sodium dodecylsulfate) supplemented with protease inhibitors (Complete, Roche). Cells were allowed to lyse by incubating them at 4^{o}C for 20 minutes with gentle shaking. The suspension was then centrifuged at 4^{o}C and 14,000 x *g* for 30 minutes and the resulting supernatant was incubated with 10 µl of protein G beads and 3 µg of RGS9-2 CT antibody for 1 hour at 4^{o}C. The beads were then washed 3 times with 500 µl of RIPA buffer and immunoprecipitated RGS9 proteins were eluted from the beads by 50 µl of SDS sample buffer. 25 µl of the samples were run on the SDS PAGE and transferred to a PVDF membrane (Bio-Rad). Membrane was air dried and incubated on a phorphor imaging screen overnight. This screen was then scanned using a STORM phosphoimager (Molecular Dynamics), and the bands were quantified using ImageQuant Software (Molecular Dynamics). Each experiment was repeated at least twice.

- ***Results***

Co-expression with R7BP increases RGS9 levels - It is well established in the literature that R7 RGS proteins are susceptible to degradation and require association with Gβ5 for their increased stability and high expression levels (35, 78, 79). Previous studies by us and others indicate that R7 RGS proteins bound to Gβ5 can readily form complexes with their partner R7BP when co-transfected into cultured cell lines (93, 153). Here, we investigated how expression levels of R7 RGS•Gβ5 complexes are affected by their co-expression with R7BP. For these experiments we chose to use complexes of Gβ5 with RGS9 as model R7 RGS protein because of its documented instability *in vivo* (107). The use of RGS9 also allowed us to compare potential effect of R7BP to the effects produced by R9AP, a protein known to stabilize the RGS9-1•Gβ5 complex in photoreceptors (89, 91). As illustrated in Figure 2.1, co-expression with R7BP in 293 cells substantially elevates the levels of both the RGS9-1•Gβ5 and RGS9-2•Gβ5 complexes. Quantification of protein expression levels indicated that R7BP increases the levels of RGS9 by approximately 3.5 fold and Gβ5 by 2 fold. Interestingly, the extent of the R7BP's effect on the RGS9-2•Gβ5 expression was similar to the one observed with R9AP. The weaker effects of R7BP and R9AP on the expression of Gβ5 is expected since this protein appears to be more stable than RGS9-1 and could be detected even when RGS9-1 was completely eliminated in

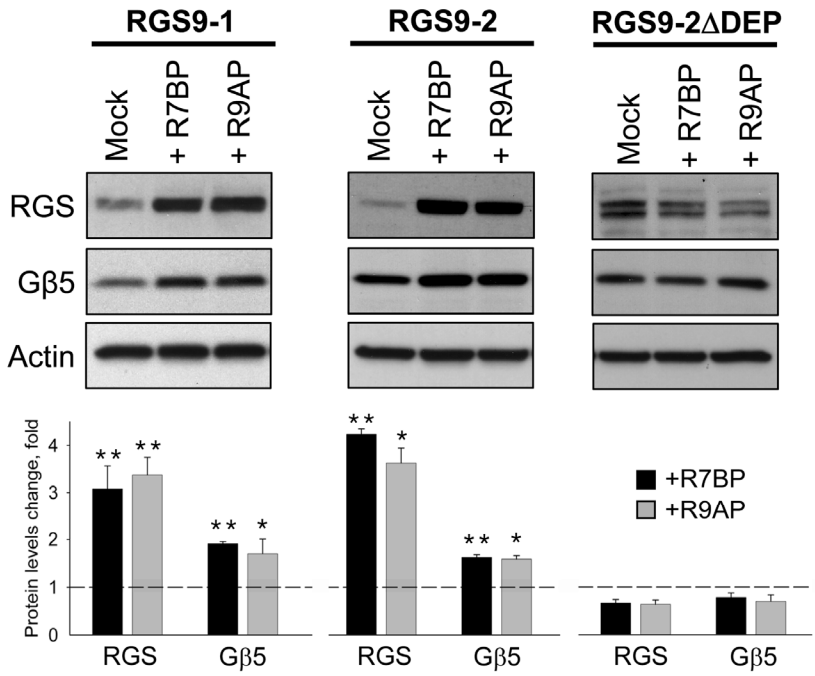

Figure 2.1: Effect of the association with membrane anchors R7BP and R9AP on the expression levels of RGS9•Gβ5. *Upper panels:* 293FT cells cultured in 6-well plates were co-transfected with pcDNA3.1 plasmids encoding RGS and Gβ5 proteins (1.3 μg/well) and either empty pcDNA3.1 vector (1.3 μg/well, mock) or vector encoding full-length mouse membrane anchors R9AP and R7BP (1.3 μg/well). 24 hours post-transfection cells were collected in SDS sample buffer, and the resulting extracts were analyzed by Western blotting using specific antibodies against RGS9-1, RGS9-2, Gβ5 and β-actin. *Bottom panels*: Band intensities for individual proteins were quantified by densitometry using ImageJ software package and normalized by the intensities of β-actin bands. Resulting values for the experiments with R7BP and R9AP were divided by the values for mock control experiments and plotted as fold change in band intensities. Statistical significance of differences in RGS and Gb5 protein levels in the absence and presence of membrane anchors R7BP and R9AP was evaluated by t-test analysis of data from three independent experiments. P values are indicated by asterisks as follows: * for $p < 0.05$ and ** for $p < 0.01$. *Error bars* represent the S.E.M. values.

photoreceptors of R9AP knockout mice (107). Control experiments utilizing RGS9-2 mutant deficient in its ability to interact with both R9AP and R7BP, RGS9-2ΔDEP reveal that its expression level is not modulated by co-expression with membrane anchors confirming that the R7BP/R9AP elicit their effects through the complex formation with RGS9•Gβ5 complexes. We have found that the effects of the membrane anchors on the expression of R7 RGS proteins did not depend on the cell line, and similar results were obtained using cultured NG108-15 cells (data not shown).

Association with R7BP reduces the rate of RGS9-2 degradation - The observed enhancement of the RGS9•Gβ5 protein levels by R7BP may be a result of either increased protein synthesis or decreased degradation. Several studies of RGS7 and RGS9 complexes with Gβ5 strongly indicate that the major regulation of their expression occurs at the post-translational level (35, 79, 107). We therefore studied the mechanism of RGS9-2 expression modulation by analyzing the effect of R7BP on the degradation kinetics of RGS9-2. We utilized a pulse-chase strategy for the metabolic labeling of proteins expressed in 293 cells. In these experiments a small fraction of newly synthesized RGS9-2 was radioactively labeled and the rate of its degradation was measured by analysing the decay of radioactivity present in the full-length RGS9-2 protein following its immunoprecipitation from cellular lysates. Data presented in Figure 2.2 demonstrate that the RGS9-2•Gβ5 complex degrades rapidly, such that by 6 hours after synthesis the proteins are nearly undetectable). However, co-expression with R7BP decreases its degradation rate by approximately 5-fold from 59.3±5.8 min to 287.1±41.3 min (Figure 2.2C). At the same time, co-transfection with R7BP did not appreciably change the extent of the RGS9-2 labeling indicating that R7BP did not increase the rate of RGS9-2 protein synthesis. Western blot analysis of RGS9-2 present in the samples served as a loading control since the total amount of RGS9-2 expressed in the cell remains constant during the time of the experiment. These results indicate that binding to R7BP binding greatly stabilizes the RGS9-2•Gβ5 complex by protecting it from proteolytic degradation.

The protective effect of R7BP requires protein binding but not membrane association.

The R7BP homologue, R9AP, has been shown to regulate RGS9-1 levels *in vivo* (20, 107). Since RGS9-1•Gβ5 and RGS9-2•Gβ5 bind to both R9AP and R7BP with approximately equal efficiency (76, 91) and result in similar modulation of the expression levels upon

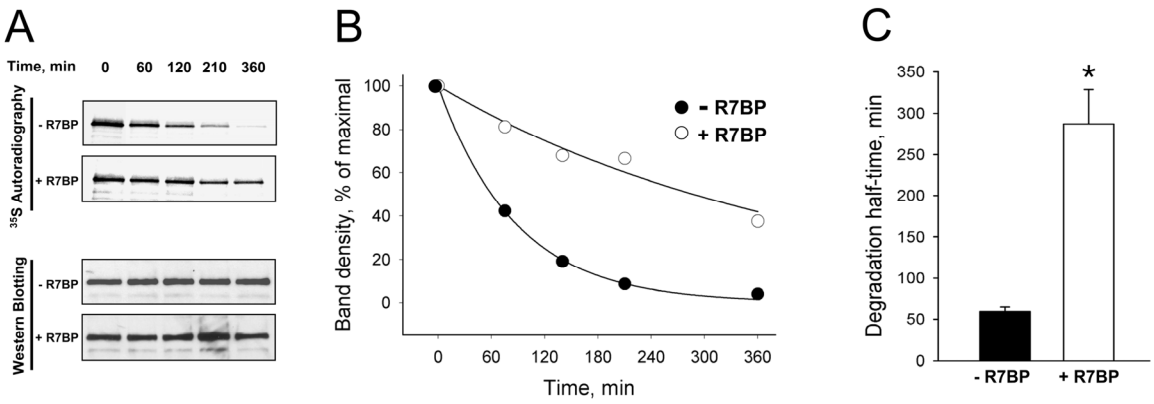

Figure 2.2:. **The effect of R7BP on the degradation kinetics of RGS9-2•Gβ5.** (**A)** Pulse-chase labeling of RGS9-2. NG108-15 cells transiently transfected with RGS9-2, Gβ5 with or without R7BP. Cells were labeled by ^{35}SMet/Cys as described in *Experimental Procedures*. The label was removed and replaced with fresh media containing non-radioactive amino acids. Cells were collected at the indicated time-points during the chase, and frozen in liquid nitrogen. Following disruption of the cells, RGS9-2 was immunoprecipitated using specific antibodies and resolved on an SDS-PAGE gel. The gel was subjected to autoradiography to reveal the radio-labeled RGS9-2, and to Western blotting to reveal the total amount of the precipitated RGS9-2. (**B)** Time-course of RGS9-2 degradation in a representative experiment. Intensities of radioactive bands in the presence or absence of R7BP were quantified using Image Quant software and plotted as a function of time. (**C**) Analysis of the degradation half-time. The values of the degradation half-time were derived by single exponential analysis of the degradation time course (as plotted in panel B). *Error bars* represent S.E.M. Asterisk indicate statistically significant difference ($p < 0.05$, n=3) between degradation half-times of RGS9-2 in the absence and presence of R7BP as revealed by the t-test.

co-transfection (Figure 2.1) we asked if R9AP and R7BP were also similar in their ability to protect RGS9-2•Gβ5 complexes from degradation in the pulse-chase degradation assays. As shown in Figure 2.3, co-transfection of RGS9-2•Gβ5 with R9AP also results in an approximately 5-fold reduction in the rate of RGS9-2 proteolysis demonstrating that R7BP and R9AP are equal in their ability to protect RGS9-2•Gβ5 complexes.

Because association of RGS9-2•Gβ5 with either R9AP or R7BP results in a translocation of the complex to the membrane (93, 153), one can imagine two potential mechanisms that can contribute to the protective effects of the anchors: targeting of RGS9-2 away from the site of proteolysis and/or stabilization via direct interaction. In order to differentiate between these two modes we examined the protection of RGS9-2 by an R7BP mutant deficient in its ability to localize to membranes. Figure 2.3 shows that R7BPΔCT, a mutant that retains full binding to RGS9-2 but has a soluble cytoplasmic localization pattern due to the deletion of its membrane localization motif (153) provides the same degree of protection as full length R7BP for RGS9-2 when co-expressed in cells. This indicates that R7BP exerts its protective effects by direct protein-protein interaction rather than by re-localization of RGS9-2 in the cell.

It has been previously shown that the interaction with R7BP and R9AP is mediated by the DEP domain of RGS9 (76, 89). Our earlier studies indicated that while full-length RGS9-1 could not be expressed without interacting with R9AP (20, 107), we were able to transgenically express a deletion variant of RGS9-1 lacking the DEP domain in photoreceptors (89). This result suggested that the DEP domain of RGS9-1/RGS9-2 might contain elements that destabilize RGS9 when it is not in complex with R9AP or R7BP (89). We used the pulse-chase degradation assay to directly determine if the deletion of the DEP domain would result in the stabilization of RGS9-2•Gβ5 in the absence of its interaction with R7BP. Data presented in Figure 2.3 show that RGS9-2 lacking the DEP domain exhibits the same rate of degradation as full length RGS9-2 arguing that the elements that destabilize RGS9 are either contained in other regions of the molecule or the stabilizing effect of R7BP is brought about by conformational re-arrangement of the RGS9-2 molecule.

Knockdown of R7BP expression reduces RGS9-2 levels in primary cultures of striatal neurons - The observation that R7BP reduces the degradation rate of RGS9-2 led us to ask whether binding to R7BP is critical for the expression of RGS9-2 in native neurons. RGS9-2 was reported to be predominantly expressed in the striatum where it is found in most subtypes of medium spiny

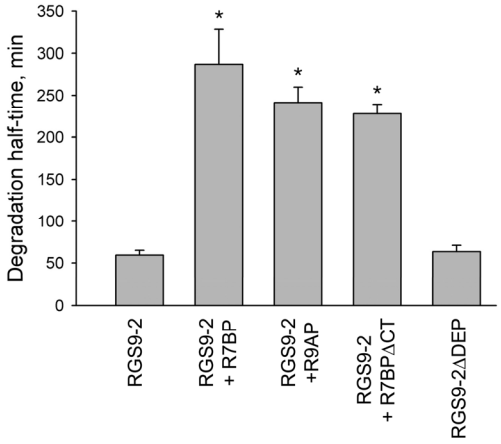

Figure 2.3: Proteolytic protection of RGS9-2•Gβ5 by R7BP is not dependent on membrane association. NG108-15 cells were transfected with RGS9-2 or its DEP-less mutant (RGS9-2ΔDEP) with Gβ5 in the absence or presence of R9AP, wild-type R7BP or R7BP mutant lacking membrane targeting sequence (R7BPΔCT) as indicated. RGS9-2 degradation half-times were determined as described in Figure 2.2 legend and plotted as bars. Each bar represents an average of two experiments. *Error bars* are S.E.M. Statistically significant differences in degradation half-times in respect to the degradation half-time of RGS9-2•Gβ5 alone are indicated by asterisks (t-test: $p < 0.05$, n=2).

neurons as well as the cholinergic interneurons (30, 137). We therefore used primary cultures ofmouse striatal neurons as a model for studying the effects of R7BP on RGS9-2 expression. To knockdown R7BP expression we employed an RNAi approach in which we used short RNA duplexes containing sequences complementary to R7BP mRNA to induce specific inhibition of its expression (157). Our screen of chemically synthesized siRNA duplexes in transfected 293 cells identified two sequences that were able to induce almost complete knockdown of R7BP expression when co-delivered with an R7BP expression construct into the cells (data not shown). Nucleotide sequences of these effective RNAs (shRNA) were incorporated into the micro RNA-155 environment in the lentiviral transfer vector pLenti6.2 (Figure 2.4A). The vector was used to produce lentiviral particles pseudotyped with the VSV-G envelop protein which upon infection delivers the construct to the cells. Our control lentiviral construct contained scrambled shRNA placed in the same position of miRNA155. The resulting lentiviruses were able to effectively infect both cultured cells and primary neurons as evidenced by the expression of the GFP reporter in the cells (Figure 2.4B). The results presented in Figure 2.4C reveal that infection of the striatal neurons with lentiviruses carrying miRNA targeting R7BP but not lentiviruses containing scrambled control miRNA result in the effective knockdown of R7BP expression. We found that our two lentiviral vectors targeting different regions of R7BP mRNA (#158 and #483, see Experimental Procedures for details) were equal in their ability to bring down R7BP expression level in striatal neurons. Notably, concomitant with decreases in R7BP protein RGS9-2 protein also showed a comparable reduction in its expression levels. At the same time, the expression of DARPP-32, a signaling protein exclusively expressed in striatal neurons (159) remained unchanged verifying the specificity of the R7BP and subsequent RGS9-2 knockdown. Together, these data demonstrate that the knockdown of R7BP expression in native striatal neurons specifically destabilizes RGS9-2 resulting in a marked reduction in its expression levels.

The RGS binding site in R7BP is formed by four putative alpha helices - In order to gain insight into the stabilizing properties of the R7BP•RGS9-2•Gβ5 complex we sought to define the molecular determinants that mediate the interaction of R7 RGS proteins with R7BP. As we previously reported (76), the core of R7BP secondary structure is predicted to be formed by 4 alpha helices, designated H1 through H4 with the weakly structured regions at both N- and C-termini (Figure 2.5). In addition to its propensity to form an alpha helix, the H4 region also contains heptad repeats (76, 93) and is identified by the COILS algorithm (160) to have more than 90% probability to form a coiled-coil fold. Interestingly, analysis of R9AP organization, the closest R7BP homolog, also predicts the same overall structural organization (89, 104).

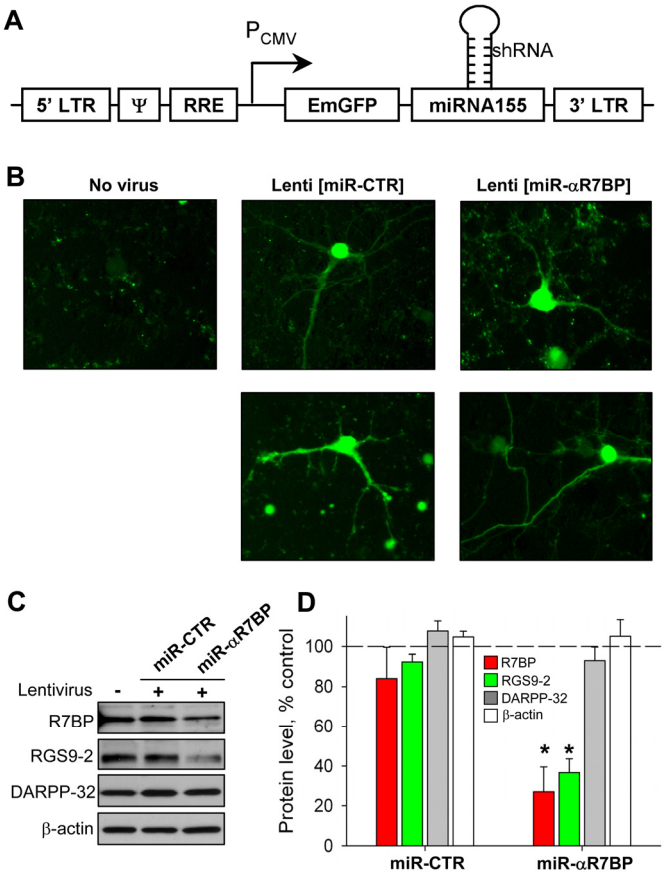

Figure 2.4: Lentivirial mediated knockdown of R7BP expression in primary cultures of striatal neurons. (**A**) Genetic construct for the inhibition of R7BP expression with lentiviruses. Short hairpin duplex with either the sequences of R7BP gene or scrambled nucleotides (shRNA) were cloned as a part of microRNA155 (miRNA155) and placed under the control of the CMV promoter. The construct also allows for the co-cistronic expression of emerald GFP with miRNA155. The expression cassette is flanked by the elements necessary for packaging into lentiviral particles (5' and 3' LTRs, Φ and RRE). (**B**) Representative striatal neurons in culture following lentiviral infection. Cultured cells were infected with equal amounts of anti-R7BP (miR-αR7BP) or control (miR-CTR) lentiviruses. The infection results in the expression of the GFP reporter as monitored by the appearance of the green fluorescence. Images were obtained using fluorescent microscopy. (**C**) Western blot analysis of protein expression in the striatal neurons infected with control or anti-R7BP viruses. When indicated, recombinant lentiviruses were added to cultured cells on day 7 in vitro and the cultures were maintained for a week after the infection. Cells were lysed in SDS sample buffer and equal amounts of lysates were loaded on the same gel. Expressed proteins were detected with specific antibodies (see Materials and Methods). (**D**) Quantification of changes in protein levels. The intensity of the protein bands were determined by densitometry using ImageJ software (NIH). The resulting values were reflected as % of the band density in the uninfected control cultures. Two lentiviruses targeting different regions of R7BP gene showed similar results and were combined in the analysis. Results were averaged from 3 experiments conducted on independently isolated primary cultures. Error bars reflect SEM. Asterisks indicate statistically significant difference in protein levels in cultures infected by miR-CTR vs. miR-αR7BP viruses ($p<0.05$, t-test).

We have used this model to perform a deletion mutagenesis of R7BP. Full-length R7BP and its deletion mutants were obtained as C-terminal fusions with GST. Recombinant proteins were expressed in *E.coli*, affinity-purified to homogeneity and assessed for their ability to bind recombinant R7 RGS•Gβ5 complexes (Figure 2.5) Among the four R7 RGS proteins RGS9 is highly homologous to RGS11 and RGS7 shares closest homology with RGS6 separating the subfamily into two groups. Therefore, in order to account for the potential differences assayed in the binding properties of R7BP mutants we analyzed their binding to both RGS9 and RGS7. As evident from Figure 2.5, the interaction pattern of both RGS proteins was similar across all deletion mutants used. Both N and C- terminal elements of R7BP were found to be dispensable for high affinity binding of R7BP to R7 RGS proteins. However, all four helices were required for its ability to form complexes with RGS proteins. Any truncations of the H1-H4 resulted in the complete loss of R7BP's binding to RGS proteins even though all generated constructs were soluble and retained their ability to bind to glutathione. This indicates that the minimal RGS binding site in R7BP is formed by helices H1-H4 which are likely to be organized in a single structural unit. This organization of the binding site is different from R9AP where only three helices H1-H3 were shown to constitute the minimal binding site for RGS proteins (104).

R7BP and R9AP have competitive but distinct modes of binding to RGS9-2 - In addition to the observed difference in the minimal RGS binding site between R7BP (H1-H4 helices) and R9AP (H1-H3 helices) these proteins also differ in their binding specificity for R7 RGS proteins. While R7BP can bind all four R7 RGS proteins, R9AP forms complexes only with RGS9 and its closest homologue RGS11. To explore the molecular basis of this specificity of binding we generated a series of R7BP/R9AP chimeric molecules in which we interchanged one or more helices and used pull down assays to determine if the ability to bind to RGS9 or to both RGS9 and RGS7 was altered (Figure 2.6). Data presented in Figure 2.6 indicate that no region from R9AP can functionally substitute for the RGS binding determinants in R7BP unless most of the protein is substituted by the R9AP sequences which alone can form an RGS binding site (chimera #4). At the same time, both R7BP and R9AP sites of interaction with RGS9 overlap, as indicated by the binding competition assays (Figure 2.7). These results indicate that despite structural and functional similarity of these two proteins, R7BP and R9AP use different modes of binding to RGS proteins.

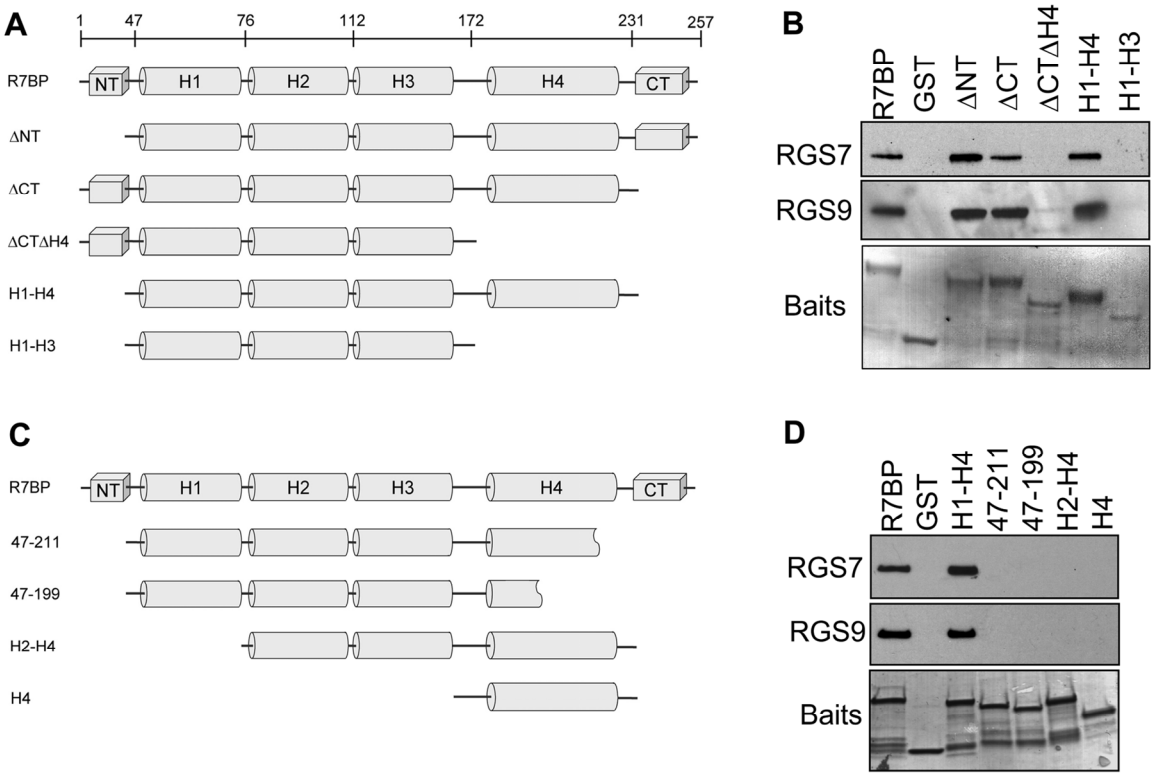

Figure 2.5: Determination of the RGS binding site in R7BP. (**A**) Schematic diagram of the R7BP deletion mutants. Cylinders (H1-H4) indicate regions predicted to form alpha helices, blocks (NT and CT) correspond to poorly structured regions. Numbers at the bar indicate the amino acid position number where the truncations were made. (**B**) Results of the GST pull-down assay. Deletion mutants were expressed as GST fusions, purified and bound to the beads. The beads were incubated with R7 RGS•Gβ5 complexes, washed and bound proteins were eluted with SDS sample buffer. The retention of the RGS proteins was analyzed by Western blotting. GST-R7BP mutants (baits) were detected by Ponceau S staining of the PVDF membrane to ensure their equal binding to the beads. (**C**) Schematic diagram of the R7BP mutants with additional truncation in the H1-H4 region. (**D**) Western blotting analysis of the RGS protein retention by the additional R7BP deletion mutants. RGS9 and RGS7 were detected using specific antibodies.

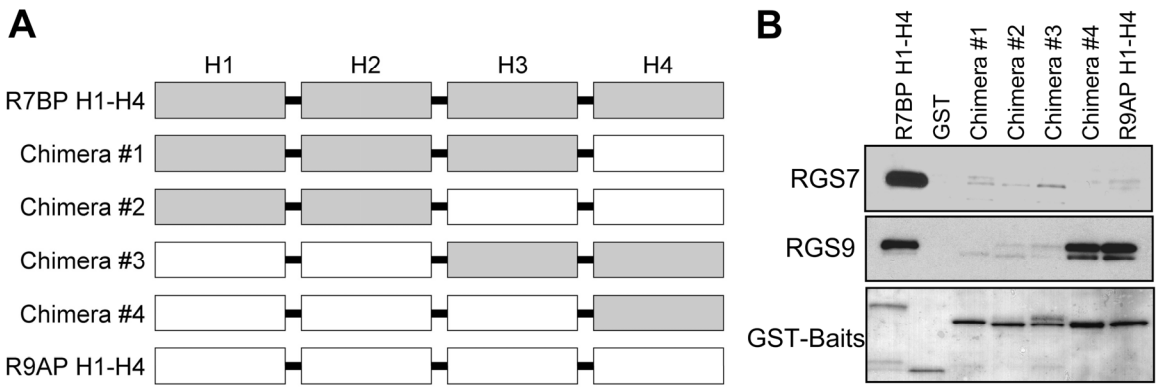

Figure 2.6: RGS binding properties of R7BP/R9AP chimeras. (**A**) Schematic representation of the generated R7BP/R9AP chimeras. Blocks indicate predicted alpha helical regions that are shared between R7BP and R9AP. Shaded blocks designate elements in R7BP, white blocks designate elements in R9AP. (**B**) Results of the pull-down binding assay between R7BP/R9AP chimeras bound to beads and RGS proteins present in the solution. RGS7•Gβ5 and RGS9•Gβ5 proteins retained by the beads were detected by Western blotting with specific anti-RGS antibodies.

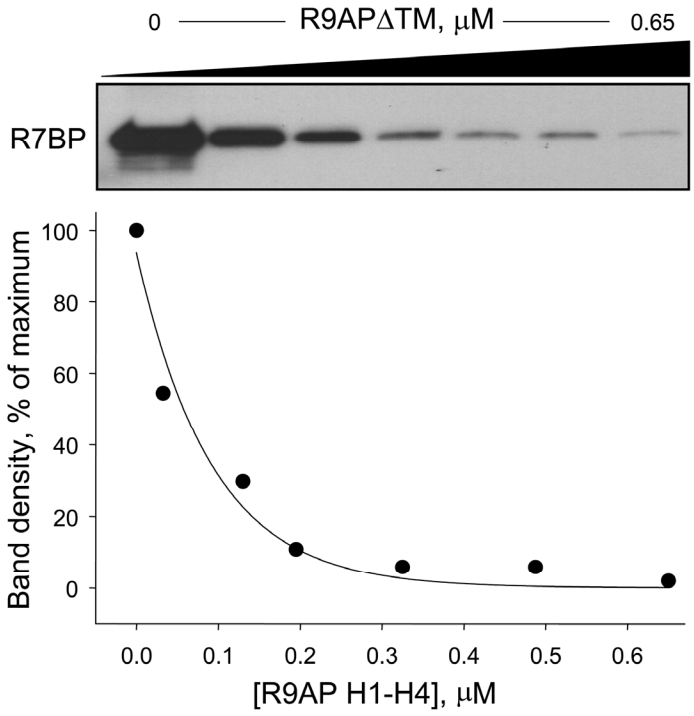

Figure 2.7: R7BP and R9AP compete for binding to RGS9-2•Gβ5. Recombinant RGS9-2•Gβ5 complex (65 nM) was incubated with recombinant R7BP (65 nM) and varying concentrations of recombinant R9AP (H1-H4) in PBS buffer. RGS9-2 was immunoprecipitated using specific anti RGS9-2 antibodies and the presence of the R7BP in the precipitates was detected by Western blotting with anti-R7BP antibodies (*upper panel*). Band intensities were determined by densitometry and plotted as a function of R9AP H1-H4 concentration (*bottom panel*). Single exponential analysis of the data was used to determine the value of IC50, which was equal to 58.3 nM.

R7BP/R9AP binding site in R7 RGS proteins is formed by both DEP and R7H domains - Continuing our search of the molecular determinants of R7BP•RGS9•Gβ5 complex formation we have next focused on the identification of the R7BP binding site in RGS proteins. Previous studies by us and others have identified the DEP domain as a critical element which was required for RGS9 binding to both R7BP and R9AP (76, 89, 90, 103). However, when expressed alone the DEP domain failed to bind R9AP indicating that by itself it is not sufficient for mediating interactions with the membrane anchors (90). Our attempts to determine the minimal binding site for R9AP and R7BP in RGS9 by deletion mutagenesis were not successful due to the high instability of resulting mutants (Dr. Sheila Baker and Kirill Martemyanov, unpublished observations).

In the experiments presented in Figure 2.8 we employed chimeric replacement strategy to identify the elements in R7 RGS proteins that form the minimal binding site for its membrane anchors. We took advantage of the fact that RGS7 and RGS9 have clearly different binding specificities for R7BP and R9AP. RGS9 forms complexes with both R7BP and R9AP whereas RGS7 can bind only to R7BP (76). Therefore, the minimal segment shared between the RGS proteins the replacement of which would completely and reciprocally reverse their respective binding specificities should reveal a minimal binding site for the membrane anchors R9AP/R7BP.

Data presented in Figure 2.8 reveal that the replacement of the DEP domain of RGS9 for the DEP domain of RGS7 did not result in the acquisition of the chimera's ability to bind R9AP. The reciprocal substitution have dramatically reduced the ability of the chimeric protein to bind to R7BP and eliminated its binding to R9AP. Consistent with our earlier observations this result indicates that the DEP domain although necessary, is not sufficient for mediating the binding of R7 RGS protein with their membrane anchors R7BP and R9AP. Strikingly, the replacement of both DEP and R7H domains in the next set of chimeras completely switched the binding specificities of the RGS proteins. RGS7 containing the DEP and R7H domains of RGS9 gained an ability to interact with R9AP whereas the ability of RGS9 to bind to R9AP was lost. Including the GGL-Gβ5 module to the parts replaced between RGS7 and RGS9 did not change this altered binding specificity pattern. Overall, these results indicate that the binding site for membrane anchors R7BP and R9AP is formed by pairing DEP and R7H domains of R7 RGS proteins.

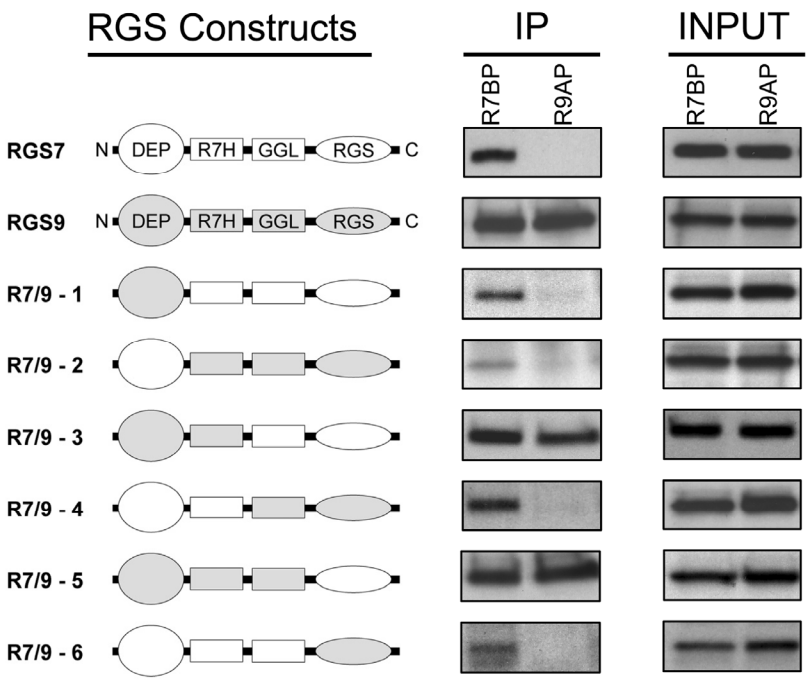

Figure 2.8: Determination of the R7BP/R9AP binding sites in RGS proteins. Left, Schematic representation of R7 RGS domain organization. RGS7 and RGS9 share similar domain composition comprising: DEP (Disheveled, EGL-10, Pleckstrin), R7H (R7 Homology), GGL (G Gamma Like) and RGS (Regulator of G Protein Signaling homology) domains. The GGL domain mediates interaction with Gβ5. RGS7 domains are represented by white elements and RGS9's by shaded figures. **Right,** Western blot analysis of either total cellular lysates prepared from 293 cells co-expressing RGS9-1, Gβ5 and R9AP/R7BP (Input) or eluates after immunoprecipitation with either anti-R7BP or anti-R9AP antibodies. RGS7, RGS9 and their chimeric constructs were detected by a mixture of anti-RGS7 and anti-RGS9 antibodies.

♦ ***Discussion***

The main finding of our study is that RGS9-2•Gβ5 is inherently susceptible to rapid degradation and requires the association with its binding partner, R7BP to maintain its stability and high expression levels. Regulation of protein stability is an emerging mechanism for the control of R7 RGS protein function at the cellular level. Previous studies have found that the stability of RGS9 as well as other members of R7 RGS family, depend on complex formation with their binding partner, Gβ5 (35, 74, 78). Studies of RGS9 and Gβ5 knockout animals firmly establish these proteins as obligate heterodimers (13, 79, 107). The results obtained in our study introduce R7BP as an additional player that in turn determines the stability of the RGS9•Gβ5 at the post-translational level. This result parallels our earlier observation that the photoreceptor specific splice isoform of RGS9, RGS9-1 is also highly unstable when present in complex only with Gβ5. The levels of the RGS9-1•Gβ5 complex in photoreceptors is controlled by its association with R7BP-like protein R9AP as the genetic ablation of the R9AP gene leads to the complete degradation of RGS9-1 in photoreceptors (20, 107).

The second major result obtained in our study is the identification of the molecular determinants that mediate the association of RGS9 with its anchors R7BP and R9AP and resultant stabilization of the complex. We have found that the binding of R7BP/R9AP to R7 RGS proteins requires contribution of not only DEP domain but also R7H domain, the functional role of which was previously unknown. Unlike DEP domain present in a number of signaling proteins, R7H domain is unique to R7 RGS proteins (149). This suggests that the ability to bind protein anchors R7BP and R9AP is a unique property of R7 RGS proteins which emerged as a result of synergistic contributions from both R7H and DEP domains. Interestingly, that despite interaction with a common binding site and significant amino acid homology R7BP and R9AP utilize different modes for RGS protein binding and lack functionally interchangeable elements. Such differences may underlie differential selectivity of R7BP and R9AP for binding to RGS proteins and also indicate for the convergent nature in the evolution of membrane anchors for R7 RGS proteins.

Overall, our results suggest that the instability of the RGS9-2•Gβ5 complex and the ability of R7BP to protect it from degradation may serve as a powerful mechanism for rapid regulation of RGS9-2•Gβ5 complex in the neurons. Recent investigations suggest that the expression level of RGS proteins serves as a rate limiting factor determining the duration in the G protein signaling thus making regulation of the RGS levels a key mechanism that control the

duration of the cellular responses to GPCR activation in the cell (20). Indeed, changes in the amount of RGS9•Gβ5 in both photoreceptors and striatal neurons were previously shown to affect the extent of their G protein signal transmission consequently resulting in the alteration of the physiological and behavioral responses of the organism (13, 20, 27, 28, 111, 127). Interestingly, conditions that alter the signaling through the μ-opioid and dopamine receptors in the striatum were reported to result in the alteration of RGS9-2 expression in the striatum. The levels of RGS9-2 increase upon chronic cocaine (27) or acute morphine (28) administration, but decrease when morphine (28) or amphetamine (139) are administered chronically. In addition, patients with the Parkinson's disease show elevated levels of RGS9-2 expression (138). These observations argue for that activity dependent modulation of RGS9-2•Gβ5 expression levels as a possible compensatory mechanism that regulates altered GPCR activity.

We propose that the regulation of the RGS9-2•Gβ5 stability by the association with its membrane anchor R7BP may serve as potent mechanism for the rapid modulation of the RGS9-2•Gβ5 protein levels in the striatal neurons. Dissociation of RGS9-2•Gβ5 from R7BP would destabilize the protein complex resulting in rapid degradation, which would in turn prolong the duration of the GPCR responses. Conversely, formation of the ternary complex would stabilize the RGS9-2•Gβ5 resulting in shorter responses. Mechanisms that regulate the RGS9-2•Gβ5 association with R7BP and mediate rapid proteolytic degradation of RGS9-2•Gβ5 heterodimer will be a timely goal for future investigations.

Acknowledgments

This study was supported by the research grants from the Minnesota Medical Foundation, the Graduate School at the University of Minnesota and National Institute on Drug Abuse (DA011806). We are grateful to Dr. Sheila Baker for critical comments on the manuscript.

Chapter 3 - Expression and localization of RGS9-2·Gβ5·R7BP complex *in vivo* is set by dynamic control of its constitutive degradation by cellular cysteine proteases.

Garret R. Anderson[1], Rafael M. Lujan[2], Arthur Semenov[1], Marco Pravetoni[1], Ekaterina N. Posokhova[1], Joseph H. Song[1], Vladimir Uversky[3,4], Ching-Kang Chen[5], Kevin Wickman[1], Kirill A. Martemyanov[1]

From the [1]Department of Pharmacology, University of Minnesota, Minneapolis, MN 55455 USA; [2]Departamento de Ciencias Médicas, Facultad de Medicina, Universidad de Castilla-La Mancha, 02006 Albacete, Spain; [3]Department of Biochemistry and Molecular Biology, Indiana University School of Medicine, Indiana, IN 46202 USA; [4]Institute for Biological Instrumentation, Russian Academy of Sciences, Pushchino, 142290, Russia; [5]Department of Biochemistry and Molecular Biology, Virginia Commonwealth University, Richmond, VA 23298 USA.

Content taken from the published manuscript:

Anderson G.R., Lujan R., Semenov A., Pravetoni M., Posokhova E.N., Song J.H., Uversky V., Chen C.K., Wickman K., Martemyanov K.A. Expression and localization of RGS9-2/Gβ5/R7BP complex in vivo is set by dynamic control of its constitutive degradation by cellular cysteine proteases. *Journal of Neuroscience*, 2007. Dec 19, 27(51):14117-27.

Specific contributions: GRA data is presented in Figures 3.4C/D, 3.5, 3.6B, 3.7B, 3.8A/C.

A member of Regulator of G protein Signaling family, RGS9-2 is an essential modulator of signaling through neuronal dopamine and opioid G protein coupled receptors. Recent findings indicate that the abundance of RGS9-2 determines sensitivity of signaling in the locomotor and reward systems in the striatum. In this study we report the mechanism that sets the concentration of RGS9-2 *in vivo,* thus controlling G protein signaling sensitivity in the region. We found that RGS9-2 possesses specific degradation determinants which target it for constitutive destruction by lysosomal cysteine proteases. Shielding of these determinants by the binding partner R7BP controls RGS9-2 expression at the posttranslational level. In addition, binding to R7BP in neurons targets RGS9-2 to the specific intracellular compartment- the postsynaptic density. Implementation of this mechanism throughout ontogenetic development ensures expression of RGS9-2•Gβ5•R7BP complexes at postsynaptic sites in unison with increased signaling demands at mature synapses.

♦ ***Introduction***

Heterotrimeric G protein signaling pathways mediate a number of fundamental cellular processes including reception, proliferation, exocytosis, chemotaxis and many others. The stimuli in these systems are transmitted via molecular switches, G proteins that oscillate between inactive GDP-bound and active GTP-bound states (5). It is well established that signaling in these pathways is critically controlled by a conserved family of proteins called Regulators of G protein Signaling (RGS) which facilitate G protein inactivation to result in faster response termination (149).

One member of this protein family, RGS9 has recently attracted significant attention due to its essential roles in regulating vision, reward behavior and locomotion in mammals. A short splice isoform, RGS9-1, is expressed only in photoreceptors where it sets the duration of light responses (13, 20), while the long splice variant, RGS9-2 is prominent in the basal ganglia, where it modulates signaling through D2 dopamine and μ-opioid receptors to regulate reward and the coordination of movement (27, 28, 111).

Accumulating evidence suggests that expression level of RGS9 critically determines signal duration in both retina and striatum. In the visual system, the absence of RGS9-1 results in delayed recovery of photoreceptors from light excitation (13) causing the disease, bradyopsia (128). Conversely, an increase in RGS9-1 levels results in faster response termination (20). In the

striatum, loss of RGS9-2 aggravates dyskinetic conditions (111) and hypersensitizes the reward system to stimulation with morphine and cocaine, whereas elevation in RGS9-2 expression blunts these behavioral responses (27, 28). Furthermore, levels of RGS9-2 were found to be specifically modulated by changes in the cascade activation induced by abused drugs (27, 28, 139), neuro-degeneratative diseases (138), or sex hormones (161), suggesting that RGS9-2 expression modulation is an important biological parameter contributing to adaptive responses.

Given its significance, surprisingly little is know about the mechanisms involved in regulating RGS9-2 expression. RGS9-2 forms complexes with two binding partners: type 5 G protein beta subunit (Gβ5) (38, 47) and R7 Binding Protein (R7BP) (76, 93) and both of these proteins were found to influence RGS9 stability (50, 78, 79).

In the current study we show that the expression level of RGS9-2 *in vivo* is set by balancing its selective degradation by cellular cysteine proteases targeted by specific degradation determinants, and macromolecular complex formation with binding partner R7BP which shields these determinants. We demonstrate that the mechanism is involved in marked upregulation of the RGS9-2•Gβ5•R7BP complex expression in ontogeny upon which it is recruited to specific signaling compartment of mature synapses - the postsynaptic density.

♦ *Material and Methods*

Antibodies and DNA constructs

Generation of rabbit anti-R7BP NT (76), rabbit anti-R9AP (94), sheep anti-RGS9d (47), and sheep anti-RGS9-2 CT (76) has been described previously. Rabbit anti-RGS7 (7RC1) and anti-Gβ5 (SGS) were generous gifts from Dr. William Simonds (NIDDK, National Institutes of Health). Commercial antibodies used include mouse monoclonal anti-β-actin (clone AC-15, Sigma), anti-Ubiquitin (Santa Cruz Biotechnology), and PSD-95 (Abcam). All custom generated antibodies were tested for the specificity to ensure that (i) they recognize single major band in brain extracts corresponding to size of detection subject, (ii) their immunoreactivity is blocked by peptide containing specific epitope sequence and (iii) antibodies efficiently performed in immunoprecipitation reactions and the identity of precipitated band was confirmed by mass-spectrometry.

RGS7, and RGS9-1 and their chimeric constructs were cloned into pcDNA3.1/V5-His-TOPO (Invitrogen) mammalian expression vector as detailed previously (50). The following RGS7/RGS9 chimeras were used: #1 (RGS9 1–115, RGS7 123–469), #2 (RGS7 1–122, RGS9

116–484), #3 (RGS9 1–209, RGS7 218–469), #4 (RGS7 1–244, RGS9 210–484). Cell transfections were performed utilizing Lipofectamine LTX reagent (Invitrogen) according to manufacturer's protocol.

Preparation of brain extracts, immunoprecipitation and Western blotting

Cellular lysates were prepared by homogenizing brain tissue by sonication in the IP buffer (1X PBS, 150mM NaCl, 1% Triton X-100, protease inhibitors) followed by 10 min centrifugation at 14,000 x *g*. The resulting extract was used for protein concentration determination by BCA assay (Pierce). This Triton X-100 extraction procedure yielded more than 90 % extraction efficiency of proteins under investigation and was followed for both direct immunoblot and immunoprecipitation experiments. Immunoprecipitation of RGS7 and RGS9-1 was performed utilizing 5 µg antibody, 10 µl protein G beads (GE Healthcare), added to the extracts. The mixtures were incubated for 1 hour, washed three times with IP buffer, and proteins bound to the beads were eluted with SDS sample buffer. Samples were resolved on SDS-PAGE gel, transferred onto PVDF membrane and subjected to Western blot analysis using HRP conjugated secondary antibodies and ECL West Pico (Pierce) detection system. Signals were captured on film, scanned by densitometer and band intensities were determined using Image J software (NIH). For quantitative analysis serial dilutions of the sample with highest concentration of antigen were loaded on the same gel and used as calibration standards for estimation of relative changes in protein levels.

Quantitative real-time RT-PCR experiments

Striatum tissue was subjected to RNA extraction with RNA isolation kit (Stratagene), and 0.08 µg RNA was used to perform quantitative real-time RT-PCR using SYBR Green QRT-PCR kit (Stratagene). QuantiTect primers (Qiagen) were used, which had been designed to be specific to either R7BP or RGS9 mRNA. PCR cycling and detection was performed on the 7500 Fast Real-Time PCR System, with quantification analysis by System Sequence Detection Software v1.3 (Applied Biosystems). In addition to using equal amounts of total RNA as defined by UV spectroscopy we have also included internal reference controls to account for the integrity of mRNA: amplification of β-actin and GAPDH mRNAs. We found that both of these messages do not show any appreciable changes during development and consequently used β-actin as endogenous reference for normalization of both R7BP and RGS9 mRNA amplification.

Generation of R7BP knockout mouse

Targeting of R7BP gene was done by homologous recombination in 128 Sv/Ev mouse ES cell lines and was performed on a commercial basis at Ingenious, Inc (Stony Brook, NY).

The targeting strategy consisted in the replacement of the first two exons of R7BP gene by neomycin resistance cassette. A ~10.8 kb region used to construct the targeting vector was first sub cloned from a positively identified BAC clone. The region was designed such that the short homology arm (SA) extends ~2.3 kb to 3' side of LoxP/FRT flanked Neo cassette. The long homology arm (LA) starts at the 5' side of LoxP/FRT flanked Neo cassette and is ~7.5kb long. The neo cassette replaces ~5.8 kb of the gene encoding exons 1-2 (including the ATG start codon). Following electroporation, G418 resistant clones were selected, confirmed for recombination by PCR and injected into blastocyst. After confirming germline transmission, mice were back-crossed with C57/Bl6 wild type mice for two generations. Resulting heterozygous animals were inbred to produce wild type, heterozygote and R7BP knockout littermates used in the experiments. R7BP knockout mice did not show any visible abnormalities in their baseline behavior or brain morphology.

Immunogold electron microscopy

Electron microscopic examination of immunoreactivity for RGS9-2 and R7BP in the striatum of WT and RGS9-2 KO and R7BP KO mice was performed as described previously using either pre-embedding or post-embedding immunogold methods (162). Briefly, brains were perfused with 4% paraformaldehyde, 0.05% glutaraldehyde and 15% (v/v) saturated picric acid in 0.1 M phosphate buffer. For pre-embedding immunogold labeling, brain sections (50-70 mm) were cut on a Vibratome and processed for immunocytochemical detection of RGS9-2 and/or R7BP using HRP and silver-enhanced immunogold techniques. For postembedding immunogold labeling, ultrathin sections (70–90 nm) from three Lowicryl-embedded blocks slices were cut on an Ultramicrotome and processed for immunocytochemical detection of RGS9-2 and/or R7BP.

Subcellular fractionation experiments

Striatums from one animal were lysed in 0.5 ml of non-detergent buffer (12 mM Na_2HPO_4/NaH_2PO_4, 287 mM NaCl, 3 mM KCl, protease inhibitors, pH=7.4), homogenized with series of needles (16, 22, 26G) and spinned down at 22,000g for 20 min. Supernatant was removed and pellet was resuspended in 0.5 ml of the above referenced buffer. Equal volume aliquotes of supernatant and pellet were mixed with SDS sample buffer and subjected to SDS-PAGE analysis following by Western blotting with anti-RGS9-2 antibodies. The procedure separates heavy plasma and synaptic membranes from cytosolic compartment and light microsomal membranes.

Recombinant lentiviruses and stereotaxic injections

Recombinant lentiviruses carrying R7BP or LacZ genes were packaged and concentrated as previously described (50). Solution containing viral particles was delivered by the means of a stereotaxic injection into the caudate putamen regions of anesthetized mice. A total of 4 injections per brain side were performed, with injection volume of 400 nl delivered at 5 nl per second via a 30G hypodermic needle. The following stereotaxic coordinates for the injection sites were used: 0.75 mm anterior to Bregma; ±1.5 mm and ± 2.25 from midline; 2.5 mm and 3.5 mm dorsal ventral from skull surface. After injection, needle was held in place for an additional 60 seconds in order to ensure proper diffusion. Holes and wounds were closed with tissue adhesive (Vetbond, 3M) and the animals were allowed to recover for one week.

Ubiquitination assays

293FT cells were transfected with either RGS7 or RGS9-2 with or without Gβ5 and/or R7BP. Twenty hours post-transfection media was supplemented with 50 μM MG132 and cells were incubated for an additional 4 hours, lysed in IP buffer supplemented with 1% SDS, protease inhibitors (Complete; Roche), 50 μM MG132, and 2 mM N-ethylmaleimide (Sigma). Lysates were heated at 70ºC for 10 minutes, diluted ten fold with IP buffer and subjected to immunoprecipitation using RGS-specific antibodies. Immunoprecipitation eluates were resolved by SDS-PAGE and the presence of ubiquitin conjugates was detected by Western blotting with anti-ubiquitin antibodies.

Pulse-chase metabolic labeling

Pulse-chase assays were conducted as previously described (50). NG108-15 or 293FT cells are grown in T-25 flasks and transfected with RGS7, RGS9-1, or RGS7/RGS9 chimera in the mammalian expression construct pcDNA3.1 (Invitrogen). Gβ5 was co-transfected with RGS proteins in all experiments.

Ex-vivo cultures of striatal slices

Striatal tissue was dissected from 1 mm thick coronal brain slices and immediately placed in culturing media (DMEM, 10% FBS, Penicillin/Streptomycin; Invitrogen). Striatal regions from one side of the brain were treated with the indicated protease inhibitor, with the contralateral side serving as vehicle control. Striatal slices were incubated for 5 hours at 37ºC with or without Leupeptin, E64 (Sigma), and lactacystin (Boston Biochem) and lysed in PBS, 150mM NaCl, 1% Triton. Total protein was normalized by concentration determined by BCA reagent (Pierce), and subjected to Western blot analysis.

Bioinformatics

Disorder predictions were done using a recently developed Various Short-Long version algorithm of the Predictor of Natural Disordered Regions (PONDR®-VSL1). This algorithm consists of an ensemble of logistic regression models that predict per-residue order-disorder (163, 164). Two models are used to predict either long or short disordered regions, greater or less than 30 residues, and the algorithm calculates a weighted average of these predictions, where the weights are determined by a meta-predictor that approximates the likelihood of a long disordered region within its 61-residue window. The output of the prediction is presented by a score ranging from 0 to 1 assigned to each residue which reflects its likelihood to adopt disordered conformation. The neutral probability score was set to 0.5.

♦ *Results*

Expression of RGS9-2 is co-induced with R7BP in late phase of neuronal differentiation.

We started examining the mechanisms that set RGS9-2 expression level by analyzing the change in its protein levels during the postnatal development of the mouse striatum. Data presented in Figure 3.1A reveal that RGS9-2 undergoes a striking pattern of late onset expression induction. Being virtually absent in neonatal tissues until approximately day 6 of postnatal development its levels dramatically increase to reach peak levels in adult animals. Interestingly, R7BP, an interaction partner of RGS9-2 exhibited an identical level of change in expression. A similar developmental expression profile was also observed for PSD-95, a postsynaptic scaffold of mature synapses, while other signaling proteins such as a striatal specific regulator of dopamine signaling, DARPP-32 (165) and Figure 3.1A), and the close RGS9-2 homolog RGS7, exhibited only modest changes in expression levels.

Co-immunoprecipitation experiments reveal that RGS9-2 forms a complex with R7BP as early as it becomes robustly detectable (around postnatal day 6), and that the extent of the complex formation is directly proportional to the increase in the protein levels of both proteins as the brain develops (Figure 3.1B). Quantitative analysis of the protein expression kinetics indicates that both R7BP and RGS9-2 follow identical patterns of exponential increase in expression resulting in approximately 200-fold increase in levels from the moment they first become detectable (Figure 3.1C).

Quantitative RT-PCR analysis revealed that at the mRNA level the expression kinetics of R7BP and RGS9-2 are substantially different (Figure 3.1D). The expression of both messages is

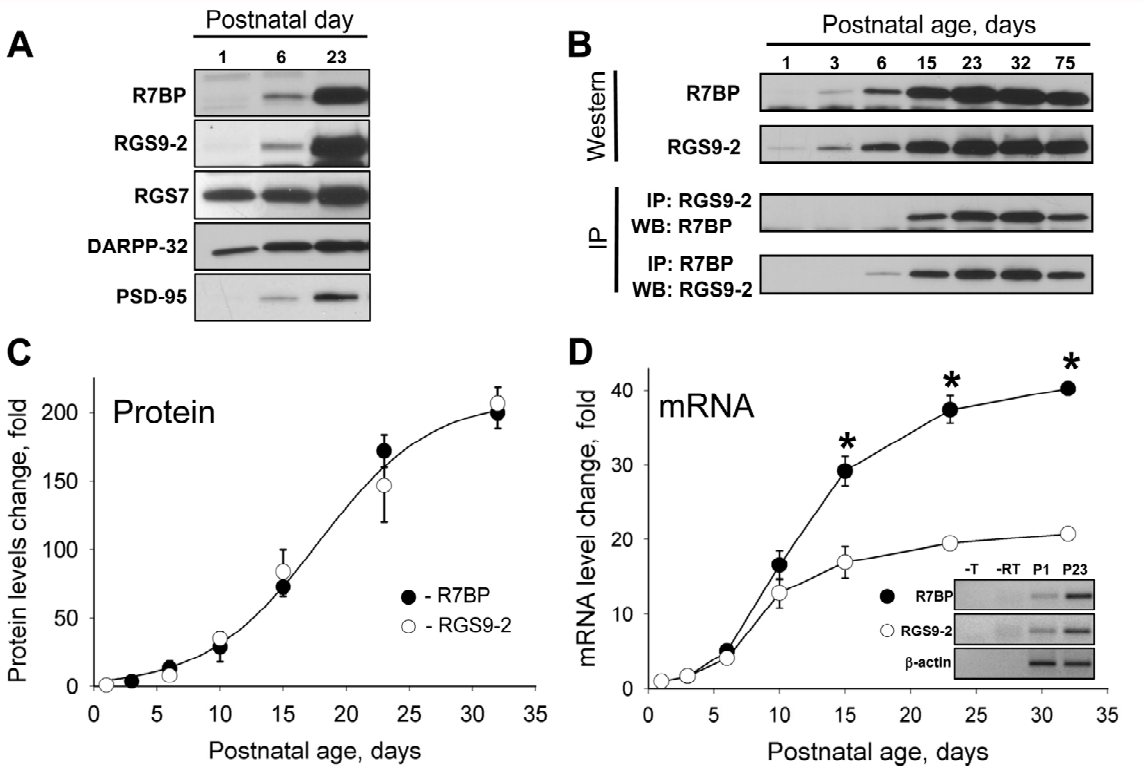

Figure 3.1: Co-regulation of RGS9-2 and R7BP expression during differentiation of striatal neurons. (**A**) Western blot analysis of change in protein expression level upon postnatal differentiation of striatum in Swiss-Webster mice. Striatal lysates (20 μg/lane) were analyzed for protein expression using specific antibodies. (**B**) Time-course of RGS9-2 and R7BP expression and their complex formation at the protein level. RGS9-2 and R7BP were immunoprecipitated and subjected to Western blot analysis. Immunoprecipitation efficiency in the experiments was greater than 90%. (**C**) Quantification of changes in levels of proteins from three separate groups analyzed as described in panel (B). Band densities were determined by ImageJ (NIH) software and used to determine changes in protein levels relative to day 1 as described in Materials and Methods. (**D**) Quantitative analysis of R7BP and RGS9-2 expression in development at mRNA level. Relative levels of RGS9-2 and R7BP mRNAs were measured by quantitative RT-PCR and normalized to the levels of β-actin mRNA amplified in parallel as an endogenous reference. Relative quantification algorithm was used where changes in amplification threshold were normalized to sample from postnatal day1. Data are averaged from three separate groups of animals. Insert shows gel electrophoresis of PCR products amplified from newborn (P1) or adult (P23) samples. No reverse transcriptase (-RT) or template (-RNA) was added in controls. Asterisks indicate statistically significant differences ($P<0.05$, t-test) between relative changes in R7BP and RGS9-2 mRNA.

very low in neonatal animals and their levels rise dramatically as animals develop. However, while R7BP mRNA essentially replicates exponential kinetics matching the change in its protein, the enrichment of RGS9-2 message stops much earlier. Even though the abundance of RGS9-2 mRNA does not substantially change after day 10, its protein levels still increases approximately 5- fold. In fact, the kinetics of RGS9-2 protein accumulation appear to follow the time course of R7BP mRNA synthesis, suggesting that the upregulation in RGS9-2 protein levels after day 10-15 of postnatal development is determined by R7BP availability.

RGS9-2 co-localizes with R7BP at postsynaptic sites of striatal neurons

The correlation of RGS9-2/R7BP late expression onset with that of major postsynaptic density organizer PSD-95, taken together with previously reported enrichment of both R7BP and RGS9-2 in postsynaptic densities (98) has prompted us to examine their fine subcellular localization at the ultrastructural level. We have first used a post-embedding immunogold labeling with specific antibodies against R7BP and RGS9-2. Although the post-embedding procedure is less sensitive and does not provide perfect ultrastructural preservation, it is the only suitable method for unequivocal localization of proteins at synaptic sites (see 166 for detailed discussion). Data presented in Figure 3.2 establishes that strong immuoreactivity for both R7BP and RGS9-2 is observed at postsynaptic densities of excitatory synapses where they are found to co-localize. To reveal the overall pattern of RGS9-2 and R7BP localization in neurons we further used a more sensitive procedure of pre-embedding immuno-gold electron microscopy (Figure 3.3). This method reveals that in addition to postsynaptic densities both RGS9-2 and R7BP are also present at the extrasynaptic plasma membrane of dendritic shafts and spines with some immunoreactivity localizing to pre-synaptic sites. Quantification of the data by counting immunogold particles (2,190 particles for RGS9-2 and 2,163 particles for R7BP) from 3 independent labeling experiments provided the following results: 1) 88% of RGS9-2 (1,752 particles) and 86% of R7BP (1,691 particles) was associated with plasma membrane while the remainder was found at intracellular membranes, 2) Immunoreactivity was predominantly found at postsynaptic sites (90.3% for RGS9-2 and 91.5% for R7BP) while only a small percentage localized presynaptically (9.7% for RGS9-2 and 8.5% for R7BP) and 3) Postsynaptic immunoreactivity was largely found in two places: dendritic shafts (966 particles or 61% for RGS9-2 and 977 or 63% for R7BP) and spines (616 particles or 39% for RGS9-2 and 570 or 37% for R7BP).

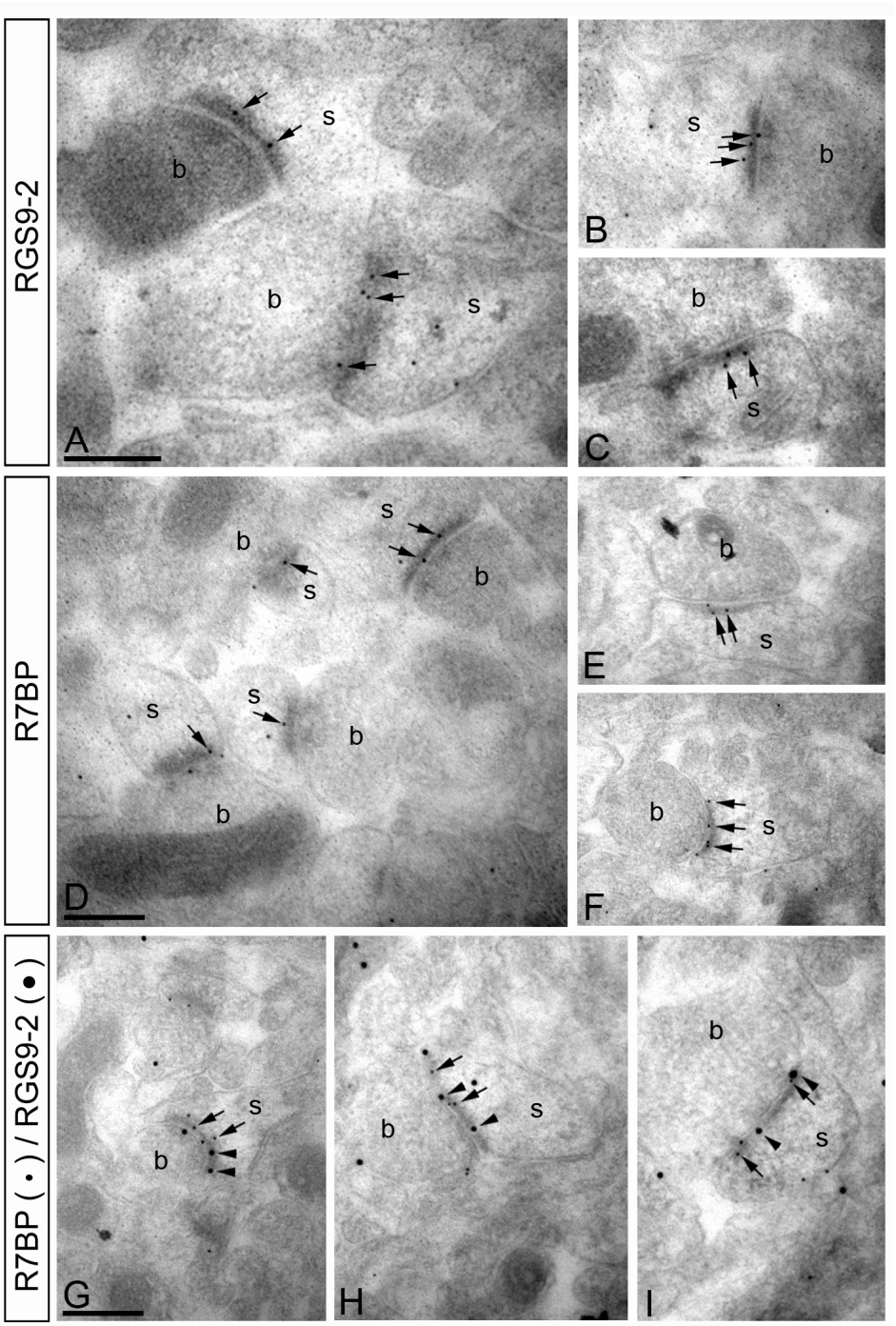

Figure 3.2: RGS9-2 and R7BP co-localize at postsynaptic densities of excitatory synapses. Electron micrographs of the striatum showing immunoreactivity for RGS9-2 and R7BP as detected using a post-embedding immunogold method. (**A-C**) Immunoparticles for RGS9-2 were found within the synaptic specialization of asymmetrical synapses (arrowheads). Gold particles were also observed at the extrasynaptic plasma membrane of spines (s) and to a lesser extent at presynaptic sites along the plasma membrane of axon terminals (b). (**D-F**) Similarly, immunoparticles for R7BP were found within the synaptic specialization of asymmetrical synapses (arrowheads). A few immunoparticles were also observed at the extrasynaptic plasma membrane of spines (s) and at presynaptic sites along the plasma membrane of axon terminals (b). (**G-I**) Double immunogold labelling showing co-localization of RGS9-2 (20 nm particles, arrowheads) and R7BP (10 nm particles, arrows) in individual synapses on spines (s) in the striatum. Scale bars: 0.2 μm.

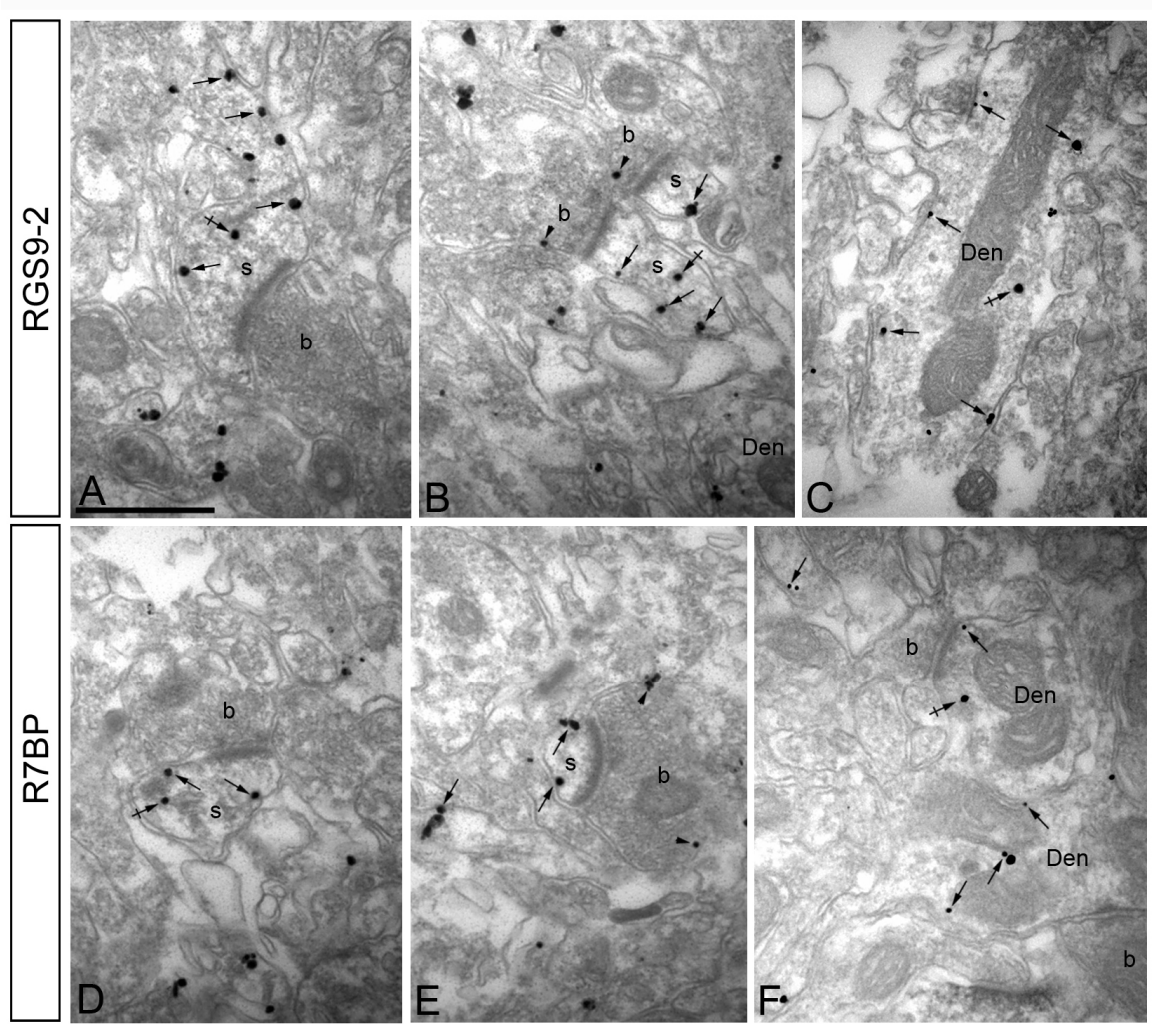

Figure 3.3: **RGS9-2 and R7BP share the same subcellular localization in striatum**. Electron micrographs of the striatum showing immunoreactivity for RGS9-2 (**A-C**) and R7BP (**D-F**), as detected using a pre-embedding immunogold method. (**A-C**) Immunoparticles for RGS9-2 were detected associated or close (arrows) to the extrasynaptic plasma membrane of dendritic shafts (Den) and dendritic spines (s) establishing excitatory asynapses with axon terminals (b). Some immunoparticles for RGS9-2 were also detected intracellularly (crossed arrows) associated with intracellular membranes of dendritic shafts and spines. To a lesser extent, RGS9-2 immunoparticles were detected at presynaptic sites associated with the plasma membrane of axon terminals (b) (arrowheads). (**D-F**) Immunoparticles for R7BP were detected associated or close (arrows) to the extrasynaptic plasma membrane of dendritic shafts (Den) and dendritic spines (s) establishing excitatory asynapses with axon terminals (b). Immunoparticles for R7BP were also detected intracellularly (crossed arrows) associated with intracellular membranes of dendritic shafts and spines. A few immunoparticles for R7BP were also detected at presynaptic sites associated with the plasma membrane of axon terminals (b) (arrowheads).

Knockout of R7BP results in a selective down-regulation of RGS9-2 expression and its subcellular mislocalization.

In order to directly test a possibility that R7BP is involved in setting the expression level of RGS9-2 *in vivo*, we generated R7BP knockout mice (Figure 3.4A). Targeting of the R7BP locus was confirmed by PCR (Figure 3.4B) and the lack of R7BP expression was confirmed at both protein (Figure 3.4C) and mRNA (Figure 3.4D) levels. Heterozygous animals contained approximately half of the R7BP mRNA and protein, demonstrating that R7BP protein levels are limited by the abundance of its mRNA. Strikingly, elimination of R7BP resulted in severe down-regulation of RGS9-2 protein (Figure 3.4C). Furthermore, reduction in R7BP levels in heterozygous mice also caused comparable reduction in the levels of RGS9-2. At the same time, both R7BP knockouts and heterozygous animals contained normal levels of RGS9-2 mRNA comparable to that of the wild-type littermates, indicating that elimination of R7BP did not affect the synthesis of the RGS9-2 message but rather destabilized the RGS9-2 protein by changing its susceptibility to proteolysis (50). Interestingly, knockout of R7BP did not have any statistically significant effect on the expression levels of RGS6, RGS7 or RGS11 (data not shown), which belong to the R7 family of RGS9-like proteins and were reported to form complexes with R7BP (76), (93). We have further investigated whether the observed reduction in RGS9-2 levels result from the inability of this protein to fold properly in the absence of its interaction with R7BP. This was done by monitoring RGS9-2 complex formation with its other binding partner, Gβ5, a process requiring appropriate post-translational processing of the complex. Data presented in Figure 3.4E reveal that RGS9-2 efficiently co-immunoprecipitated with Gβ5 when anti-Gβ5 antibodies were used in the assay. Quantification of data from three independent experiments demonstrated that the ratio of RGS9-2 between wild-type and R7BP knockout samples remained unchanged before and after the immunoprecipitation (8.9±1.7 before IP and 9.7±1.8 after the IP) indicating that the extent of RGS9-2 association with Gβ5 in R7BP knockout is equal to that observed in wild-type mice. Since RGS9-2 complex formation with Gβ5 was previously shown to be sufficient for its functional activity (32, 33, 78) we conclude that the elimination of R7BP has reduced the lifetime of RGS9-2•Gβ5 complex in the cell rather than affected its folding and/or assembly.

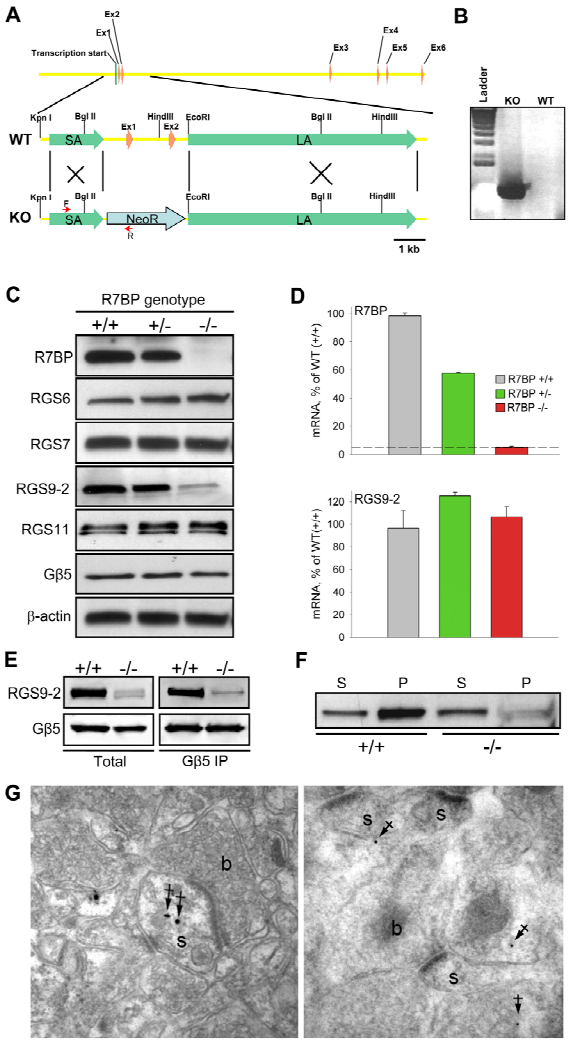

Figure 3.4: Knockout of R7BP selectively destabilizes RGS9-2 at post-transcriptional level. (**A**) R7BP gene structure and strategy for targeting homologous recombination. Targeting construct contained neomycin resistance cassette (NeoR) flanked by short (SA) and long (LA) homology arms. The positions of primers used to confirm the replacement are shown as red arrows. (**B**) Confirmation of homologous recombination in genomic DNA isolated from the founder animal (KO) as compared to wild-type parental strain (WT) by PCR. (**C**) Western blot analysis of protein expression in the brains of wild type (+/+), heterozygous (+/-) and R7BP knockout (-/-) mice. The blot shows a representative experiment out of three conducted. (**D**) Analysis of R7BP and RGS9-2 transcript levels by quantitative RT-PCR. Total mRNA was isolated from striatal regions of adult mice, quantified by UV spectroscopy and equal amounts were subjected to Q-RT PCR amplification. Each experiment was conducted with samples isolated from two to three mice. Dashed line indicates the limiting level for mRNA detection. *Error bars* represent S.E.M. (**E**) Immunoprecipitation of RGS9-2•Gβ5 complexes from wild-type and R7BP knockout striatal tissues. Extraction and immunoprecipitation with anti-Gβ5 antibody was conducted as described in Materials and Methods. 2 mg total protein was used in each immunoprecipitation experiment with 14 μg of anti-Gβ5 antibody. Equal protein amounts of whole cell extracts and volumes of the immunoprecipitation eluates were loaded in each well. The data are representative out of 3 experiments conducted. (**F**) Subcellular fractionation of striatal neurons into synaptic- and plasma- membrane containing pellet (P) and supernatant (S) containing primarily cytosol and small microsomal membranes. Striatal regions of wild type (WT) and R7BP knockout (R7BP KO) mice were homogenized and subjected to one step centrifugation as described in Materials and Methods. Knockout samples were loaded at four time excess of total protein over wild-type samples. (**G**) Pre-embedding (left) and post-embedding (right) immunogold EM analysis of RGS9-2 localization in striatum of R7BP knockout mice. Closed arrows indicate location of immunogold particles at intracellular sites, a predominant localization pattern of RGS9-2 in neurons of R7BP knockouts.

The presence of low levels of RGS9-2•Gβ5 in R7BP knockouts also made it possible to address the question whether R7BP is important in driving the localization of RGS9-2 *in vivo*. We first addressed this question by performing subcellular fractionation of brain lysates into membrane containing pellet and cytosol containing supernatant (Figure 3.4F). We found that while in wild-type striatal neurons most of RGS9-2 was associated with membrane fraction, in the R7BP knockout neurons RGS9-2 is predominantly cytoplasmic. This observation was further confirmed by immunogold labeling of RGS9-2 in the striatum of R7BP knockout mice. Figure 3.4G indicate that RGS9-2 immunoreactivity was never found in postsynaptic densities, but rather was predominantly located at various intracellular sites in the spines and cell bodies. Taken together, these results demonstrate that in addition to being essential for maintaining high expression levels of RGS9-2, R7BP is also responsible for the localization of RGS9-2•Gβ5 complex to postsynaptic sites in native neurons.

Overexpression of R7BP in vivo leads to selective up-regulation of RGS9-2 expression.

We next directly tested whether the availability of R7BP limits the expression of RGS9-2 and whether an increase in R7BP levels would be sufficient to augment RGS9-2 expression. To address this question we delivered an R7BP lentivirus (Figure 3.5A) into the striatum via stereotaxic injection (Figure 3.5B). Data presented in Figures 3.5C and 3.5D illustrate that we were able to achieve about 50% overexpression of R7BP. Importantly, elevation in R7BP levels resulted in marked increase in levels of RGS9-2 but not other R7 RGS proteins. Although no statistical significance was detected, it is curious that over-expression caused larger change in RGS9-2 levels as compared to R7BP (2-fold vs. 1.5-fold). This is likely explained by the lower levels of endogenous RGS9-2 as compared to R7BP, which is present in excess over RGS9-2 as it additionally forms complexes with other R7 family members.

Selective degradation of RGS9-2 is mediated by its R7BP binding site.

Knockout and overexpression data (Figures 3.4 and 3.5) argue that the effect of R7BP on protein expression level is specific for RGS9-2 among all other R7 RGS protein members that form complexes with R7BP. We therefore hypothesized that the selective regulation of RGS9-2 expression by R7BP results from its higher susceptibility to degradation among the R7 family. We tested this hypothesis by comparing proteolytic degradation rates of RGS9-2 and RGS7, a representative R7 RGS protein that is not regulated in its expression by R7BP. To simplify the

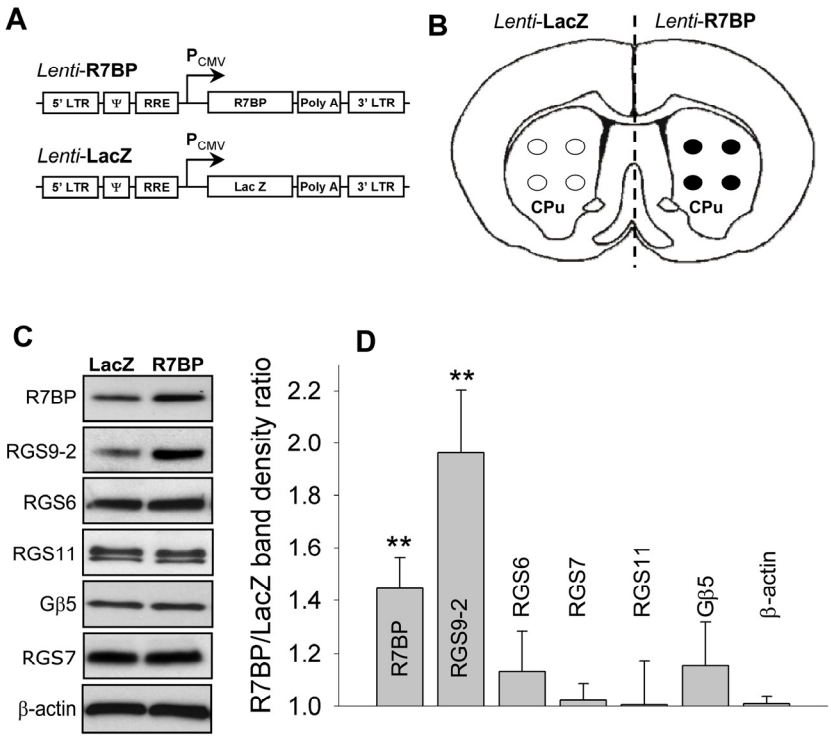

Figure 3.5: Lentivirus-mediated over-expression of R7BP in the striatum. (A) Schematic representation of lentiviral constructs used for the expression experiments. Open reading frames for R7BP or LacZ were placed under the control of strong CMV promoter in the context of lentiviral packaging elements (LTR, Ψ and RRE). (B) Strategy for the lentivirus mediated protein expression *in vivo*. Each side of the brain received four injections with either R7BP or control LacZ lentiviruses within the caudate/putamen region (CPu). (C) Western blot analysis of protein expression in the CPu induced following lentiviral transduction. (D) Quantification of Western blot data shown in panel (C) from three independent experiments. Band densities were determined by densitometry and used to calculate the ratio of band intensity between R7BP side to LacZ side. Asterisks mark statistically significant changes ($p<0.01$, t-test) in the levels of proteins as compared to changes in β-actin expression (last bar). *Error bars* are S.E.M.

analysis, we used the short isoform (RGS9-1) which is the closest in its amino-acid sequence to RGS7 yet has the same degradation rate as RGS9-2 (50). Pulse-chase metabolic labeling experiments (Figure 3.6A) reveal that in contrast to an unstable RGS9-1•Gβ5 complex (half-time to degradation 39.7±5 min) the complex of RGS7 with Gβ5 is about 10 times more stable (half-time to degradation 462±75 min).

Because protein modification by ubiquitination is a major cellular mechanism for selective targeting of proteins to degradation, we next checked whether RGS9-2 and RGS7 are differentially ubiquitinated. Figure 3.6B shows that without Gβ5, both RGS9-2 and RGS7 are heavily poly-ubiquitinated. However, co-expression with Gβ5 completely abolishes RGS7 ubiquitination. Yet Gβ5 only had a modest effect on the RGS9-2 ubiquitination, which was only significantly reduced in the presence of R7BP (Figure 3.6B). Ubiquitination of RGS7 when expressed alone was reported in the past (118) and its prevention by Gβ5 observed in our study correlates very well with the requirement of the entire R7 RGS family to be associated with Gβ5 for their folding and stability (35, 73, 79). The inability of Gβ5 to fully prevent RGS9 ubiquitination and decrease its degradation rate suggests a presence of secondary instability elements in this protein that are controlled by the association with R7BP. To identify such elements, we employed a chimeric mutagenesis approach exploiting the homologous nature of RGS9-1 and RGS7. We reciprocally replaced conserved domains between these proteins and analyzed the stability of the resulting chimeras in the pulse chase degradation assays in the presence of Gβ5 (Figure 3.6C). Quantification of the data shows that replacing the DEP domain of RGS9 with that of RGS7 partially rescues RGS9-1 instability, and an additional replacement of the R7H domain makes chimeric RGS9•Gβ5 in the absence of R7BP as stable as RGS7. Conversely, replacing either N-terminal DEP domain or DEP in combination with R7H in RGS7 dramatically destabilized this protein. This result parallels with our previous study, where the binding site for R7BP in R7 RGS proteins was mapped to be formed by both DEP and R7H domains of R7 RGS proteins (50). This suggests that R7BP exerts its degradation protective effects by masking the unique instability element(s) in RGS9-2 located within its R7BP binding site.

Multiple determinants at the N-terminus target RGS9-2 to degradation by cysteine proteases.

In order to gain insights into possible structural characteristics of the instability elements within DEP/R7H domain of RGS9-2 we performed a comparative sequence analysis between RGS7 and RGS9-2. First, RGS9-2 and RGS7 were analyzed for the presence of naturally

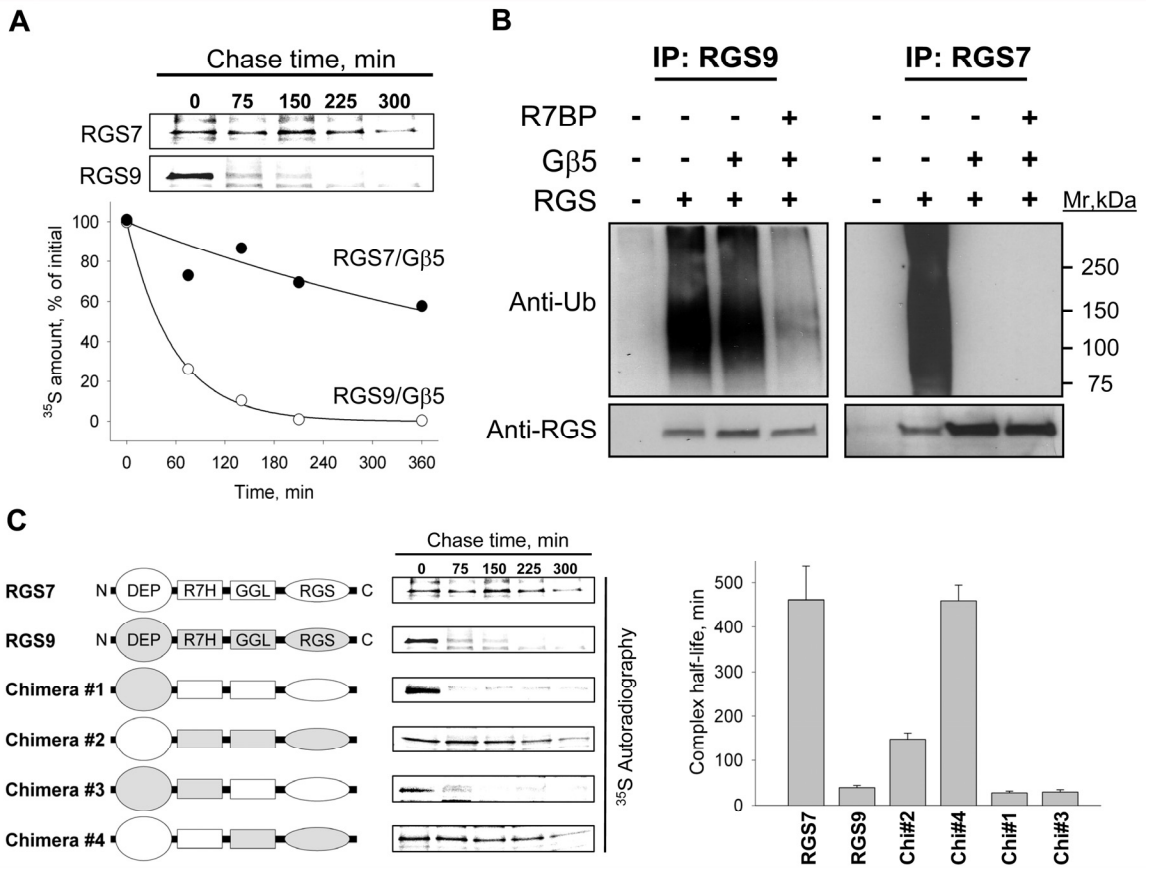

Figure 3.6: Selective degradation of RGS9-2•Gβ5 in the absence of R7BP is determined by N-terminal instability elements. (**A**) Pulse-chase metabolic labeling experiments comparing degradation rates of RGS7 and RGS9-1 in 293FT cells. The blot shows the time-course of ^{35}S-Met/Cys dissipation from imunoprecipitated RGS proteins, quantified on a graph below. About 25% of recombinant proteins was recovered in the immunoprecipitation eluates. (**B**) Detection of RGS protein modification with ubiquitin in transfected 293FT cells. Upper panel: Ubiquitination of RGS7 or RGS9-2 in the presence or absence of Gβ5 and R7BP was detected by Western blotting with anti-ubiquitin antibodies following protein immunoprecipitation with specific anti-RGS antibodies (~25% immunoprecipitation efficiency). Lower panel: Western blot detection of respective RGS protein from same immunoprecipitation fractions. (**C**) Proteolytic stability of RGS7/RGS9 chimeras as determined by pulse-chase metabolic labeling experiments. Right panel shows quantification of protein half-life calculated from exponential fitting of degradation time course. *Error bars* are S.E.M.

disordered regions, predominantly unstructured segments within proteins or domains that are increasingly accepted to underlie much of the functional flexibility in proteins and serve as sites for posttranslational modifications and for association with interaction partners and ligands (167, 168). We reasoned that a higher probability for the presence of these regions in RGS9-2 as compared to RGS7 might account for the observed differences in their proteolytic stability, for example, by providing recognition sites for cellular degradation machinery. Analysis of disordered prediction profiles shows that both RGS7 and RGS9 have a very similar pattern of distribution for local minimums and maximums of disorder scores along the DEP/R7H domains (Figure 3.7A). However, peak scores and the number of regions which exceeded the disorder threshold were significantly greater in RGS9-2.

The second noticeable feature that distinguishes RGS9-2 is the high occurrence of so called 'KFERQ-like' motifs which are short (5-6 amino acid long) sequences that have the unusual combination of oppositely charged amino acids with hydrophobic residues and glutamates. Occurrence of these motifs in proteins is linked to their increased instability mainly by routing them to the lysosomal degradation pathway (169). The DEP/R7H domains of RGS9-2 contain 6 KFERQ-like sequences, while in contrast, only 1 such motif is present in RGS7. Superimposing positions of the KFERQ-like motifs over the disorder prediction profiles reveal that most of these sequences in RGS9 are localized to disorder peaks (Figure 3.7A), while the only KFERQ motif present in RGS7 localized to a region of low disorder score.

Our next step was to test whether the prediction of KFERQ lysosomal degradation targeting sequences in RGS9 would be consistent with the main pathway of its degradation in cells in the absence of R7BP. Culturing striatal slices in the presence of cysteine protease inhibitors (E64 and Leupeptin), which are the major destruction enzymes of lysosomes, potently prevent RGS9-2 degradation in R7BP knockout tissues (Figure 3.7B). In contrast, the specific proteasome inhibitor lactacystin had no effect on rescuing RGS9-2 levels. Furthermore, inhibitors had similar effects on the levels of the intact RGS9-2•R7BP complex in wild type slices suggesting that even in the presence of R7BP the regulation of RGS9-2 levels is dynamic. The effect is specific for RGS9-2•R7BP since it does not affect the levels of other R7 RGS proteins. These results suggest that the degradation of the RGS9-2•R7BP complex in native neurons is mainly controlled by cellular cysteine proteases (lysosomal pathway), rather than by proteasome.

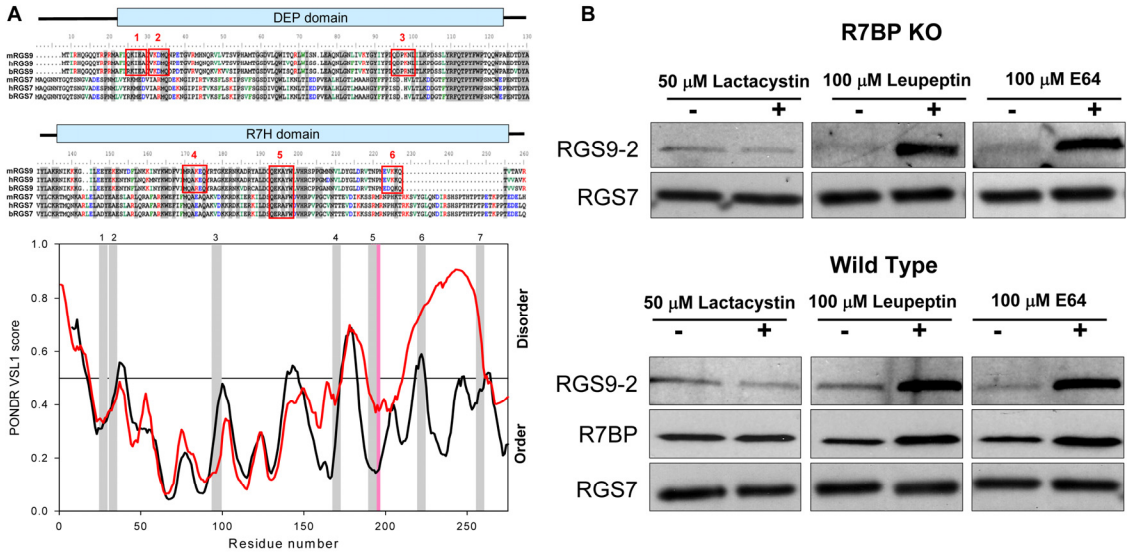

Figure 3.7: Degradation determinants and route of RGS9-2 proteolysis. (**A**) Prediction of RGS9-2 instability elements. Upper panel: multiple sequence alignment of RGS9 and RGS7. Shaded areas indicate conserved regions, red boxes mark the positions of KFERQ-like sequences. Lower panel: prediction of naturally disordered regions in N-terminal domains of RGS9 (black traces) and RGS7 (red traces) by PONDR-VSL1 algorithm. Positions of KFERQ-like motifs are marked by gray (RGS9) or pink (RGS7) bars. (**B**) Effect of protein degradation inhibitors on RGS9-2 levels. Striatal slices from wild type or R7BP knock-out mice were cultured *ex vivo* for 5 hours in the presence or absence of indicated inhibitors after which protein levels were determined by Western blotting. Note that wild type and knockout blots were exposed for different times to reveal the extent of protein up-regulation by inhibitors rather than differences in RGS9-2 levels between knockout and wild type samples.

The stability of R7BP is reciprocally controlled by its association with R7 RGS proteins.

Further, we observed that the inhibition of proteolysis in wild type slices led not only to RGS9-2 upregulation but also to an increase in R7BP levels (Figure 3.7B, lower panel). This suggested the possibility that R7BP could also be an unstable protein whose stability might be in turn controlled by protein-protein interactions. We first tested this possibility by analyzing the stability of R7BP in transfected cells. Co-transfection with either RGS9-2•Gβ5 or RGS7•Gβ5 markedly increased the expression level of R7BP (Figure 3.8A). Pulse-chase degradation experiments (Figure 3.8B) revealed that like RGS9-2, R7BP is rapidly degraded (half-time to degradation is 114±18 min) but is greatly stabilized when co-expressed with an R7 RGS protein. In fact, no significant degradation of R7BP•RGS7•Gβ5 complex was observed during the time course of an experiment (half time to degradation >48 hours). This observation predicts that interaction with R7 RGS proteins is essential for the stable expression of R7BP. Indeed, analysis of protein expression in Gβ5 knockout animals which lack all four R7 RGS proteins (79), no detectable R7BP could be found in the striatum (Figure 3.8C). Elimination of RGS9-2 from the striatum did not significantly affect the level of R7BP suggesting that in the absence of RGS9-2, R7BP is stabilized by association with other R7 family members which bind to this protein in the same striatal neurons. Interestingly, R7BP appears to be unique in its requirement of RGS protein association for stable expression since a homologous protein, R9AP, which serves to anchor RGS9-1 and RGS11 in the retina (170) have normal expression levels in the Gβ5 knockout.

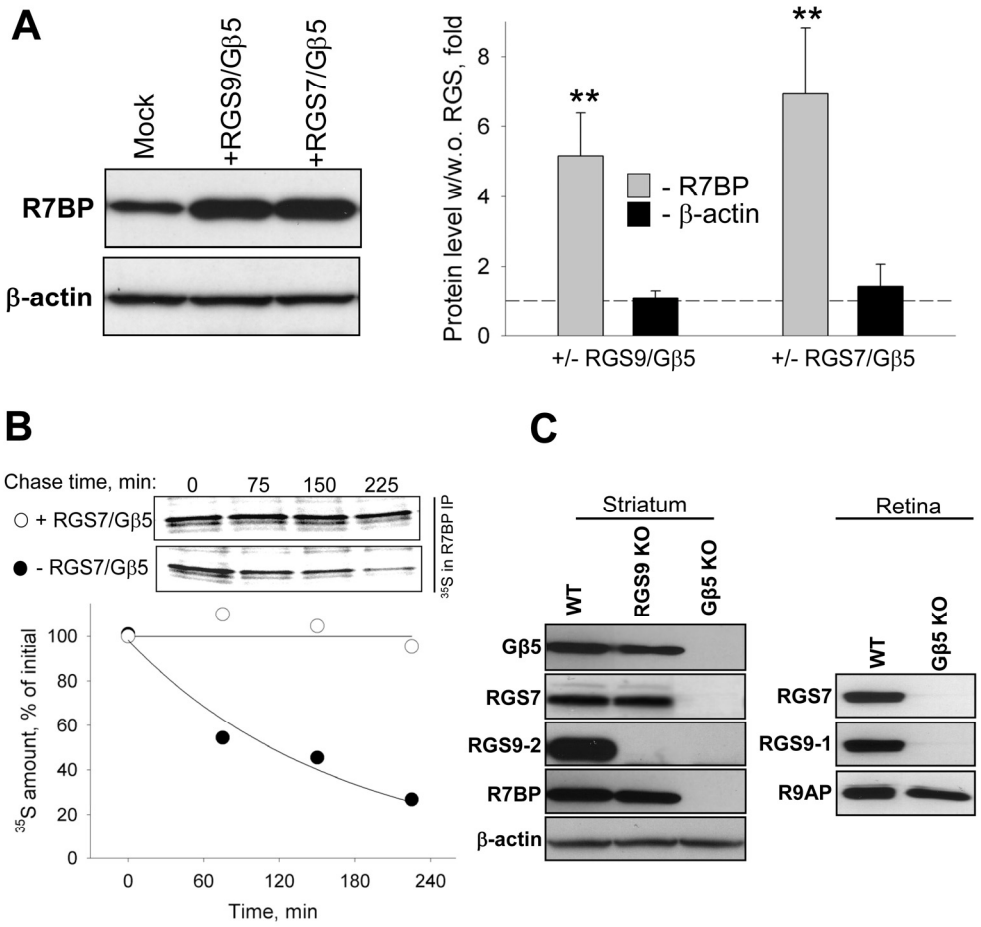

Figure 3.8: R7BP degradation is reciprocally regulated by complex formation with R7 RGS•Gβ5 proteins. (**A**) Co-transfection with RGS7•Gβ5 and RGS9-2•Gβ5 augment R7BP expression. 293FT cells were transfected with R7BP either alone (mock) or in combination with the indicated RGS construct and Gβ5. Right panel shows quantification of changes in protein levels from three independent experiments. Asterisks indicate statistically significant differences in R7BP levels with and without co-expression with R7 RGS proteins ($p<0.01$, t-test). (**B**) RGS7•Gβ5 slows down the rate of R7BP proteolysis as determined by pulse- chase degradation assays. (**C**) Effect of Gβ5 knockout on the expression of R7BP and R9AP in striatum and retina. Tissue lysates containing equal protein concentrations were analyzed by Western blotting with the indicated antibodies.

♦ ***Discussion***

In this study we propose a mechanism for the regulation of the expression and localization of the key regulator of dopamine and opioid receptor signaling in the brain. In this mechanism, RGS9-2 expression level in the striatum is set by posttranslational regulation acting to rescue the protein from constitutive degradation. RGS9-2 belongs to the R7 RGS family, members of which have been found to form macromolecular complexes with two binding partners: Gβ5 and R7BP. Association with Gβ5 is required for the folding of all R7 RGS proteins which as a result, exist as constitutive RGS-Gβ5 heterodimers (35, 74, 79). In turn, association of RGS9-2•Gβ5 complex with R7BP was shown to increase the proteolytic stability of the complex (50). Here we used genetic knockout and overexpression strategies to demonstrate that unlike Gβ5, R7BP selectively regulates the expression levels of RGS9-2 but not other R7 RGS protein complexes *in vivo*. We found that in the absence of R7BP, RGS9-2 is translated and forms complexes with Gβ5, but is destined to be quickly degraded by the cell's proteolytic machinery. The binding site for R7BP in RGS9-2 contains specific instability elements that target it for proteolysis by cysteine proteases. Binding of R7BP masks these degradation determinants and results in elevation of RGS9-2 expression. The instability elements are absent in other homologous R7 RGS proteins, allowing them to be stably expressed independently from R7BP association. Consequently, the expression level of the RGS9-2•Gβ5 signaling complex is determined by the availability of R7BP and is not dependent on the synthesis of RGS9-2 mRNA. Interestingly, a similar posttranslational mechanism also appears to regulate the expression of the short splice isoform, RGS9-1 whose levels in photoreceptors are determined by the R7BP homologue, R9AP (20, 107).

Comparative bioinformatics analysis of RGS9-2 revealed a unique combination of sequence features in the R7BP binding site, DEP/R7H domain, that confer higher susceptibility to degradation. First, this region of RGS9-2 has a high probability of local disordered regions which are increasingly viewed as hot spots of posttranslational protein modification as well as sites for association with ligands and binding partners (167, 168, 171). Second, most of the RGS9-2 regions with high disorder prediction also display unique composition of positively and negatively charged as well as hydrophobic residues in conjunction with glutamines known as KFERQ-like motifs. Although DEP/R7H domains are conserved in R7 RGS proteins, this specific combination of determinants is a unique feature of RGS9-2. Notably, KFERQ-like motifs were previously reported to target proteins to degradation mainly via the lysosomal

pathway (169, 172). Consistent with these reports, our data indicate that in the absence of R7BP, degradation of RGS9-2 in striatum is prevented by the inhibition of cysteine proteases of the lysosomes, but not by the specific inhibition of the proteasome. Although the present study does not unequivocally demonstrate how targeting of RGS9-2 for lysosomal degradation is accomplished, two possibilities emerged from our studies. One possibility revealed by bioinformatics analysis was the presence of disordered regions within RGS9-2 correlating with KFREQ motifs, which could serves as chaperone mediated binding sites for entry into lysosomes (173). Alternatively, another lysosomal targeting signal could be accomplished by ubiquitination within DEP/R7H disordered regions of RGS9-2, as recent data suggests that such regions could underlie ubiquitin attachment sites (171, 174). Further, it is becoming increasingly accepted that protein ubiquitination is involved in targeting some proteins for lysosomal degradation rather than to the proteasome (175, 176). Although in this study we show that in transfected cells RGS9-2 can be ubiquitinated, the importance of this modification for targeting RGS9-2•Gβ5 degradation in striatal neurons remains to be elucidated.

The second main finding of this work is that the RGS9-2•Gβ5•R7BP complex shows striking developmental co-regulation. Both RGS9-2 and R7BP are virtually absent in the brains of neonatal mice and are rapidly induced at late stages of postnatal neuronal differentiation. Similar expression time course is observed for a few postsynaptic proteins that are involved in the elaboration of the synaptic organizing characteristic of differentiated neurons such as NR2A, PSD-95, and PSD-93 (177, 178). In contrast, many proteins such as DARPP-32, GluR1, SAP102 that are involved in constitutive signaling at synapses are normally expressed from early embryonic stages and exhibit rather modest upregulation (177, 178). Provocatively, this suggests that the RGS9-2•R7BP complex is involved in setting signaling characteristics of the mature nervous system. Consistent with this idea, we found that both RGS9-2 and R7BP co-localize at postsynaptic densities of excitatory synapses. Importantly, this localization of the complex is mediated by R7BP, as RGS9-2 is completely absent from the postsynaptic densities of R7BP KO striatum. This result taken together with the importance of R7BP complex formation with RGS9-2 for its stabilization, ensures this localization pattern for RGS9-2. In addition to localizing RGS9-2, R7BP may also be important for targeting other R7 RGS proteins such as RGS6, RGS7, RGS11, with which it associates, to postsynaptic sites upon nervous system development.

The described posttranslational mechanism of RGS9-2 expression and localization regulation by R7BP has several implications. First, it suggests that RGS9-2 levels could be regulated by attenuation of the lysosomal degradation pathway, perhaps, as part of the cellular

response to receptor activation. Second, it suggests that changes in R7BP concentration provide a new regulatory input for modulating the sensitivity of dopamine and opioid receptor signaling set by RGS9-2. Third, the mechanism provides the specificity for the rapid alteration in concentration of one regulator amongst highly similar homologues. Fourth, the mechanism ensures that at the postsynaptic density RGS9-2•Gβ5 functions only in complex with R7BP. Fifth, the elimination of R7BP in Gβ5 knockout mice indicates that R7BP is unlikely to have any independent signaling roles outside of its complex with R7 RGS proteins.

Acknowledgments:

We thank Dr. William Simonds (NIH) for the generous gift of anti-RGS7 and anti-Gβ5 antibodies and Dr. Sheila Baker for critical comments on the manuscript. This work was supported by NIH grants EY018139 and DA021743 (to KAM), MH61933 (to KW), EY013811 (to CKC) and DA 011806 (KAM and KW), the Graduate School and Academic Health Center at the University of Minnesota (to KAM), grant from the Spanish Ministry of Education and Science (BFU-2006-01896) to RL.

Chapter 4 - Changes in striatal signaling induce remodeling of RGS complexes containing Gβ5 and R7BP subunits

Garret R. Anderson[1], Rafael Lujan[2], and Kirill A. Martemyanov[1]

[1]Department of Pharmacology, University of Minnesota, Minneapolis, MN 55455, USA
[2]Departamento de Ciencias Médicas, Facultad de Medicina*, Universidad de Castilla-La Mancha, 02006 Albacete, Spain*

Content taken from the published manuscript:

Anderson G.R., Lujan R., Martemyanov K.A. Changes in striatal signaling induce remodeling of RGS complexes containing Gβ5 and R7BP subunits. *Molecular and Cellular Biology*, 2009. Jun 29, (11):3033-44.

Specific contributions: GRA data presented in Figures 4.1, 4.2, 4.4, 4.5, 4.6, 4.8, 4.9.

Neurotransmitter signaling via G protein coupled receptors is crucially controlled by Regulators of G Protein Signaling (RGS) proteins that shape the duration and extent of the cellular response. In the striatum, members of the R7 family of RGS proteins modulate signaling via D2 dopamine and μ-opioid receptors controlling reward processing and locomotor coordination. Recent findings have established that R7 RGS proteins function as macromolecular complexes with two subunits: G beta, type 5 (Gβ5) and R7 Binding Protein (R7BP). In this study we report that subunit composition of these complexes in striatum undergoes remodeling upon changes in neuronal activity. We found that under normal conditions two equally abundant striatal R7 RGS proteins, RGS9-2 and RGS7, are unequally coupled to the R7BP subunit which is present in complex predominantly with RGS9-2 rather than with RGS7. Changes in the neuronal excitability or oxygenation status resulting in extracellular calcium entry, uncouples RGS9-2 from R7BP, triggering its selective degradation. Concurrently, released R7BP binds to mainly intracellular RGS7 and recruits it to the plasma membrane and the postsynaptic density. These observations introduce activity dependent remodeling of R7 RGS complexes as a new molecular plasticity mechanism in striatal neurons and suggest a general model for achieving rapid posttranslational subunit rearrangement in multi-subunit complexes.

♦ *Introduction*

Members of the Regulator of G protein Signaling (RGS) family are ubiquitous negative regulators of signal transmission via G protein coupled receptors (GPCR). RGS proteins act to limit the extent and duration of GPCR signaling by accelerating the GTP hydrolysis rate on the α subunits of heterotrimeric G proteins, thus promoting their inactivation (see 10, 149 for review). The action of RGS proteins is essential for normal functioning of a wide range of fundamental processes including cell division (179), neuronal excitability (180), photoreception (88), angiogenesis (181), vasoconstriction (182) and many others.

R7 RGS subfamily is one out of six distinct groups of more than 30 diverse RGS proteins (10, 183). This subfamily is comprised of four proteins: RGS6, RGS7, RGS9 and RGS11 with similar multi-domain organization (10, 183) and predominant neuronal expression pattern (30). Studies in mice indicate that R7 RGS proteins crucially regulate several critical aspects of

nervous system function such as vision (148, 184), motor control (111, 135) and nociception (28, 29, 141) placing a significant emphasis on the elucidation of their mechanisms.

A unique property of R7 RGS proteins is their constitutive association with the type 5 G protein beta (Gβ5) subunit (46, 47). Binding to a G protein gamma-like domain (GGL) in the core of R7 RGS proteins (185), Gβ5 is tightly integrated into the structure of the RGS molecule (48). The ability to form complexes with Gβ5 was shown to be essential for folding and stability of R7 RGS proteins (32, 35) and knockout of Gβ5 in mice results in complete abrogation of expression of all four R7 RGS proteins (79). More recent studies revealed that, in addition to Gβ5, R7 RGS proteins bind to a two-member family of SNARE-like membrane proteins: R7 family Binding Protein (R7BP) (76, 93) and RGS9 Anchor Protein (R9AP) (91, 170) which interact with the DEP/R7H domain of the RGS proteins and constitute the third subunit in the complex.

The role of R7BP/R9AP proteins is perhaps best studied for the R7 RGS subfamily member, RGS9. This RGS protein exists in two splice variants exhibiting very restricted and non-overlapping expression pattern (52, 186). The short splice isoform, RGS9-1 is expressed exclusively in photoreceptors (88) where it sets the timing of phototransduction cascade recovery from the light excitation (125). The long splice isoform is mostly found in the striatum region of the brain (54, 57, 186) and regulates the duration of the G protein signaling through D2 dopamine (27, 111) and μ-opioid receptors (28, 131). Accordingly, knockout of RGS9 in mice results not only in deficits in light adaptation (13) but also affects striatal control of movement and reward (27, 28, 111, 135). We have previously shown that both R9AP and R7BP play crucial roles for both targeting and expression of RGS9 splice isoforms. While retina specific R9AP delivers RGS9-1 to the specific subcellular compartment, the outer segment of photoreceptors (89), R7BP is indispensable for targeting RGS9-2 to the postsynaptic densities of striatal neurons (92). Furthermore, knockout of either R9AP (107) or R7BP (92) leads to severe down-regulation in RGS9 protein levels in retina and striatum, respectively. It has been proposed that exposure of specific degradation determinants normally shielded by R7BP/R9AP tag RGS9•Gβ5 to degradation by cellular cysteine proteases, and that balance of RGS9•Gβ5 association with R7BP/R9AP sets its expression levels *in vivo* (20, 92, 107).

Striatal neurons contain multiple R7 RGS proteins that bind to R7BP, however only RGS9-2 requires R7BP for its expression (50, 92). In turn, R7BP itself is an unstable protein and is eliminated upon ablation of all R7 RGS proteins (92, 100). Interestingly, knockout of only RGS9 does not affect the stability of R7BP (92) suggesting that multiple striatal R7 RGS•Gβ5 complexes are pivoted by R7BP to allow several possibilities for subunit composition.

The goal of the present study was to investigate the principles and factors that regulate coupling of R7 RGS•Gβ5 complexes to R7BP in striatal neurons. We report that in the striatum, R7BP mainly exist in complex with two RGS complexes: RGS9-2•Gβ5 and RGS7•Gβ5. However, despite the equimolar amounts of these RGS proteins in striatal neurons, R7BP is coupled preferentially to RGS9-2•Gβ5, whereas the majority of RGS7•Gβ5 is free from R7BP due to its substantially lower binding affinity. As a result, RGS9-2•Gβ5 complex is targeted by R7BP to the plasma membrane while RGS7•Gβ5 is predominantly found at the intracellular sites. Strikingly, we find that this background complex composition undergoes dramatic remodeling upon which R7BP re-couples to RGS7 to recruit it to the plasma membrane and the postsynaptic density. This remodeling involves selective proteolytic degradation of RGS9-2 during which it uncouples from R7BP. We report that RGS9-2 degradation is controlled by signaling pathways that mediate synaptic activity and oxygen sensing, converging at an elevation of intracellular $Ca2^{+}$ via extracellular $Ca2^{+}$ entry. These findings suggest a novel plasticity mechanism for dynamically regulating subunit composition for major G protein signaling regulators in striatum depending on changes in synaptic activity.

- ***Materials and Methods***

Antibodies, recombinant proteins and DNA constructs - Generation of sheep anti-R7BP NT (76), and sheep anti-RGS9-2 CT (76) has been described previously. Rabbit anti-RGS7 (7RC1), rabbit anti-R7BP (TRS) and anti-Gβ5 (SGS) were generous gifts from Dr. William Simonds (NIDDKD/NIH). All custom generated antibodies were tested for the specificity to ensure that (1) they recognize single major band in brain extracts corresponding to size of detection subject, (2) their immunoreactivity is blocked by peptide containing specific epitope sequence and (3) antibodies efficiently performed in immunoprecipitation reactions and the identity of precipitated band was confirmed by mass-spectrometry. Recombinant his-tagged and GST-tagged R7BP were expressed in *E.coli* and affinity purified on Ni-NTA beads (Qiagen) as previously described (50, 76). RGS7 and RGS9-2 were expressed in Sf-9 insect cells together with Gβ5 via baculoviral mediated delivery and recombinant complexes were purified by Ni-NTA chromatography utilizing his-tag present at the N-termini of RGS proteins as described (76). Protein concentration was determined by BCA kit (Pierce) and adjusted to reflect protein purity (ranging between 55% and 90%) determined by densitometry of Coomasie stained gels.

Urea-treated bovine rod outer segment membranes (uROS) were obtained as described (187). The plasmid encoding His_6-$G\alpha_{o1}$ was a gift from Dr. N.O. Artemyev; the plasmid encoding His_6-$G\alpha_{i1}$

was a gift from Dr. N.P. Skiba; both recombinant proteins were purified from E. coli as described (188). $G\alpha_t$ and $G\beta_1\gamma_1$ subunits were purified from bovine retinas as described (189).

Preparation of brain extracts, immunoprecipitation, and Western blotting - Cellular lysates were prepared by homogenizing brain tissue by sonicating in immunoprecipitation (IP) buffer composed of PBS (pH=7.4, Fisher) supplemented with an additional 150 mM NaCl, 1% Triton X-100 and Complete protease inhibitors (Roche), followed by 15 minute centrifugation at 14,000 x *g*. The resulting extract was used for protein concentration determination by BCA assay (Pierce, Rockford, IL). This Triton X-100 extraction procedure yields >90% extraction efficiency of proteins under investigation and was followed for both direct immunoblot and immunoprecipitation experiments. Immunoprecipitation of R7BP was performed using 3 μg of sheep anti-R7BP NT antibody, 10 μl of protein G beads (GE Healthcare, Little Chalfont, UK), added to the extracts. The mixtures were incubated for 1 h, washed three times with IP buffer, and proteins bound to the beads were eluted with SDS sample buffer. Samples were resolved on SDS-PAGE gel, transferred onto PVDF membrane and subjected to Western blot analysis using HRP conjugated secondary antibodies and ECL West Pico (Pierce) detection system. Western blots that were quantified, were subjected to analysis of specific bands performed on an Odyssey Infrared Imaging System (LI-COR Biosciences) according to the manufacturer's protocols using IRDye 680 and IRDye 800 labeled secondary antibodies.

Cell Culture and Transfections - 293FT cells were obtained from Invitrogen and cultured at 37 °C and 5% CO_2 in DMEM supplemented with 100 units/ml of penicillin, and 100 μg/ml of streptomycin, 10% fetal bovine serum, 4 mM L-glutamine, and 1 mM sodium pyruvate. Cells were transfected at ~70% confluency, using Lipofectamine LTX reagent (Invitrogen) according to the manufacturer's protocol. The ratio of Lipofectamine to DNA used was 6.25 μl : 2.5 μg per 10 cm^2 of cell surface. A constant level of R7BP-pcDNA3.1 (0.2 μg) vector was co-transfected with an excess of Gβ5-pcDNA3.1 (1.2 μg), variable RGS7-pcDNA3.1 and RGS9-2-pcDNA3.1, balanced with empty pcDNA3.1 vector. The quantity of RGS7-pcDNA3.1 (1 μg) and RGS9-2-pcDNA3.1 (0.2 μg) vector necessary to establish a 1:1 protein expression level was determined by comparing to recombinant protein standard curves. The cells were grown for 36–48 h post-transfection prior to collection.

GST Pulldown Assays - The assays were performed by preparing cellular lysates in Triton X-100/PBS buffer (1x PBS, 150 mM NaCl, 1% Triton X-100, protease inhibitors), clarified by centrifugation at 14,000 x *g* for 15 minutes. Concentration of Triton X-100 in lysate was then reduced to 0.2% with binding buffer (1x PBS, 150 mM NaCl, protease inhibitors) prior to the

addition of purified recombinant R7BP-GST fusion proteins (175 pmol) attached to 10 µl of glutathione agarose beads (GE Healthcare). Samples were incubated on rocker for 3 hr at 4 °C, and the beads were subsequently washed with binding buffer three times. The proteins were eluted in SDS sample buffer, and RGS proteins retained by the beads were detected by Western blotting with specific antibodies.

Surface Plasmon Resonance Spectroscopy - The specific interaction between recombinant R7BP and RGS9-2•Gβ5, and between R7BP and RGS7•Gβ5 was analyzed using a BIAcore Processing Unit (BIAcore 1000) at 23-25°C. R7BP was covalently coupled to CM5 chip flow cells (BIAcore) using an Amine Coupling Kit (BIAcore) according to the manufacturer's instructions. R7BP (30 µl) was flowed across the flow cell at a concentration of 10 µg/ml in 10 mM ammonium acetate pH=6.0 at a rate of 5 µl/min, resulting in a net increase of 1500-3000 resonance units (RU) after immobilization. A control flow cell surface was reacted with the amine coupling reagents in the absence of R7BP. RGS protein of several concentrations in HBS buffer (10 mM HEPES pH=7.4, 150 mM NaCl, 3.4 mM EDTA, and 0.005% Surfactant p20) was injected over the control and immobilized R7BP flow cell surfaces at a flow rate of 10 µL/min, and the resonance changes were recorded with BIACORE 1000 Control Software v2.1. Changes in surface refraction were recorded for 1 minute during protein binding and dissociation. The response from the R7BP surface, which was in the 25% - 35% range of the RU response observed in the R7BP cell, was subtracted from that of the control, and the dissociation constants (K_D) were determined using BIAevaluation v3.0.2 software. R7BP surfaces were removed of RGS protein and regenerated by running 100 µL of 10 mM NaOH through the flow cell at 100 µl/min.

Coronal brain slice preparation and pharmacological treatments - The whole brain from 1-2 month old C57BL/6 mice was quickly removed and placed in an ice-cold slicing solution containing 85mM NaCl, 2.5mM KCl, 4 mM $MgCl_2$, 1 mM NaH_2PO_4, 25 mM $NaHCO_3$, 25 mM glucose, and 75 mM sucrose (all from Sigma, St. Louis, MO) pH=7.4. When indicated the media was continuously bubbled with 95% O_2-5% CO_2. Coronal slices were prepared 300 µm in thickness using a Vibratome 3000 Plus sectioning system (Vibratome, St Louis, MO). Slices were then cut sagittally down the midline, with striatal tissue being isolated from one side and directly frozen in liquid N_2. The contralateral half slice was subsequently placed into artificial CSF (ACSF; in mM: 119 NaCl, 2.5 KCl, 1 NaH_2PO_4, 26.5 $NaHCO_3$, 1.3 $MgSO_4$, 2.5 $CaCl_2$, and 11 glucose) with the indicated pharmacological agent, brought to 37°C, and continuously bubbled with 95% O_2-5% CO_2. 30 mM KCl treatments were performed by concurrently reducing the ACSF NaCl concentration to 91.5 mM. (+)-Bicuculline was purchased from Ascent Scientific

(Weston-Super-Mare, UK), Nimodipine and Phorbol 12-myristate 13-acetate (PMA) from Sigma. Striatal tissue was isolated from the slice after one hour of culturing and frozen in liquid N_2 prior to protein extraction and western blot analysis.

Immuno electron microscopy - Electron microscopic examination of immunoreactivity for RGS9-2, R7BP and RGS7 in the striatum of WT and RGS9-2 KO mice was performed as described previously using either pre-embedding or post-embedding immunogold methods (92, 162). Briefly, brains were perfused with 4% paraformaldehyde, 0.05% glutaraldehyde and 15% (v/v) saturated picric acid in 0.1 M phosphate buffer. For pre-embedding immunogold labeling, brain sections (50-70 μm) were cut on a Vibratome and processed for immunohistochemical detection of RGS9-2 and/or R7BP using HRP and silver-enhanced immunogold techniques. For post-embedding immunogold labeling, ultrathin sections (70–90 nm) from three Lowicryl-embedded blocks slices were cut on an Ultramicrotome and processed for immunohistochemical detection of RGS9-2 and/or R7BP. The specificity of RGS7 antibodies (7RC1) for electron microscopy conditions was confirmed by staining the striatal regions of Gb5 knockout mice and observing marked down-regulation of characteristic staining as the levels of RGS7 in these mice are severely reduced (data not shown).

- ***Results***

R7BP•RGS complexes in the striatum are remodeled upon induced degradation of RGS9-2 - We have previously shown that RGS9-2•Gβ5 complexes are proteolytically labile and rapidly degrade when not bound to R7BP. Furthermore, we hypothesized that the concentration of RGS9-2•Gβ5 *in vivo* may be quickly regulated by dynamically changing RGS9-2•Gβ5 association with R7BP. To investigate whether levels of RGS9-2•Gβ5 is subject to these posttranslational alterations, we studied modulation of RGS9-2 expression in cultured striatal slices. Data presented in Figure 4.1A illustrate that upon culturing a 300 μm thick coronal slice through the striatum, RGS9-2 protein levels rapidly decline, reaching ~30% of initial amount in only 3 hours in culture. During this time-frame, the levels of other investigated signaling proteins including the RGS9-2 homolog, RGS7 were unaffected, suggesting a selective nature of this modulation. Inclusion of the cysteine protease inhibitor E64 into the culture medium, which was previously shown to be effective for its prevention of RGS9-2•Gβ5 degradation, completely blocked its decay, indicating for the proteolytic mechanism of the effect (Figure 4.1B).

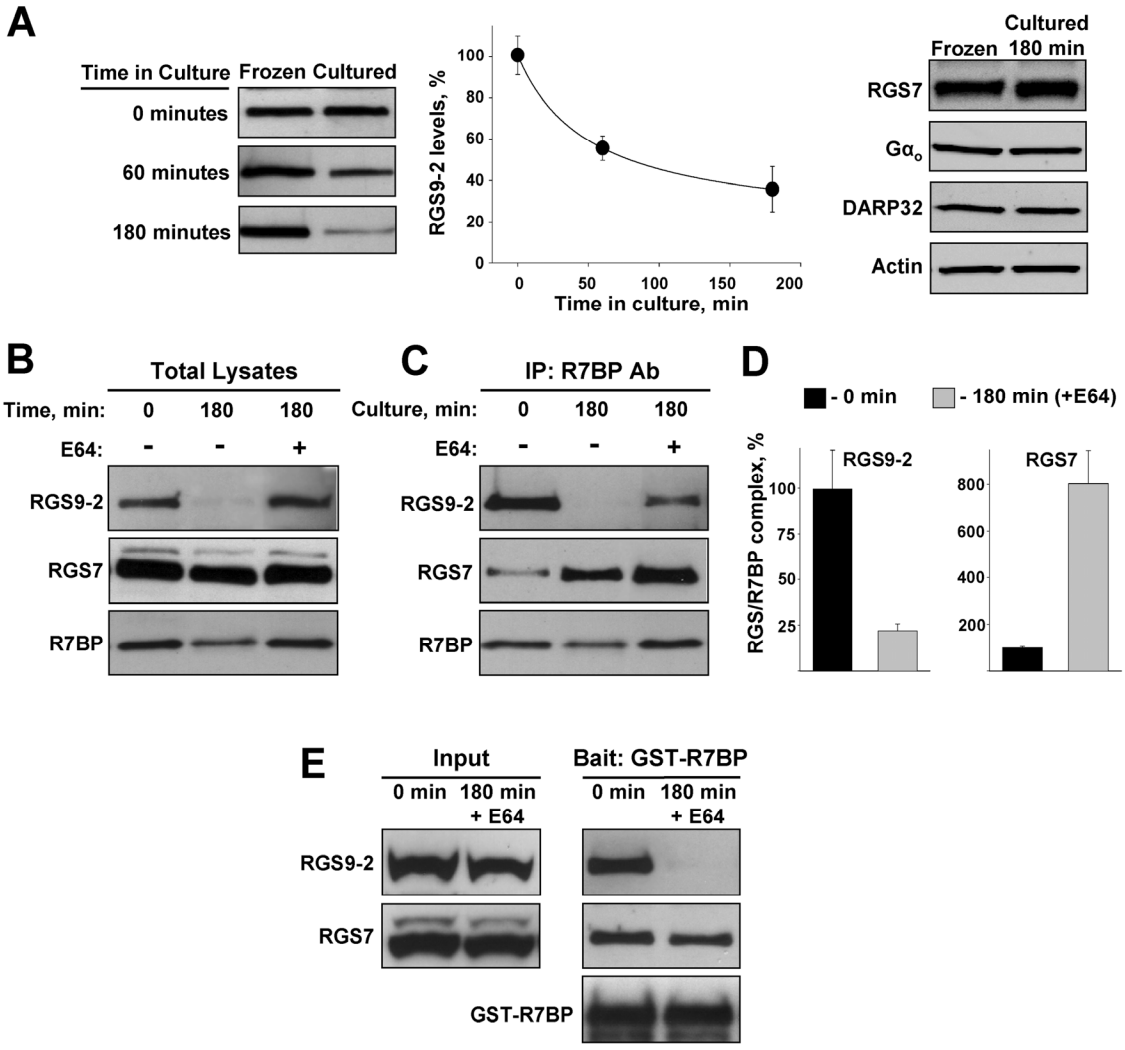

Figure 4.1: R7BP recouples to RGS7 upon induced degradation of RGS9-2. (A) Culturing striatal slices results in overt RGS9-2 degradation. 300 μm coronal sections were prepared and cut in half down the midline. One side of the section served as control, with striatal tissue isolated and directly frozen in liquid nitrogen. The contra-lateral section was subsequently cultured for 0, 60, or 180 minutes in ACSF prior to analysis. Subsequently, tissue was lysed and subjected to Western blot analysis using anti-RGS9-2 antibodies (left panels) or antibodies against striatally enriched signaling proteins (right panels). Protein bands were quantified by densitometry and resulting values were plotted as a function of time. (**B**) Degradation of RGS9-2 in slices is prevented by the inhibitor of cysteine proteases, E64. 1% Triton X-100 lysates were obtained from striatal slices (300 μm) cultured for 3 hours in the absence or presence of 50 μM E64 and analyzed for the expression of RGS9-2, RGS7 and R7BP by Western blotting. (**C**) Western blot Analysis of proteins immunoprecipitated by 5 μg of sheep anti-R7BP from extracts
in panel B. (**D)** Quantitative analysis of protein band density in panel C. RGS9-2 and RGS7 band densities from 3 independent experiments were obtained by ImageJ software and normalized against R7BP content. *Error bars* represent S.E.M. values. (**E)** Pull-down binding assay between immobilized recombinant GST-R7BP and native RGS proteins. Extracts obtained from slices either immediately frozen or cultured in the presence of E64 inhibitor were applied to GST-R7BP beads. After washing, bound proteins were eluted with the SDS-PAGE sample buffer and detected by Western blotting.

Because it was previously found that stable expression of RGS9-2•Gβ5 *in vivo* requires its binding to R7BP, we next investigated whether degradation of RGS9-2•Gβ5 upon culturing could be explained by the loss of its association with R7BP. In these experiments, R7BP was immunoprecipitated from the striatal slices cultured in the presence of E64 inhibitor, and co-precipitating proteins were analyzed by Western blotting. Data presented in Figure 4.1C reveal two key observations. First, the amount of RGS9-2 co-precipitating with R7BP markedly drops after culturing slices for 3 hours despite similar levels of RGS9-2 protein present in the total lysates before and after culturing in the presence of protease inhibitor. Second, culturing striatal slices substantially increases the amount of RGS7 co-precipitating with R7BP, despite the lack of modulation in its expression level. Indeed, quantitative analysis of data from three independent experiments (Figure 4.1D) indicates that while RGS9-2•R7BP complex formation is decreased approximately 5-fold, the extent of RGS7•R7BP association is increased by a comparable factor.

These observations suggest that R7BP remains competent for binding R7 RGS proteins and switching of its binding from RGS9-2 to RGS7 is likely induced by the changes affecting RGS proteins during culturing. In order to determine which RGS protein is responsible for the observed remodeling we conducted a pull-down assay where we studied the ability of recombinant R7BP immobilized on the beads to capture RGS7 and RGS9-2 from striatal slices prepared before and after culturing. As evident from Figure 4.1E, R7BP was able to efficiently pull-down both RGS9-2 and RGS7 from uncultured tissue. However, after culturing, R7BP completely lost the ability to retain RGS9-2 while still effectively pulling down RGS7. This suggests that degradation of RGS9-2 in culture and subsequent upregulation of RGS7-R7BP complexes is induced by changes in RGS9-2 protein, leading to its uncoupling from R7BP and subsequent targeting for degradation.

Quantitative analysis of R7 RGS•Gβ5•R7BP complex compositions in the striatum - Observation of R7BP complex remodeling in slices, and previous reports that R7BP is capable of forming complexes with all R7 RGS proteins, have prompted us to investigate the composition and stoichiometry of R7BP complexes with R7 RGS•Gβ5 in the striatum. We have immunoprecipitated R7BP from striatal lysates and determined the amount of co-precipitating R7 RGS proteins by quantitative Western blotting using recombinant protein standards for each individual R7 RGS protein (Figure 4.2A). Plotting the densities of protein standards against their concentration resulted in linear relationship (data not shown) which was used to determine the concentration of proteins in the lysates from values of their band densities. Out of 4 RGS proteins reported to interact with R7BP, RGS7 and RGS9-2 were found to be predominant binding

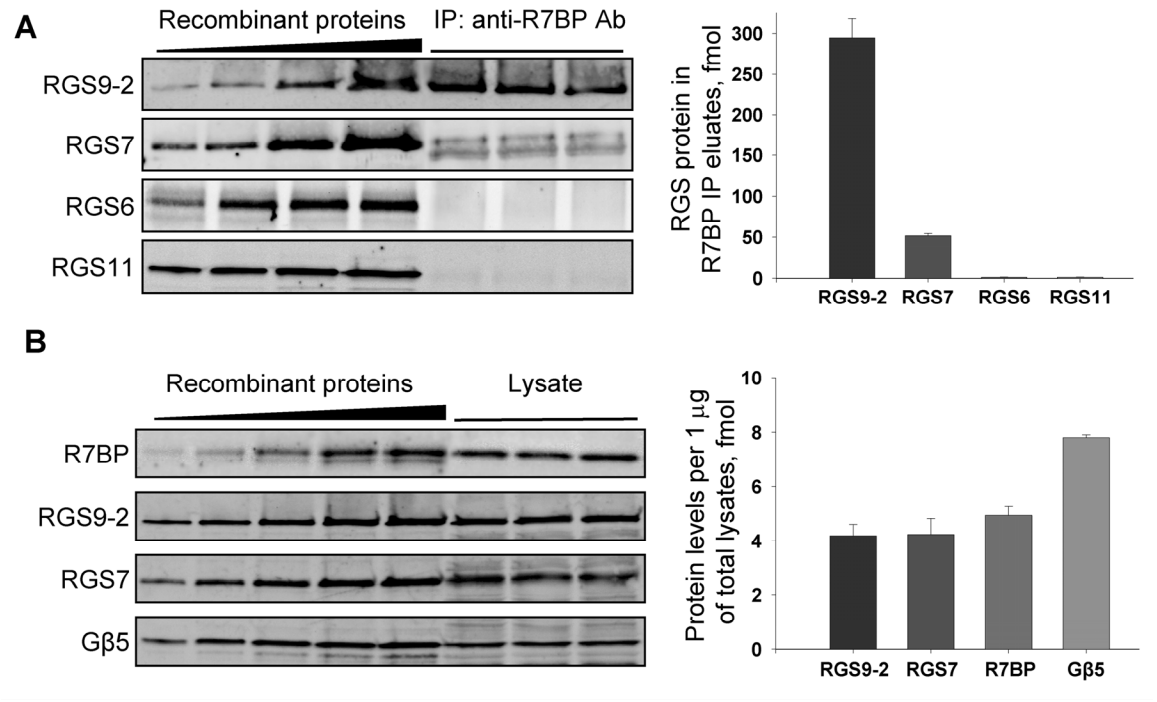

Figure 4.2: RGS9-2 is the primary R7 RGS protein in complex with R7BP in the striatum. (**A)** Quantification of proteins co-immunoprecipitating with R7BP. Fresh striatal tissue was lysed in 1% Triton extracts and incubated with 5 μg of sheep anti-R7BP antibody. Eluates were loaded on 4-20% PAGE adjacent to recombinant protein standards containing 50, 100, 250, and 500 fmoles of indicated RGS proteins. Upon incubation with IR-dye conjugated secondary antibodies images were scanned on Odyssey infrared imager. Band densities were quantified using Odyssey 2.0 software. Calibration curve was plotted from densities of recombinant protein standards. The linear range, typically extending throughout the calibration standard concentrations, was used to determine RGS protein content in striatal extracts obtained from 3 separate mice. (**B**) Quantification of the total levels of R7BP complex components in striatum. 20 μg of total protein from each out of three lysates was loaded next to recombinant protein standard of 20, 50, 100, 150, 200 fmol for RGS7, RGS9-2 and R7BP or 40, 100, 200, 300, 400 fmol for Gβ5.Note that the range of protein standards is different from that used in the experiment presented in panel A. *Error bars* are S.E.M

partners of R7BP. Furthermore, RGS9-2•R7BP complexes were approximately 5 times more abundant as compared to RGS7•R7BP. Neither RGS6 nor RGS11 were present in R7BP immunoprecipitate fractions in appreciable quantities indicating that their association with R7BP and/or abundance in the striatum is substantially lower than that of RGS9-2 and RGS7.

We have next measured the absolute amounts of RGS7 and RGS9-2 as well as their binding partners Gβ5 and R7BP in mouse striatum using quantitative Western blotting with recombinant protein standards. Data presented in Figure 4.2B illustrate that RGS9-2, RGS7 and R7BP are present in near stochiometric amounts (~4 fmol per mg of total striatal protein). At the same time Gβ5 was twice more abundant (~8 fmol per mg) in a close agreement with the requirement of its 1:1 association with both RGS9-2 and RGS7 and the fact that other R7 RGS proteins were found to be considerably less abundant in the striatum (Figure 4.2A). These data indicate that despite the equimolar concentration of RGS9-2•Gβ5 and RGS7•Gβ5 in the striatum, R7BP is coupled predominantly to RGS9-2.

RGS9-2 and RGS7 co-localize in the same neurons of mouse striatum – Given equal amounts of RGS9-2 and RGS7 in the striatum, the disproportionate association of R7BP preferentially with RGS9-2 called for an examination of interaction partner co-localization across striatal neurons. We used double labeling techniques at the electron microscopic level, combining pre-embedding immunogold with HRP detection, to study co-localization of RGS7, R7BP and RGS9-2 in three different double-labeling experiments (Figure 4.3). Consistent with previous reports we have found that RGS9-2 is localized in essentially all striatal neurons where it co-localized with R7BP (27, 92, 111). As reported earlier, we found that RGS9-2•R7BP complexes were predominantly found on the plasma membrane of dendritic spines and shafts. Most of the RGS7 immunoreactivity was found to localize in the cells positive for RGS9-2 and R7BP (Figure 4.3). Similarly to RGS9-2 and R7BP, RGS7 antibodies strongly labeled dendritic but not axonal compartments suggesting its compartmentalization in striatal neurons. These data indicate that RGS9-2, R7BP and RGS7 extensively overlap in their expression in the same striatal neurons and their subcellular compartments.

Recombinant R7BP has higher affinity for RGS9-2•Gβ5 over RGS7•Gβ5 – In search for the mechanisms behind the preferential complex formation of R7BP with RGS9-2, we have compared the binding affinities of R7BP to RGS9-2•Gβ5 and RGS7•Gβ5 using purified recombinant proteins. Association of proteins was monitored by surface plasmon resonance technology using BiaCore 1000 instrument. Recombinant R7BP was immobilized on the surface of CM5 chip which was exposed to either RGS9-2•Gβ5 or RGS7•Gβ5 complexes in solution.

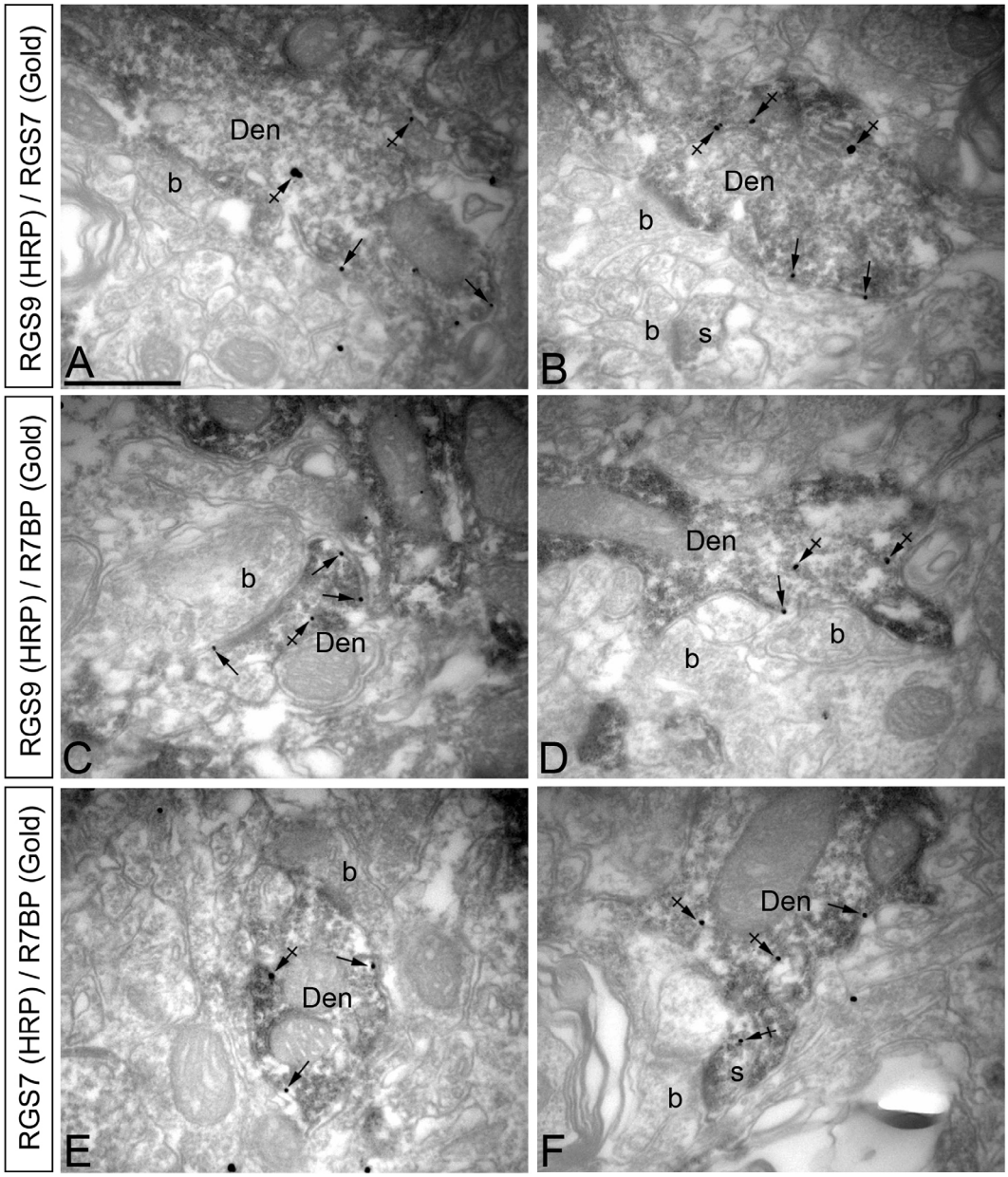

Figure 4.3: RGS9-2, RGS7 and R7BP co-localise in the same cell type and subcellular compartment in the mice striatum. Electron micrographs showing double labelling for RGS9, RGS7 and R7BP in the mice striatum, as revealed using pre-embedding techniques. (**A-B**) Double labelling approach showing co-localisation for RGS9-2 and RGS7. The peroxidase reaction product (HRP) indicating RGS9 immunoreactivity filled dendritic shafts (Den) and spines (s), whereas immunoparticles (RGS7 immunoreactivity) were mainly located along the extrasynaptic plasma membrane (e.g. arrows) and at intracellular sites (e.g. crossed arrows). (**C-D**) Double labelling approach showing co-localization for RGS9-2 and R7BP. The peroxidase reaction product (HRP) indicating RGS9 immunoreactivity filled dendritic shafts (Den) and spines(s), whereas immunoparticles (R7BP immunoreactivity) were mainly located along the extrasynaptic plasma membrane (e.g. arrows) and at intracellular sites (e.g. crossed arrows). (**E-F**) Double labelling approach showing colocalisation for RGS7 and R7BP. The peroxidase reaction product (HRP) indicating RGS7 immunoreactivity filled dendritic shafts (Den) and spines (s), whereas immunoparticles (R7BP immunoreactivity) were mainly located along the extrasynaptic plasma membrane (e.g. arrows) and at intracellular sites (e.g. crossed arrows). b, axon terminal. Scale bar: A-F, 0.5 μm.

Performing protein-protein interaction measurements over a range of analyte concentrations have yielded consistent differences in the binding constants (Figure 4.4A). The affinity of R7BP for the RGS9-2•Gβ5 (K_D=1.1 ± 0.4 nM) complex was approximately ten-fold higher than for RGS7•Gβ5 (K_D=12.7 ± 2.6 nM). We have further determined whether RGS9-2•Gβ5 and RGS7•Gβ5 can simultaneously interact with R7BP using competition binding experiments. We incubated GST tagged R7BP with a fixed concentration of RGS7•Gβ5, and an increasing concentration gradient of RGS9-2•Gβ5. Following pull-down with the glutathione agarose beads, the amounts of retained RGS7 and RGS9-2 were determined. Data in Figure 4.4B demonstrates that increasing concentrations of RGS9-2•Gβ5 result in elevation in its binding to R7BP concomitant with the decreased association between RGS7•Gβ5 and R7BP. This result indicates that RGS9-2 and RGS7 compete for R7BP association binding to the same or overlapping determinants, yet with different affinities.

Modulation of R7BP•R7 RGS complex composition in transfected cells – Significantly different affinities of R7BP for RGS7•Gβ5 and RGS9-2•Gβ5 has prompted us to analyze how decrease in individual RGS protein concentration affect the composition of the whole complex. We have addressed this issue by modeling competitive association of R7BP with RGS9-2•Gβ5 and RGS7•Gβ5 in transfected HEK 293FT cells which do not express R7BP, Gβ5, RGS7, or RGS9-2 endogenously (Figure 4.5).

Using transient transfection, we delivered a fixed amount of R7BP and Gβ5 message, and either a fixed amount of RGS9-2 and variable amounts of RGS7, or a fixed amount of RGS7 and variable amounts of RGS9-2. The amount of Gβ5 construct was kept in six fold excess to ensure that RGS proteins at all concentrations are not competing for Gβ5. Further, by using quantitative Western blotting with recombinant standards and native striatal extracts we confirmed that RGS7 and RGS9-2 were present in equimolar concentrations when equal amounts of their expression constructs were delivered into cells (data not shown). Cellular extracts containing variable amounts of RGS7 or RGS9-2 were subjected to immunoprecipitation with anti-R7BP antibodies and changes in amounts of each precipitated protein were determined by Western blotting. Data presented in Figure 4.5A reveal that RGS9-2 in complex with R7BP is minimally affected by changes in concentration of RGS7, which can only decrease the abundance of RGS9-2•R7BP complexes by 20% upon reaching equimolar concentration with RGS9-2. In agreement with this estimation, the reciprocal experiment (Figure 4.5B) shows that at an equal stochiometric ratio of RGS proteins, as much as 80% of RGS9-2 is complexed with R7BP. However, unlike the model

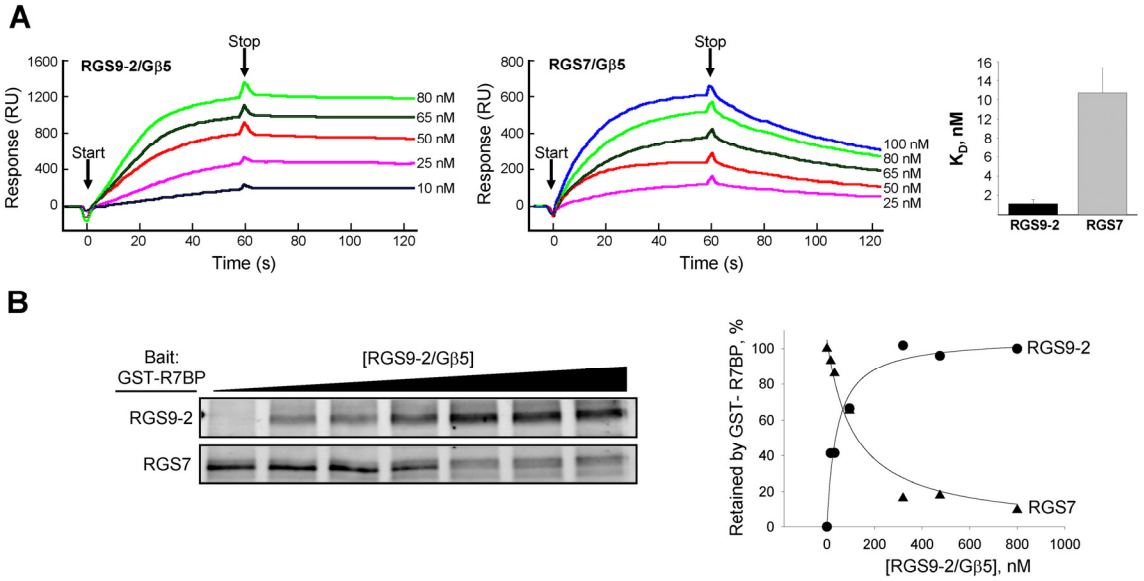

Figure 4.4: RGS9-2•Gβ5 has higher affinity for R7BP over RGS7•Gβ5 and competes for its binding. **(A)** Surface plasmon resonance analysis of R7BP association with RGS7•Gβ5 and RGS9-2•Gβ5 performed on Biacore 1000 instrument. Purified recombinant R7BP was immobilized on the surface of CM5 chip and exposed to varying concentrations of RGS7•Gβ5 (25, 50, 65, 80, 100 nM) or RGS9-2 (10, 25, 50, 65, 80 nM). Analyte solutions were injected at a 10 µl/min rate for 1 minute, and analyzed for RGS•R7BP association rates, as was dissociation rates during the first minute after RGS solution injection stopped. Each plotted curve is representative of duplicate repetition. K_D values were calculated using BiaCore Evaluation software and were: 1.1 nM $\pm$ 0.4 nM (S.D.) for R7BP binding to RGS9-2•Gβ5 and 12.7 nM $\pm$ 2.6 nM for R7BP interaction with RGS7•Gβ5. **(B)** RGS7•Gβ5 and RGS9-2•Gβ5 compete for binding to R7BP. 16 nM of immobilized GST-R7BP bait was incubated with a fixed concentration of RGS7•Gβ5 (55 nM) and varying concentration of RGS9-2•Gβ5 (0, 16, 32, 95, 320, 475, and 800nM). Beads were washed and bound proteins were analyzed by Western blotting. Right panel represents quantification of the protein densities normalized to maximal binding in the absence of RGS•Gβ5 and plotted as a function of RGS•Gβ5 concentration.

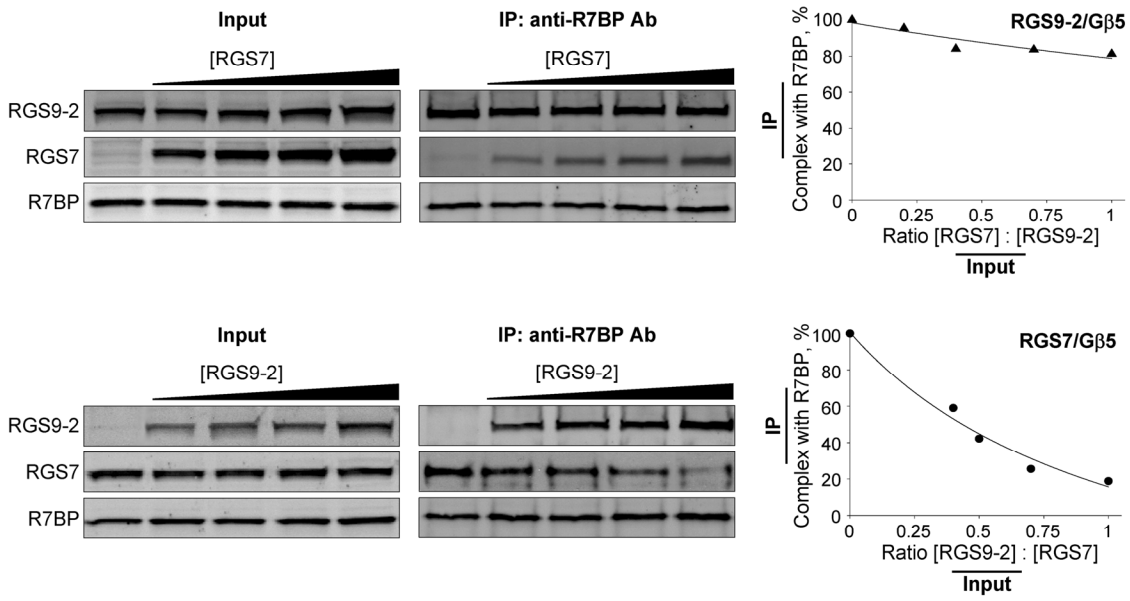

Figure 4.5: Modeling of competitive association of R7BP with RGS9-2•Gβ5 and RGS7•Gβ5 complexes in transfected cells. (**A)** HEK 293FT cells were transfected with equal and amounts of R7BP and RGS9-2 expression constructs (0.2 μg) and varying amounts of RGS7 plasmid. Six fold excess of Gβ5 expression construct was used (1.2 μg) to ensure that its concentration does not limit RGS protein expression. Actual levels of expressed RGS proteins (left panels) were determined by quantitative infrared Western blotting. The equality of RGS9-2 and RGS7 protein levels at the maximal concentration of RGS7 construct was verified by comparing band densities to recombinant protein standards and brain extracts (not shown). Cells were lysed in 1% Triton and incubated with 3 μg of sheep anti-R7BP antibody. Eluates were subjected to SDS-PAGE separation followed by Western blot analysis using specific and IR-conjugated secondary antibodies (right panels). Images were scanned on Odyssey infrared imager and band densities were quantified using Odyssey 2.0 software. The density of RGS9-2 bands were normalized against that of R7BP and used to define Y-axis with 100% reflecting maximum band density in the absence of RGS7. The ratios of actual RGS7 and RGS9-2 band densities present in total lysates before immunoprecipitation (left panels) were used to define X-axis. (**B)** Inverse experiment was performed with constant RGS7 expression construct and varying RGS9-2 amounts. Protein levels in inputs and immunoprecepitation eluates were determined exactly as described for panel A. The experiments shown on both panels are representative out of at least three conducted yielding similar results.

with variable RGS7, modulation of RGS9-2 concentration appears to markedly affect the extent of RGS7 coupling to R7BP. This indicates that while change in RGS7 expression minimally affects the balance in RGS9-2•R7BP complexes, changes in RGS9-2 levels cause proportionate rebalancing of R7BP coupling to RGS7.

Elimination of RGS9-2 leads to the R7BP mediated recruitment of RGS7 to the plasma membrane - Modeling of the complex formation in transfected cells makes a prediction that reduction of RGS9-2 in the striatum would entail upregulation in RGS7•R7BP complex formation. In order to investigate if this is the case, we have compared RGS7 coupling to R7BP between striatal regions of wild type and RGS9 -/- mice in which the expression of RGS9-2 was ablated by gene targeting. The results of the immunoprecipitation experiment presented in Figure 4.6 illustrate marked enhancement of RGS7-R7BP association in the absence of RGS9-2 providing further evidence that changes in RGS9-2 expression cause remodeling of R7BP containing complexes.

To begin to analyze the consequences of this remodeling we have examined whether loss of RGS9 affected localization of RGS7 in the striatal neurons. Immunogold labeling indicate that in wild type neurons most of the dendritic RGS7 is found at intracellular sites (Figure 4.7A,B) and almost none of it is detected within the postsynaptic density (Figure 4.7C). Quantitative analysis of 1781 gold particles revealed 1478 (83%) of them at the intracellular sites and only 303 (17%) at the plasma membrane. Since nearly all of the R7BP was previously found associated with the plasma membrane compartment this distribution is in the close agreement with ~ 20% fraction of RGS7 associated with R7BP in wild type striatums (Figure 4.2). In contrast, in striatal neurons of RGS9 knockout mice only 22% (374 particles) were found at intracellular sites and 78% (1322 particles) residing at the plasma membrane (Figure 4.7D,E) and postsynaptic densities (Figure 4.7F). No significant change in RGS7 localization was observed in the striatal neurons of R7BP knockout mice (Figure 4.7 G,H). This result is consistent with the small extent of RGS7 association with R7BP in the presence of RGS9-2 and suggests that it is the physical association with vacant R7BP rather than changes in the G protein signaling resulting from RGS9 elimination that are responsible for the recruitment of RGS7 to the postsynaptic plasma membrane compartments.

Multiple signaling pathways regulate RGS9-2 degradation in striatal neurons - Since RGS9-2 protein levels is the determining factor for remodeling R7 RGS complexes, we investigated signaling mechanisms that are involved in regulation of RGS9-2 posttranslational stability. Observation that RGS9-2 undergoes spontaneous degradation upon acute culturing of

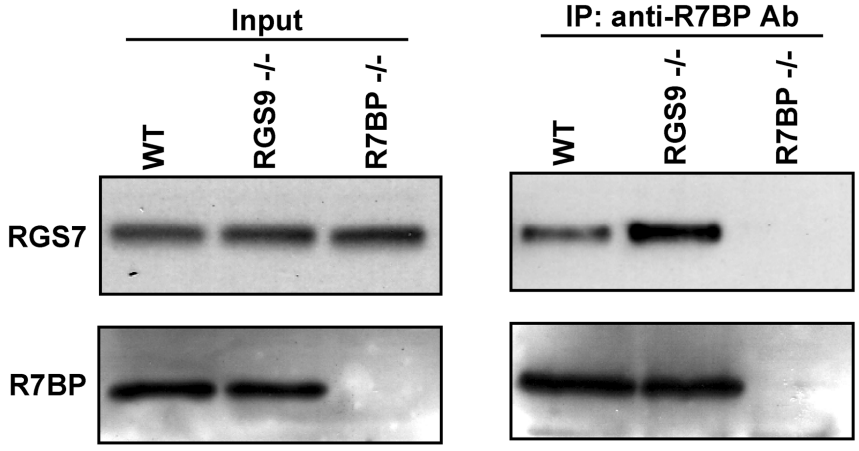

Figure 4.6: Complexes of RGS7 with R7BP are upregulated in striatums of RGS9 knockout mice. Striatal regions were dissected from C57BL/6 wild-type (WT), RGS9 knock-out (RGS9 -/-), and R7BP knock-out (R7BP -/-) mice, lysed in 1% Triton and used to determine total protein concentration. 20 μg aliquots of each lysate were separated on SDS-PAGE and analyzed by Western blotting (left panels, "input").. Equal amounts of lysates were subjected to immunoprecipitation with 5 μg of sheep anti-R7BP antibody. Immunoprecipitated proteins were analyzed by Western blotting. The experiment shown is representative of 3 conducted and yielding similar results.

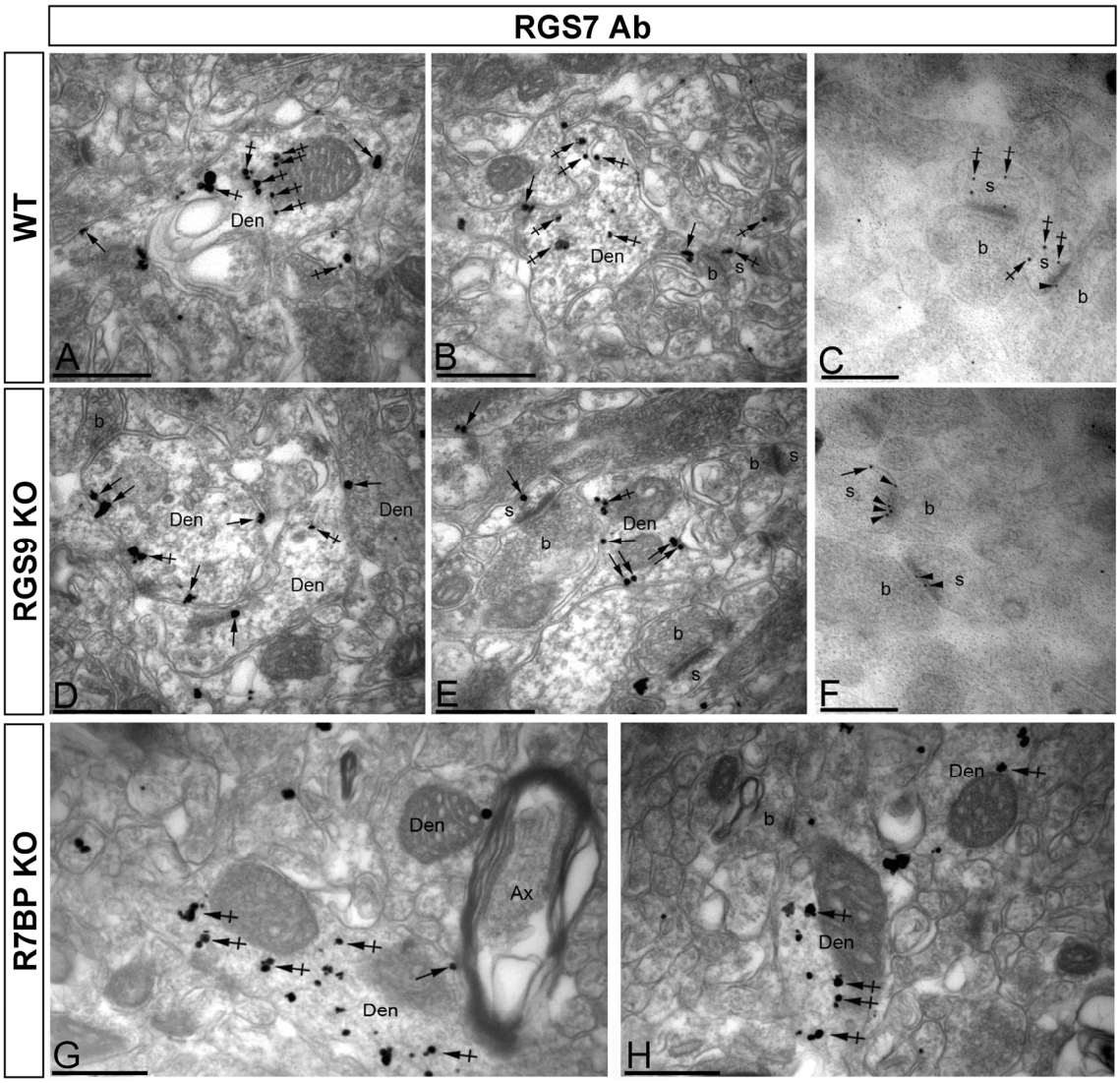

Figure 4.7: Loss of RGS9-2 but not R7BP induces changes in RGS7 localization in striatal neurons. Electron micrographs showing immunoreactivity for RGS7 in wild type (WT), RGS9 knockout (RGS9 KO) and R7BP knockout (R7BP KO) mice in the striatum, as revealed using pre-embedding (A, B, D, E, G, H) and post-embedding (C, F) immunogold techniques. Using the pre-embedding immunogold method, immunoparticles for RGS7 in wild type neurons (A,B) were mainly located at intracellular sites (e.g. crossed arrows), associated with intracellular membranes within dendritic shafts (Den) and spines (s) establishing excitatory synapses with axon terminals (b). In less proportion, immunoparticles for RGS7 were also detected along the plasma memebrane (e.g. arrows). Using the post-embedding immunogold method (panel C), immunoparticles for RGS7 in wild type neurons were mainly located at intracellular sites (e.g. crossed arrows) and occasionally along the postsynaptic density of excitatory synapses (e.g. arrowheads). Using the pre-embedding immunogold method, immunoparticles for RGS7 in RGS9 KO neurons (D, E) were mainly located along the plasma membrane (e.g. arrows) of dendritic shafts (Den) and spines (s) establishing excitatory synapses with axon terminals (b). In less proportion, immunoparticles for RGS7 were also detected at intracellular sites (e.g. crossed arrows), associated with intracellular membranes. Using the post-embedding immunogold method (F), immunoparticles for RGS7 in the RGS9 KO were mainly located along the postsynaptic density of excitatory synapses (e.g. arrowheads) and occasionally at intracellular sites (e.g. crossed arrows). RGS7 immunoreactivity in R7BP KO neurons (G, H) replicated the pattern observed in wild-type samples. That is, immunoparticles for RGS7 in the R7BP KO were mainly located along the plasma membrane (e.g. arrows) of dendritic shafts (Den) and spines (s), establishing excitatory synapses with axon terminals (b). In less proportion, immunoparticles for RGS7 were also detected at intracellular sites (e.g. crossed arrows), associated with intracellular membranes. Scale bar: A,B,D,E,G, H - 0.5 μm; C,F - 0.2 μm.

striatal slices under standard conditions has prompted us to modify culturing conditions in order to minimize RGS9-2 loss. We found that saturating media with 95% oxygen was very effective for maintaining RGS9-2 stability, reducing the rate of its degradation to only 10% per hour (Figure 4.8A). Therefore we used the culturing system with constant oxygenation for subsequent pharmacological manipulations.

We reasoned that increased degradation rate of RGS9-2 protein upon culturing could be caused by uncontrollable neuronal activity exacerbated by insufficient oxygenation. Indeed, stimulating neuronal firing by either application of 30 mM KCl, which induces membrane depolarization, or 50 μM bicuculline, which inhibits inhibitory GABA transmission and thus indirectly stimulating synaptic transmission, caused marked RGS9-2 destabilization, essentially abrogating a protective effect of high oxygen concentration (Figure 4.8B). Because rise in the intracellular calcium concentration is the hallmark of increased neuronal activity we next investigated whether RGS9-2 instability could be mediated by the calcium entry. Preventing extracellular calcium entry by removing it from the medium completely blocked not only depolarization-induced but also residual spontaneous RGS9-2 degradation. Blocking a major class of voltage gated calcium channels (L-type VGCC) by specific inhibitor nimodipine, also abolished depolarization induced RGS9-2 loss suggesting that rise in the intracellular calcium entering through plasma membrane calcium channels is the major signaling event that triggers RGS9-2 degradation. Finally, we found that activation of Protein Kinase C (PKC), a major downstream effector influenced by calcium entry directly enhances RGS9-2 loss, indicating that PKC plays a critical role in controlling RGS9-2 stability.

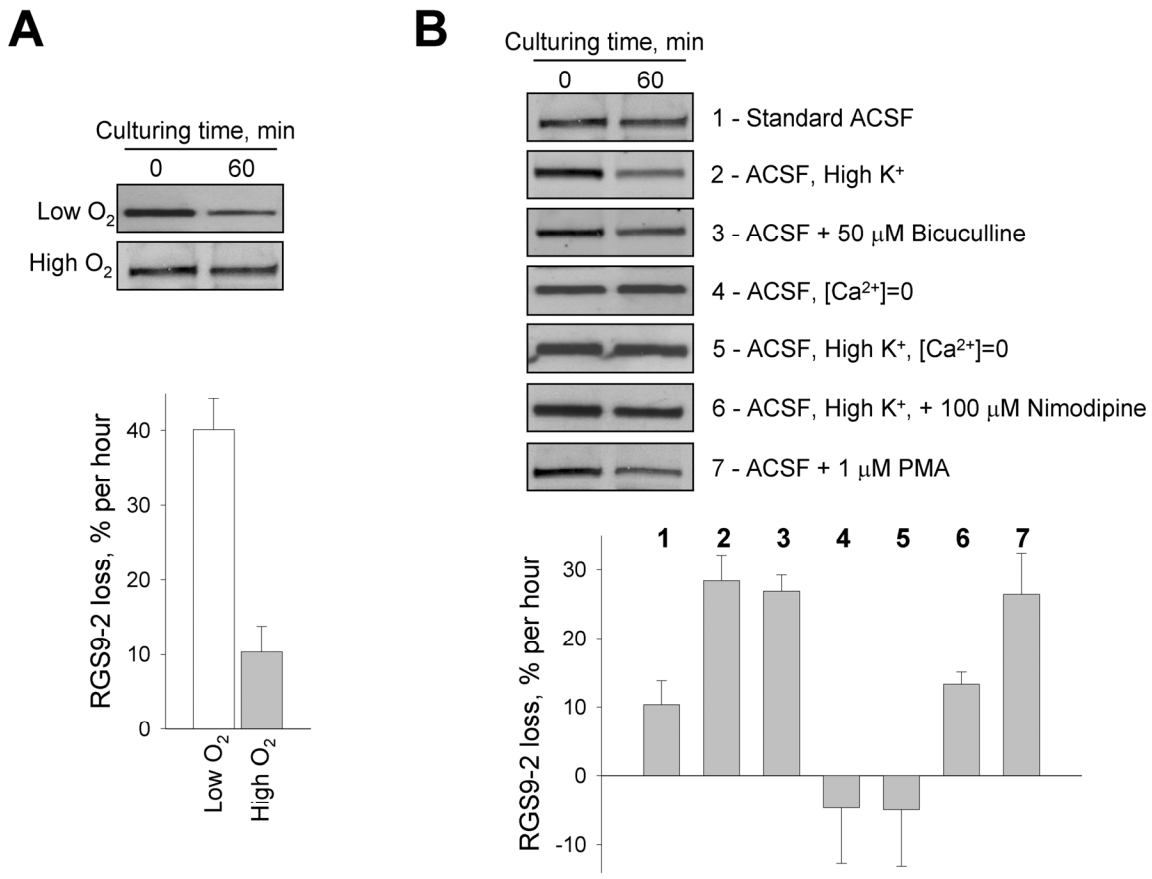

Figure 4.8: Oxygenation status, neuronal activity and extra-cellular calcium entry regulates RGS9-2 protein levels. (**A)** Overt RGS9-2 degradation upon striatal slice culturing can be slowed down by increasing oxygenation. Coronal brain slices were prepared and cut in half down the midline. One side of the section served as control, with striatal tissue isolated and directly frozen in liquid nitrogen. The contra-lateral section was subsequently cultured for 60 minutes in ACSF at atmospheric oxygen levels, 5% CO_2 (Low O_2), or ACSF bubbled with 95% O_2, 5% CO_2 (High O_2) prior to analysis. Subsequently, tissue was lysed in 1% Triton, and equal amounts of lysates were subjected to Western blot analysis using RGS9-2 specific antibody. Upon incubation with IR-dye conjugated secondary antibodies images were scanned on Odyssey infrared imager. Band densities were quantified using Odyssey 2.0 software, and cultured tissue RGS9-2 % loss was calculated as compared to uncultured tissue control band density (n = 8-12). (**B)** Neuronal depolarization initiates RGS9-2 loss in an extra-cellular calcium dependent fashion. All striatal coronal sections were prepared similarly as in panel A and cultured for 60 minutes in ACSF with the indicated media modification or pharmacological treatment, and actively bubbled with 95% O2, 5% CO2. Western blot analysis and RGS9-2 % loss quantitation was performed as in (A) and plotted as cumulative results (n = 8-12).

♦ ***Discussion***

The main finding of this study is that complexes of neuronal R7 RGS proteins with their subunits R7BP and Gβ5 undergo remodeling of their composition in response to changes in neuronal signaling. Striatal neurons express equal amounts of two R7 RGS proteins: RGS9-2 and RGS7 both forming equimolar complexes with Gβ5 subunit. The third subunit in the complex, R7BP, is unequally distributed and forms preferential complexes with RGS9-2 owning to the order of magnitude higher affinity over RGS7 (Figure 4.7). An intrinsic proteolytic instability of RGS9-2•Gβ5 in the absence of R7BP binding further shifts this balance, driving virtually all RGS9-2•Gβ5 to be present as a ternary complex with R7BP, while largely leaving RGS7 a dimer with only Gβ5. Remarkably, this equilibrium undergoes dramatic re-arrangement when R7BP uncouples from RGS9-2•Gβ5 complex, targeting RGS9-2 for degradation and funneling R7BP into complex formation with RGS7•Gβ5, generating nascent RGS7•Gβ5•R7BP trimer (Figure 4.9). R7BP, because of its proteolytically labile nature, requires association with R7 RGS proteins to maintain stable expression (92, 100), which further ensures high efficiency of this complex remodeling process. Indeed, while completely absent in striatums of Gβ5 knockouts lacking both RGS7 and RGS9-2 (92), the levels of R7BP are not altered upon RGS9-2 elimination ((92) and Figure 4.5) providing further support to the large extent of R7BP switching from RGS9-2 to RGS7.

Changes in subunit composition of the macromolecular complexes is a fundamental mechanism that underscores the plasticity of many biological processes including chromatin remodeling (190), immune cell differentiation (191), proteasome mediated protein degradation (192), synaptic activity (193-195), gene transcription (196) and many others. While the tremendous significance of this organizational flexibility is undoubted much remains to be learned about their underlying mechanisms. In our study, we describe a mechanism for rapid posttranslational changes in subunit composition of G protein signaling regulators which could serve as a general model for understanding remodeling principles of many complexes build from proteolytically labile components. In a proposed three way equilibrium model, a stable protein complex of three unstable subunits (ABC) donates one of the subunits (A) to the alternatively configured stable dimer (DC) while the remaining unstable components (BC) undergo selective degradation. These events allow for the rapid shift in subunit composition from the basal state of ABC to a new ADC state in a conditional dependent manner, and could be easily reversed by events that promote stabilization of BC subunits thus providing a point for regulatory input.

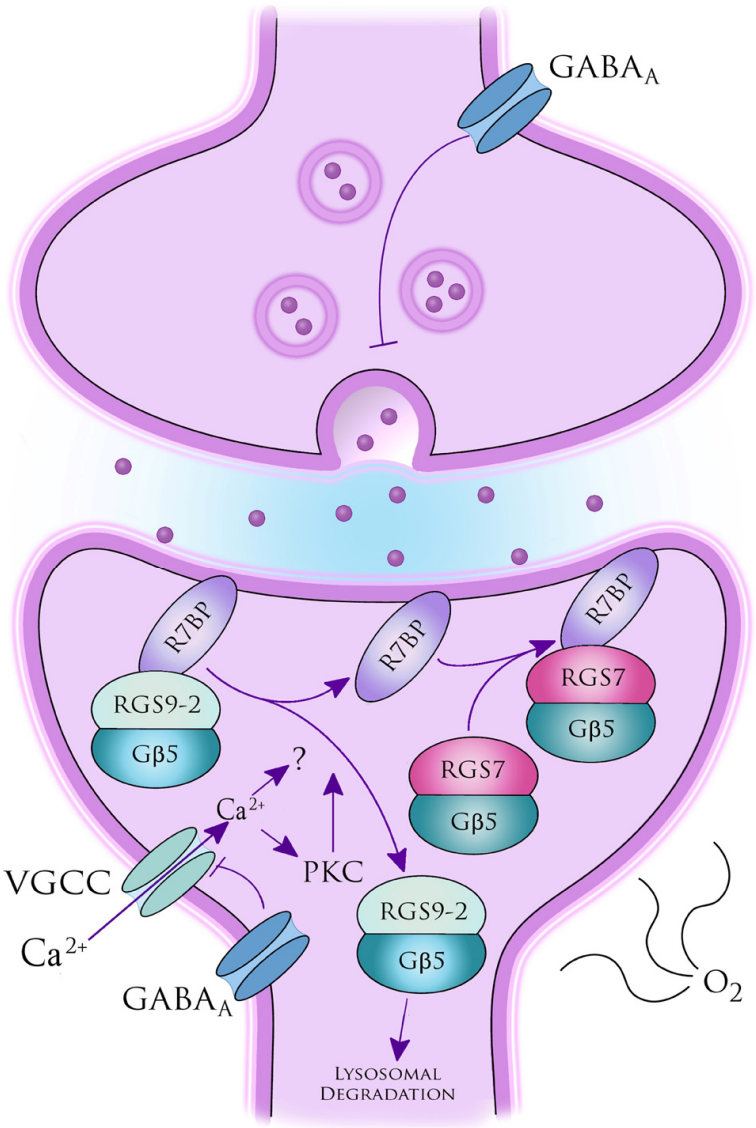

Figure 4.9: Proposed model for activity-dependent regulation of R7 RGS subunit composition. Under basal conditions, striatal neurons contain RGS9-2•Gβ5•R7BP trimer located at the postsynaptic sites and RGS7•Gβ5 dimer located intracellularly. Several signaling events can trigger RGS9-2 uncoupling from R7BP targeting RGS9-2•Gβ5 complex for degradation. Released R7BP becomes available for RGS7•Gβ5 binding resulting in production of RGS7•Gβ5•R7BP trimer which undergoes targeting to the postsynaptic density. This process is sensitive to oxygenation status, level of neuronal excitability, and is regulated by changes in calcium influx and PKC activation.

Our results indicate that remodeling of trimeric R7 RGS complexes is triggered by changes that affect binding of RGS9-2•Gβ5 to R7BP. More specifically, we found that it is RGS9-2 that is modified in a way which renders it unable to associate with R7BP, targeting it for degradation. Although, the molecular identity of the modification(s) remains unknown at the moment, several changes in neuronal signaling status appear to specifically modulate RGS9-2•R7BP coupling and resultant RGS9-2 degradation. Our pharmacological data argue for the involvement of at least two major mechanisms: oxygen sensing and synaptic activity along voltage gated Ca^{2+} channels — PKC axis. The disruption in cellular Ca^{2+} homeostasis appears to be the common element unifying both mechanisms. Indeed, changes in neuronal signaling and excitotoxicity is a well documented occurrence that accompanies hypoxia/ischemia in the brain (197). One of the major mechanisms contributing to neuronal excitotoxicity associated with increased neuronal excitability under hypoxic stress, is calcium dysregulation. Hypoxic stress leads to elevated Ca^{2+} influx, release from intracellular Ca^{2+} stores, and generalized disruption in Ca^{2+} buffering, resulting in constant activation of tightly regulated signaling molecules (i.e. PKC) which can ultimately culminate in neuronal injury and subsequent long-term disabilities for stroke victims (198, 199). However, it is also possible that oxygen sensing and changes in neuronal excitability are separate mechanisms that converge only at the level of modulating RGS9-2•R7BP coupling. In any case, our findings strongly suggest that changes in R7 RGS complex composition is another molecular hallmark of changes induced by oxygen deprivation and excessive synaptic activity.

It is interesting to consider the observed degradation-triggered remodeling in the context of the recent finding that R7BP•RGS9-2 complexes are enriched in postsynaptic densities of excitatory striatal synapses (92). Formidable body of evidence implicates dynamic regulation of postsynaptic density components as a central mechanism underlying plasticity of synaptic communication between neurons (reviewed in 200). Studies in mice have shown that both elimination and overexpression of RGS9-2 affect the sensitivity of the μ-opioid and D2 dopamine receptor signaling and influence movement control and reward processing, two highly adaptable functions of the striatum. Here, we report that fluctuations in RGS9-2 levels result in an unexpected molecular consequence: change in the targeting of RGS7•Gβ5•R7BP GAP complex to the postsynaptic density. It is tempting to speculate that these changes in subunit composition and localization of the major G protein signaling regulator in the region underlie activity dependent modulation of the opioid and dopamine systems in striatal neurons and thus could be viewed as a molecular substrate of synaptic plasticity. Indeed, levels of RGS9-2 expression has

been reported to be sensitive to a number of manipulations that alter opioid and dopamine signaling in the region (27, 28, 138, 161) and are therefore expected to cause remodeling of RGS complexes. In this light, it appears noteworthy that major determinants of various forms of neuronal plasticity such as Ca^{2+} influx (201) and oxygen deprivation (202) also regulate homeostasis of R7 RGS complexes. Furthermore, alterations in the activity of proteolytic machinery have been implicated as the earliest and most rapid mechanism utilized in neurons as a part of the biochemical and structural remodeling that occurs in response to changes in synaptic activity. Both the ubiquitin-proteasome system (203) and lysosomal autophagy (204) pathways have been shown to play a key role in the rapid synaptic remodeling that is observed with ischemic tolerance. A connection to the lysosomal degradation mechanisms is particularly intriguing because degradation of RGS9-2•Gβ5 dissociated from R7BP was shown to be mediated by cysteine proteases, major proteolytic enzymes of the lysosomes (92).

Finally, we would like to discuss potential consequences of the described R7 RGS complex remodeling on striatal signaling the extreme case of which is observed in RGS9 knockout mice where all of R7BP is re-coupled to RGS7. First, re-localization of RGS7 to the postsynaptic sites is expected to reduce its regulatory influence on the G proteins located at the intracellular sites. Secondly, binding of R7BP to RGS7•Gβ5 has been shown to negatively affect the capacity of the RGS7•Gβ5 dimer to dampen $G\alpha_q$ mediated signaling (82) suggesting that the remodeling would also lead to an enhancement in $G\alpha_q$ signaling events. Third, it has been demonstrated that RGS9-2 and RGS7 proteins differ in their substrate selectivity for members of the Gi/o family of proteins with RGS9 being more potent than RGS7 in regulating GTPase activity of $G\alpha_i$ (34). This is expected to lead to the selective reduction in regulation of the $G\alpha_i$ mediated signaling pathways at the postsynaptic density. Taken together, the R7 RGS complex remodeling upon decrease in RGS9-2 concentration suggests that global changes in G protein inactivation specificity would occur, rather than a simple decrease in RGS9-2 specific GAP activity in the striatum. These global changes in signaling events may in fact play in RGS9 knockout mice, where increased behavioral responses to the stimulation of μ-opioid and D2 dopamine receptors (27, 28, 205) might stem from the global remodeling rather than simple loss of RGS9-2's GAP activity. This model and its role in the sensitization of μ-opioid and D2 dopamine receptors observed in RGS9-2 knockout mice therefore requires further investigation. It is clear however, that changes in multiple signaling pathways beyond that normally controlled by RGS9-2 alone occurs upon its elimination, providing additional complexity to the molecular

mechanisms that determine basal ganglia responses to the action of psycostimulants and addictive drugs.

Acknowledgments:

The authors would like to thank Dr. Chris Pennell (University of Minnesota Cancer Center) for invaluable assistance with conducting BiaCore experiments, Ms. Ekaterina Posokhova for performing transcardiac perfusions in mice, Dr. Bill Simonds (NIDDKD/NIH) for the generous gift of the RGS7 and R7BP antibodies, Mr. Perry Anderson for his help with illustrations, Dr. Vadim Arshavsky (Duke University Eye Center), Drs. Yan Cao, Ikuo Masuho, Keqiang Xie and Ms. Posokhova for critical comments on the manuscript. The work was supported by the National Institute of Health, National Institute on Drug Abuse grant DA021743 (KAM), National Research Service Awards T32 DA007097 and F31 DA024944 (GRA) and Spanish Ministry of Education and Science grant BFU-2006-01896/BFI and Junta de Comunidades de Castilla-La Mancha grant PAI08-0174-6967 (RL).

Chapter 5 - R7BP complexes with RGS9-2 and RGS7 in the striatum differentially control motor learning and locomotor responses to cocaine

Abbreviated title: Behavioral role of R7BP and RGS7 in striatal signaling

Garret R. Anderson[1]*, Yan Cao[1]*, Steve Davidson[2], Hai V. Truong[2], Marco Pravetoni[1], Mark J. Thomas[2], Kevin Wickman[1], Glenn J. Jr. Giesler[2], Kirill A. Martemyanov[1]

From the [1]Department of Pharmacology, University of Minnesota, Minneapolis, MN 55455, and [2]Department of Neuroscience, University of Minnesota, Minneapolis, MN 55455

* Equally contributed to this work

Content taken from the manuscript in press:

Anderson, G.R.*, Cao Y.*, Davidson S., Pravetoni M., Truong H.V., Thomas M., Wickman, K., Giesler G.J., Martemyanov K.A. R7BP complexes with RGS9-2 and RGS7 in the striatum differentially control motor learning and locomotor responses to cocaine. *Neuropsychopharmacology*, *In Press*.

Specific contributions: GRA data is presented in Figures 5.3, 5.5, 5.6.

In the striatum, signaling via G protein-coupled dopamine receptors mediates motor and reward behavior, and underlies the effects of addictive drugs. The extent of receptor responses is determined by RGS9-2•Gβ5 complexes, a striatally-enriched regulator that limits the lifetime of activated G proteins. Recent studies suggest that the function of RGS9-2•Gβ5 is controlled by the association with an additional subunit, R7BP, making elucidation of its contribution to striatal signaling essential for understanding molecular mechanisms of behaviors mediated by the striatum.

In this study we report that elimination of R7BP in mice results in motor coordination deficits and greater locomotor response to morphine administration consistent with the essential role played by R7BP in maintaining RGS9-2 expression in the striatum. However, in contrast to previously reported observations with RGS9-2 knockouts, mice lacking R7BP do not exhibit higher sensitivity to locomotor-stimulating effects of cocaine. Using a striatum-specific knockdown approach, we demonstrate that the sensitivity of motor stimulation to cocaine is instead dependent on RGS7, whose complex formation with R7BP is dictated by RGS9-2 expression. These results indicate that dopamine signaling in the striatum is controlled by concerted interplay between two RGS proteins, RGS7 and RGS9-2, which are balanced by a common subunit, R7BP.

♦ *Introduction*

Dopamine signaling in the striatum plays an essential role in controlling movement and reward processing (206, 207). Dopamine acts on two classes of G protein coupled receptors (GPCR) which are differentially expressed in distinct populations of striatal neurons. While G_{olf}-coupled D1 receptors are mainly expressed on striatonigral ("direct") medium spiny neurons, $G_{i/o}$-coupled D2 receptors are enriched in striatopallidal ("indirect") neurons (reviewed in (208). It is commonly accepted that balancing of signaling via these dopamine receptors is essential for the striatal control of movement and reward (209, 210). At a molecular level, the extent of dopamine action is controlled both pre-synaptically via regulating the rate of the dopamine release and re-uptake, and post-synaptically by regulating the lifetime of receptor activity. Both of these mechanisms contribute essentially to normal dopamine signaling homeostasis (5) and their dysregulation has been implicated in a range of disorders including Parkinson's and Huntington's diseases, schizophrenia and drug addiction (211, 212).

Regulator of G protein Signaling (RGS) proteins are powerful negative regulators of GPCR responses that act to accelerate the inactivation of G protein α subunits, thereby controlling the duration of receptor signaling (23, 149). A member of the RGS family, RGS9-2, is selectively enriched in the striatum where it has been linked to the regulation of D2 receptor activity (27, 111, 137). Mice lacking RGS9-2 develop motor coordination deficits (135) and show enhanced locomotor responses to the administration of psychostimulants and opioids (27, 28, 111). Furthermore, inactivation of RGS9-2 in mice (111) has been reported to exacerbate the development of haloperidol-induced tardive dyskinesia, whereas its over-expression in rats and primates (136) substantially reduced L-dopa induced involuntary movements in Parkinsonian models. Together, these and other observations (see (213) for a comprehensive review) firmly establish RGS9-2 in the control of striatal dopamine signaling. However, details linking these behavioral observations to RGS9-2 function at the molecular level have been very limited.

RGS9-2 forms as a constitutive complex with the type 5 G protein β subunit (Gβ5) (reviewed in 73), and knockout of Gβ5 in mice leads to the elimination of detectable RGS9-2 (79). More recently, a third subunit in the complex was identified, the membrane anchor R7 Binding Protein (R7BP) (76, 93) which further controls the proteolytic stability of RGS9-2•Gβ5 complex and targets it to postsynaptic sites (92). In addition to RGS9-2, both Gβ5 and R7BP in the striatum form complexes with another equally abundant RGS9-2-like protein, RGS7 (214). RGS9-2•Gβ5 and RGS7•Gβ5 are coupled to R7BP in a dynamic fashion and changes in RGS9-2 levels (*e.g.* as seen in RGS9 knockout mice) dramatically affect RGS7•Gβ5 localization. The behavioral implications of this complexity in subunit organization of RGS complexes are unknown however, largely due to the lack of functional understanding of the role of R7BP and RGS7 in the basal ganglia.

In this study, we report that elimination of R7BP results in motor coordination deficits and increase in sensitivity to locomotor-stimulating effects of morphine, consistent with the essential role of R7BP in maintaining RGS9-2 expression in the striatum. However, in contrast to previously reported observations with RGS9-2 knockouts, the motor responses of mice lacking R7BP to acute or chronic administration of cocaine were indistinguishable from their wild-type littermates. Using a striatum-specific knockdown approach, we demonstrate that the sensitivity of locomotor responses to cocaine is instead dependent on the expression of RGS7. These results suggest that dopamine signaling in the striatum is controlled by concerted interplay between two RGS proteins, RGS7 and RGS9-2, and balanced by a common subunit, R7BP.

♦ ***Materials and Methods***

Animals

All studies were carried out in accordance with the National Institute of Health guidelines and were granted formal approval by the Institutional Animal Care and Use Committee of the University of Minnesota. The generation of R7BP knockouts ($R7BP^{-/-}$) was described earlier (92). The line was out-bred onto the C57BL/6J background for 5 generations. All animals used for comparison of $R7BP^{-/-}$ and $R7BP^{+/+}$ genotypes were littermates derived from heterozygous breeding pairs. Viral rescue studies were done with R7BP-/- mice derived from homozygous R7BP-/- breeding pairs. Striatal knockdown studies for RGS7 were done with C57BL/6J mice purchased from Charles River and bred in house. Mice were housed in groups on a 12h light/dark cycle with food and water available *ad libitum*. Only males 2-4 month of age were used.

Accelerating rotarod test

Motor coordination was measured by performance on an accelerating rotarod device equipped with drums sized for mice (IITC Life Science). Littermate mice were habituated in the test room for an hour before the testing. Three trials were performed per day over 3 days for a total of nine trials for each animal. After placing a mouse on the rod, it was accelerated from 4 to 27 rpm in 5 min. The endurance of mice on the rotarod was measured by time to fall to the floor of the apparatus, or to turn around one full revolution while hanging onto the drum.

Open field locomotor activity test

Littermate mice were habituated to the test room environment for 1 h before testing. Activity studies were performed in Plexiglas chamber (ENV-515; 170 W×170 L ×120 H; Med Associates, Inc., St. Albans, VT, USA) as described previously (215). Briefly, a mouse was placed in the center of the open field arena and allowed to freely move for 60 or 180 min while being tracked by an automated tracking system consisting of three 16 beam infrared arrays, the data from which were analyzed by Open Field Activity software (Med Associates, Inc.). Infrared beam break data was collected in 5 min bins and used to extract ambulatory activity (crossing 4 beams within 500 ms), and distance traveled. Beam break activity in the absence of consecutive crossing of beams was defined as steretotypic movements. Thigmotaxis (wall hugging) for each subject was determined by dividing the distance traveled in the 7.5-cm wide perimeter of the environment by the total distance traveled during the 180-min session. The number of entries in the central area of the open field (total area minus outer perimeter) was also measured. In studies measuring the

dose-dependence effects of the drugs on the locomotor activity, mice were injected subcutaneously with saline or increasing doses of morphine or cocaine (1 mg/kg, 5 mg/kg, 10 mg/kg, and 20 mg/kg) freshly dissolved in saline with a 3-d interval between the injections. For cocaine sensitization studies, mice were injected intraperitonealy daily: first with saline for three days, followed by 10 mg/kg cocaine for 5 consecutive days. Animal activity was measured immediately upon the injection and recorded for 60 (cocaine) or 180 (morphine) min.

RNA Interference and generation of recombinant lentiviruses

RGS7 expression was down-regulated by short interfering RNA duplexes similarly as described before for R7BP (50). Target regions in RGS7 were identified and miR RNAi sequences were designed by BLOCK-iT RNAi Designer Program (Invitrogen). RNAi molecules were generated by targeting the 427-447 coding region of the RGS7 gene (RNAi 427, sequence CTAGAGCTAGCAGATTATGAA). Synthetic double stranded oligonucleotides corresponding to the designed RNAi was cloned into the pcDNA6.2GW/EmGFP vector in the middle of the micro RNA 155 (miR155) sequence supplied as a part of the BLOCK-iT Lentiviral Pol II miR RNAi expression system kit (Invitrogen). In the pcDNA6.2GW/EmGFP vector, the chimeric miR155-RGS7 sequence is located under the control of the cytomegalovirus promoter co-cistronically with EmGFP. Upon processing in the cells by the endogenous machinery, the construct is used to produce anti-RGS7 RNA duplex (miRNA-αRGS7). The control construct (miRNA-CTR) was created by cloning a scrambled sequence AAATGTACTGCGCGTGGAGAC into the miR155 environment identically as described for miRNA-αRGS7. The expression cassette was transferred to the lentiviral shuttle vector pLenti6/V5-DEST vector (Invitrogen) by Gateway recombination following the kit instructions.

For the generation of infectious lentiviral particles, pLenti6/V5-DEST vectors containing miRNA-αRGS7 or miRNA-CTR cassettes were co-transfected with the packaging plasmid mixture (kindly provided by Prof. Didier Trono of the Universite de Geneve): pRSV-Rev, pMDLg/pRRE, and pMD2.G into 293T cells using Lipofectamine 2000 (Invitrogen). Fifteen T75 flasks were used to produce each batch of lentivirus. Virus containing media was collected 60–65 h after transfection, filtered through a 0.45-μm filter (Millipore), and viral particles were enriched by passing through a 500 kDa MidiKros hollow fiber column (Spectrum Labs) until the retentate volume was reduced to approximately 20-25 ml of media. Viral particles were further concentrated as described (156) with some modifications. Virus-containing supernatants were carefully loaded on 60% OptiPrep (Sigma) cushion (150–200 μl) in 30-ml conical-bottomed

polyallomer centrifuge tubes (Beckman) and centrifuged at 20,000 x *g* for 2.5 h at 4 °C using a swinging bucket rotor SW-28 (Beckman). The medium just above the media/OptiPrep interface was carefully removed and discarded. The residual medium containing OptiPrep and viruses (~ 200 µl each tube) were resuspended by gentle pipetting, aliquoted and stored at -80 °C until use.

Infectious titers of viruses were determined by Lenti-X qRT-PCR Titration Kit (Clontech). Our preparations of concentrated lentiviral stocks consistently yielded titers of 1-3 x 10^{12} viral copies/ml. The titers of all viral stocks were equalized by adjusting the concentration of viral particles to 1 x 10^{12}/ml.

Cell culture and gene transfer

293T cells were obtained from ATCC and cultured at 37°C and 5% CO_2 in DMEM supplemented with antibiotics, 10% fetal bovine serum, 1 mM sodium pyruvate, and 1X non-essential amino acids (Invitrogen). Cells were transfected at ~70% confluency, using Lipofectamine 2000 (Invitrogen) according to the manufacturer's protocol. The ratio of Lipofectamine to DNA used was 4 µl:2.5 µg/4 cm^2 of cell surface. The cells were grown for 24–48 h post-transfection, washed with PBS, lysed in SDS sample buffer (62 mM Tris, 10% glycerol, 2%SDS, 5% β-mercaptoethanol) and analyzed by 4–20% PAGE (Cambrex).

Primary cultures of striatal neurons were essentially prepared as described previously (50). The cultures were transduced by lentiviral constructs on day 4 *in vitro* by adding specified amounts of high-titer lentiviral stocks and the media was substituted on day 7. On day 14, cells were washed with PBS, and lysed in SDS sample buffer.

Preparation of striatal tissue extracts, immunoprecipitation, and Western blotting

The whole brain from 25 day old C57/BL6 mice was quickly removed and placed in an ice-cold slicing solution containing 85mM NaCl, 2.5mM KCl, 4mM $MgCl_2$, 1mM NaH_2PO_4, 25mM $NaHCO_3$, 25mM glucose, and 75mM sucrose (all from Sigma, St. Louis, MO) pH=7.4. Coronal slices were prepared 300 µm in thickness using a Vibratome 3000 Plus sectioning system (Vibratome, St Louis, MO). Striatal tissue was then isolated corresponding to viral type injection and directly frozen in liquid N_2. Cellular lysates were prepared by homogenizing the isolated striatal tissue by sonication in immunoprecipitation (IP) buffer (1X PBS, 150 mM NaCl, 1% Triton X-100, Complete (Roche) protease inhibitors) followed by 15 minute centrifugation at 14,000 x *g*. The resulting extract was used for protein concentration determination by BCA assay (Pierce, Rockford, IL). Immunoprecipitation of R7BP was performed using 2 µg of sheep anti-

R7BP NT antibody, 10 µl of protein G beads (GE Healthcare, Little Chalfont, UK), added to the extracts. The mixtures were incubated for 1 hour, washed three times with IP buffer, and proteins bound to the beads were eluted with SDS sample buffer. Samples were resolved on SDS-PAGE gel, transferred onto PVDF membrane and subjected to Western blot analysis using HRP conjugated secondary antibodies and ECL West Pico (Pierce) detection system.
Analysis was performed using sheep anti-RGS9-2 CT (76), rabbit anti-RGS7 (7RC1), rabbit anti-R7BP antibodies (generously provided by William Simonds, National Institute of Diabetes and Digestive and Kidney Diseases, National Institutes of Health), and mouse monoclonal anti-β-actin (clone AC-15) antibodies purchased from Sigma.

Immunohistochemistry

Immunohistochemical detection of R7BP protein in striatal sections was performed following transcardiac perfusion of mice with 4% paraformaldehyde in 0.1 M sodium phosphate buffer (pH=7.4). Brains were cryoprotected with 30% sucrose in PBS for 2 days at 4ºC, and embedded in Tissue-Tek OCT compound (Sakura Finetek). Embedded brains were frozen on dry ice, and 40 micrometer frozen sections were obtained by cryostat (Leica). Sections were blocked in PT1 (PBS with 0.1% Triton X-100 and 10% goat serum) for 1 hour and incubated with 1:500 dilution of primary rabbit anti-R7BP (TRS) antibody (generously provided by William Simonds, National Institute of Diabetes and Digestive and Kidney Diseases, National Institutes of Health) in PT2 (PBS with 0.1% Triton X-100 and 2% goat serum) for 1 hour, washed four times for 5 minutes in PT2, and incubated with fluorophore-conjugated secondary antibodies (goat anti-rabbit Alexa 546, 1:1000) in PT2 for 1 h. Sections were washed three times for 5 minutes in PT2 and mounted in Mounting Medium (Pierce). Images were taken by an Olympus Fluoview 1000 confocal microscope.

Stereotaxic injections

The development of the method for the regional delivery of substances to the brains of embryonic and neonatal mice is described in detail in a separate publication (Davidson et. al, Brain Research, *in press*). Briefly, five-day-old mice were anaesthetized with ice-induced hypothermia, and concentrated lentivirus at a titer of $1x10^{12}$ copies/ml was bilaterally injected into the striatum at four depth locations per hemisphere with the tip of the microinjection pipette advanced to the deepest (ventral) position for the first injection; additional injections were made every 0.3 mm while withdrawing the injection needle. The coordinates for each bilateral injection from Bregma

were: anterior 0.35 mm, mediolateral 1.75 mm, at dorsoventral depths of 3.1, 2.8, 2.5, and 2.2 mm. For animals used for behavior analysis, 90 nl of virus was injected at each depth point and the same virus was delivered bilaterally. For verification of protein expression or knockdown, 600 nL of virus was used at each depth point and each animal received both control and experimental viruses on different sides. We used an electrode manipulator stand with a 3-axis manipulator and an attached microinjection unit (Model 1449 Electrode Manipulator Stand, Model 1460-61 Electrode Manipulator, and Model 5000 Microinjection Unit; David Kopf Instruments, Tejunga, CA). A 5 μL manual syringe (Model 95, Hamilton, Reno, NV) was fitted to the Microinjection Unit. Pipette tips were pulled from thin walled borosilicate glass capillary tubes (with filament) with an outer diameter of 1.0 mm and inner diameter of 0.76 mm. Pipettes were backfilled with light mineral oil and then forward filled with concentrated lentiviruses or 4% Fluorogold (Fluorochrome, LLC, Denver, CO) for visualization of injection site. All injections were done with the aid of a dissecting microscope. Anatomical borders in the perinatal mouse brain were determined with the assistance of the Atlas of the Developing Mouse Brain (216).

Statistical analysis

Data were analyzed by statistics suite of SigmaPlot v. 11 software package. Two-way analysis of variance (ANOVA) was conducted on all of the experimental data using genotype and session number as grouping factors. Dunnet's and Tukey's posthoc tests were employed for individual pair wise comparisons. Biochemical data were evaluated by Student's t-test. All data are reported as means with SEM values.

♦ ***Results***

Knockout of R7BP does not alter basal behavioral responses of mice.

Mice with constitutive disruption of the R7BP gene ($R7BP^{-/-}$) were born in accordance to normal Mendelian inheritance patterns, had overall appearance indistinguishable from their wild-type littermates, were fertile, and exhibited normal development. By age 2-4 months, adult $R7BP^{-/-}$ mice reach normal body weights (27.21±0.96 g male and 21.56±0.62 g female) compared to their wild-type $R7BP^{+/+}$ littermates (27.12±0.96 g male and 21.54±0.47 g female). Analysis of $R7BP^{-/-}$ behavior in the open field test revealed normal baseline ambulatory activities both in terms of total distance traveled during the assay (Figure 5.1B) and average movement velocities (Figure 5.1C). As compared to their wild-type littermates, $R7BP^{-/-}$ mice exhibited the same level of heightened exploratory behavior when introduced into the novel environment of the chamber. Both genotypes also showed indistinguishable habituation behavior, reducing their locomotor activities 5-6 fold during the first two hours (Figure 5.1A). Similarly, $R7BP^{-/-}$ mice were indistinguishable from their wild-type littermates for their repetitive (Figure 5.1 D, E) and anxiety-related (Figure 5.1 F, G) behaviors. In summary, these experiments demonstrate overall preservation of basal behavioral responses in $R7BP^{-/-}$ mice.

Loss of R7BP in the striatum leads to motor coordination deficits.

Consistent with the severe reduction in the levels of RGS9-2 in the striatum upon the loss of R7BP (92), evaluation of $R7BP^{-/-}$ mice in the accelerated rotarod test revealed their substantial deficiencies in gross motor coordination (Figure 5.2). Indeed, during three days of training, $R7BP^{-/-}$ mice showed consistently lower performance reflected by the shorter durations of balancing on the rotating drum (Figure 5.2A). Analysis of the data by two-way ANOVA indicated statistically significant effects of genotype (Figure 5.2B; $F_{(1,180)}=23.955, p<0.001$) and trial number (not shown; $F_{(8,180)}=20.601$, $p<0.001$). Post-hoc pair-wise comparison of animals grouped by trial day (Figure 5.2C) showed that while prominent upon later trials, the genotype differences in animal performance upon initial trials was absent, suggesting that slower rates of motor learning might underlie deficiencies of $R7BP^{-/-}$ mice in the rotarod test.

Similar motor coordination deficits are also observed upon elimination of R7BP's binding partner, RGS9-2 (135), which is selectively enriched in the striatum (reviewed by (213). Because R7BP was reported to be broadly expressed in the central nervous system, including regions outside of the striatum (76, 100) that are also implicated in controlling motor coordination

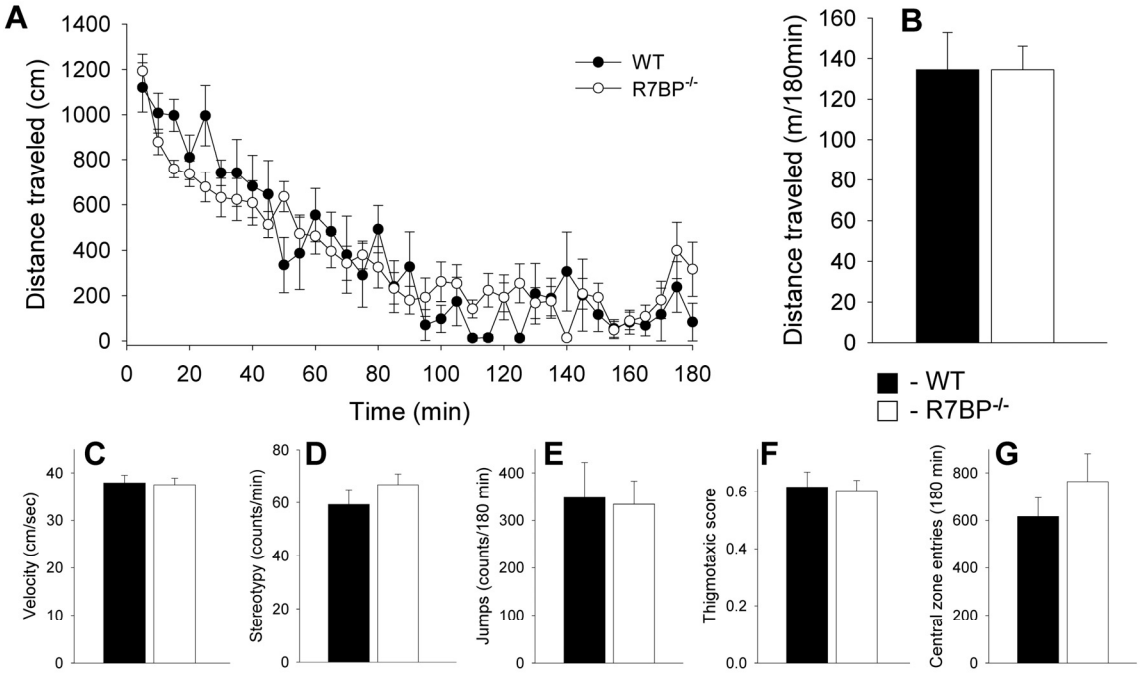

Figure 5.1: Baseline behavioral characteristics are unaltered upon the genetic elimination of R7BP. R7BP knockout ($R7BP^{-/-}$) mice (n = 9) and Wild-type ($R7BP^{+/+}$, WT) litter mates (n = 5) were placed in locomotor open field test chamber for 3 h and analyzed for the behavioral traits. (**A)** Distance traveled per 5 min interval was plotted over the 3 h evaluation period, or used to calculate cumulative total distance traveled (**B**). Quantification and one-way ANOVA reveals that travel velocity (**C**), stereotypy counts (**D**), vertical jumps (**E**), thigmotaxis (**F**), and central zone entries (**G**) between $R7BP^{-/-}$ and $R7BP^{+/+}$ littermates were all statistically insignificant.

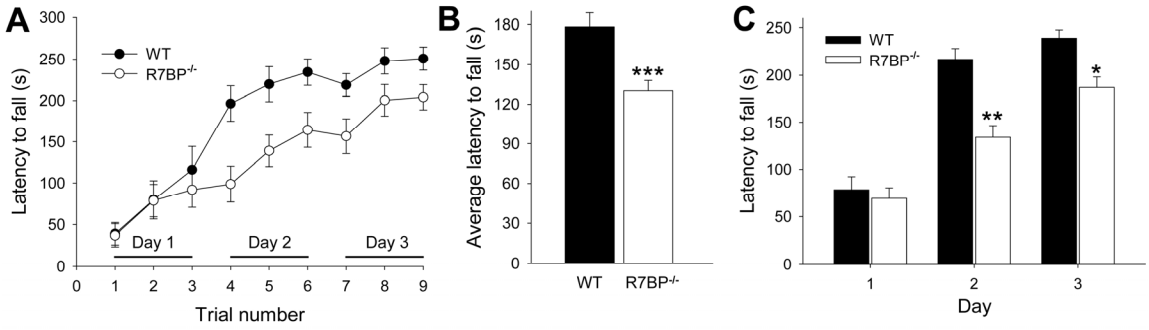

Figure 5.2: R7BP$^{-/-}$ mice show deficits in motor coordination. (**A**) R7BP$^{-/-}$ mice (n = 14) and WT (n = 8) were analyzed using an accelerated rotarod test over the course of 3 trials/d, for 3 d totaling 9 trials. A two-way ANOVA (trial by genotype) revealed a significant effect of genotype ($F_{(1,180)} = 23.96$, $p < 0.001$), and a significant effect of trial ($F_{(8,180)} = 20.601$, $p < 0.001$). (**B**) Calculated mean latencies to fall off the rotarod across all trials were 178 ± 8 (R7BP$^{+/+}$) and 130 ± 6 (R7BP$^{-/-}$). (**C**) The mean latency to fall off the rotarod for the 3 trials for each day revealed a significant difference between genotypes on days 2 ($p<0.01$) and 3 ($p<0.05$).

(*e.g.* cerebellum), we next addressed the specific contribution of striatal R7BP to the observed phenotype. This was achieved by selective expression of R7BP in the dorsal striatum of $R7BP^{-/-}$ mice by lentiviral gene transfer in neonatal mice. Before proceeding with the lentiviral manipulations in multiple mice to be used for behavioral experiment, control experiments evaluating the efficiency of the approach have been conducted with a few animals. Following confirmation of selective targeting of the striatal regions in neonatal mice by Fluorogold injections, test $R7BP^{-/-}$ mice received unilateral injections of lentiviral particles driving the expression of R7BP into the dorsal striatum (Figure 5.3A). The contra-lateral sides of the same animals were injected with the control virus expressing the unrelated LacZ gene. When mice reached maturity, their striatal regions within the injection plane were collected and analyzed for the expression of proteins of interest. Data presented in Figure 5.3B revealed significant restoration of R7BP expression in $R7BP^{-/-}$ mice driven by lentiviral gene transfer. Consistent with earlier findings (50, 92), lentiviral expression of R7BP resulted in the selective up-regulation of the RGS9-2, but not RGS7 levels presumably due to the increased proteolytic protection of the complex. Furthermore, lentiviral expressed R7BP co-precipitated with RGS9-2, and to a lesser extent with RGS7, an indication of its functional status.

Having confirmed the effectiveness of the manipulations, for subsequent behavioral studies neonatal mice were injected bilaterally (Figure 5.3A). The mice were tested two months after the injection at which point the expression of R7BP in the striatum was verified immunohistochemically (Figure 5.3C). Data presented in Figure 5.3D and Figure 5.3E illustrate that selective restoration of R7BP expression in the striatum leads to a substantial improvement of mouse performance in the rotarod test. Two-way ANOVA analysis (trial by virus) revealed a significant increase in fall latencies upon R7BP restoration into the striatum ($F_{(1,125)} = 16.41$, $p < 0.001$), and a significant effect of trial ($F_{(8,125)} = 9.62$, $p < 0.001$) These data suggest that the motor coordination deficits observed in R7BP knockout mice are likely explained by the de-regulation of RGS9-2 function in the striatum.

Elimination of R7BP does not alter locomotor responses to cocaine administration

In addition to motor coordination deficits, mice lacking RGS9-2 have been reported to develop hypersensitivity to the administration of drugs that increase synaptic dopamine concentration such as amphetamine, cocaine and morphine (27, 28, 111). We have therefore evaluated how elimination of R7BP affects locomotor responses of mice to psychostimulant administration. Both $R7BP^{-/-}$ and $R7BP^{+/+}$ littermates demonstrated progressively greater

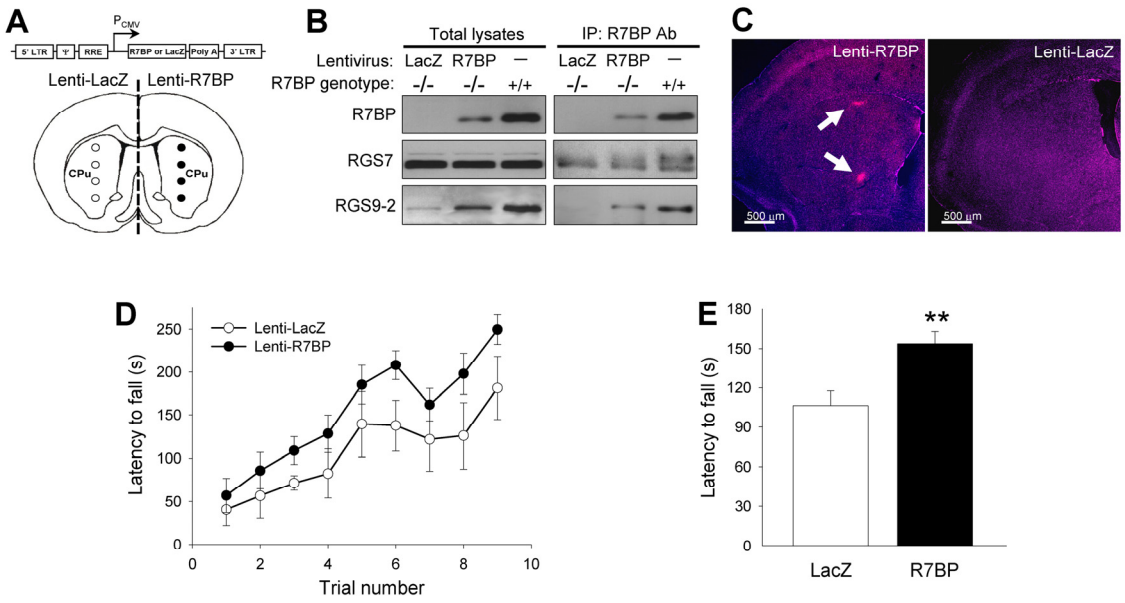

Figure 5.3: Lentiviral expression of R7BP in dorsal striatum improves the performance of R7BP$^{-/-}$ in rotarod task. (**A**) Strategy for lentivirus mediated protein expression *in vivo.* Shown schematic illustrates location of lentiviral construct (R7BP or LacZ) unilateral injection sites at 4 depth points (3.1, 2.8, 2.5, and 2.2 mm) of 5-day old R7BP$^{-/-}$ mice. Each side of the brain received four 600 nL injections with either R7BP or control LacZ lentivirus within the striatum. (**B**) Verification of lentiviral mediated R7BP expression in adult R7BP$^{-/-}$ mice. *Left*, at post natal day 25, brains were sectioned at 300 μm thickness, and LacZ/R7BP lentivirus injected striatum was isolated. Tissue sections were solubilized with 1% Triton X-100 containing buffer, lysates containing 10 μg of total protein were separated on 12.5% PAGE, and subjected to Western blotting with the indicated antibodies. Shown is maximal expression of R7BP detected within the isolated sections. Maximal R7BP mediated lentiviral expression in R7BP$^{-/-}$ mice was estimated to be ~30% of the corresponding levels in R7BP$^{+/+}$ mice using quantitative densitometry analysis with ImageJ software package. *Right*, Western blot analysis of proteins immunoprecipitated from the total lysates by 2 μg of anti-R7BP antibodies. (**C**) Verification of R7BP expression around injection sites by immunostaining with anti-R7BP antibodies. R7BP$^{-/-}$ mice were injected with 90 nL of R7BP expressing lentivirus at each injection site, and sacrificed at 10-weeks. 1-2 injection sites in a 40 μm brain slice were typically observed in one plane, with 2 injection sites shown. (**D**) Performance of R7BP$^{-/-}$ mice bilaterally injected with either R7BP (n = 9) or LacZ (n = 5) expressing lentiviruses (90 nL per injections site) in rotarod test. ANOVA analysis revealed a significant increase in fall latencies upon R7BP restoration into the striatum ($F_{(1,125)} = 16.41$, $p < 0.001$) as well as a significant effect of trial ($F_{(8,125)} = 9.62$, $p < 0.001$) (**E**). Mean latency to fall off the rotarod across all trials. Values are: 106 ± 11 seconds for LacZ injected mice and 153 ± 9 seconds for mice injected with R7BP expressing virus.

responses to increasing doses of cocaine (Figure 5.4A; $F_{(4,80)}$=23.128, p<0.001). However, no statistically significant differences in locomotor activities were observed between genotypes at any concentration of the tested drug (two way ANOVA: $F_{(1,80)}$=3.248, p=0.075). Similarly, repetitive administration of the same cocaine concentration caused pronounced sensitization of mice to the drug, yet no differences in the extent of the responses were observed (Figure 5.4B). Two-way ANOVA revealed that a significant effect of trial number ($F_{(7,211)}$=13.382, p<0.001) with no effect of genotype ($F_{(1,211)}$=0.3023, p=0.858). Because morphine, in addition to increasing dopamine levels via pre-synaptic mechanisms, can also affect signaling in striatal neurons directly by acting at μ-opioid receptors (reviewed in (217), we have additionally compared locomotor responses of mice to morphine (Figure 5.5). $R7BP^{-/-}$ mice robustly responded to the administration of 5 mg/kg of morphine, a dose that failed to elicit a response in wild- type littermates. A significant difference in sensitivity remained apparent at the higher dose of 10 mg/kg, while no differences was observed at the maximal concentration used (20 mg/kg). These data suggest that like RGS9-2 deficient mice, $R7BP^{-/-}$ mice show increased sensitivity to the administration of morphine, however unlike $RGS9^{-/-}$ mice, $R7BP^{-/-}$ mice do not have altered responses to the locomotor stimulating effects of cocaine.

Striatal RGS7 plays an essential role in controlling cocaine locomotor sensitization

Since RGS9 deficient mice demonstrate increased cocaine sensitivity (27), the lack of the effect of R7BP ablation observed in this study is unexpected since the levels of RGS9 in striatum of $R7BP^{-/-}$ mice are severely reduced and mice exhibit similar coordination deficits in rotarod test. However, in addition to RGS9-2, striatal R7BP also binds to RGS7, and the abundance of RGS7-R7BP complexes is determined by RGS9-2 concentration (214). This prompted us to evaluate the contribution of striatal RGS7 to determining the sensitivity of cocaine action on locomotor activity. Our strategy was to analyze behavioral responses of mice with selective reduction in RGS7 expression in the striatum. We first screened for synthetic micro-RNA constructs identified sequences that could effectively knock down RGS7 expression in transfected cell lines, and the construct that showed the highest efficiency (miR-427) was used to generate a recombinant lentivirus. As with the lentiviral rescue of R7BP, effectiveness of RGS7 knockdown virus was also tested at the *in vivo* level (Figure 5.6A, B). Given the large volume of the dorsal striatum and the expected confinement of knockdown effectiveness limited to the population of neurons around the site of injection, test experiments were performed with a larger amount of the viruses than normally used for the behavioral experiments (~6-fold increase). Furthermore, for the

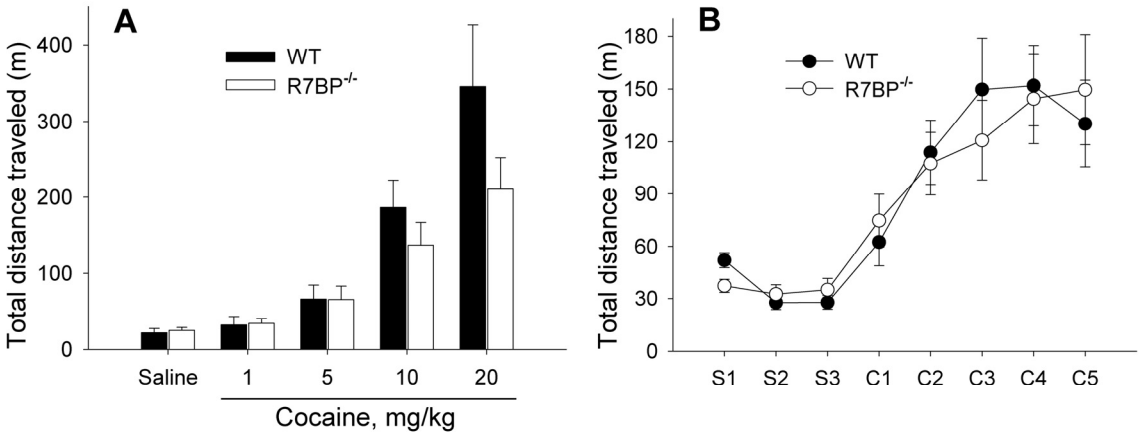

Figure 5.4: Locomotor stimulatory effects of cocaine administration are unaltered in R7BP$^{-/-}$ mice. (**A**) Locomotor activities of R7BP$^{-/-}$ (n=12) and their wild-type litermates (n= 6) in response to increasing dozes of cocaine administration. Mice were injected with saline or cocaine (1, 5, 10, 20 mg/kg) and their locomotor activity was measured for one hour. A two-way ANOVA (dose by genotype) revealed a significant effect of dose ($F_{(4,80)}$=23.128, p<0.001) but no effect of genotype ($F_{(1,80)}$=3.248, p=0.075). (**B**) Locomotor sensitization to repeated cocaine administration. Mice of both genotypes (n=18 for R7BP$^{-/-}$ and n=11 for R7BP$^{+/+}$) were given daily injections of saline for 3 days (S1-3), followed by 5 daily injections of 10 mg/kg cocaine (C1-C5). A two-way ANOVA (day by genotype) revealed a significant effect of trial number ($F_{(7,211)}$ = 13.38, p < 0.001) as both groups demonstrated higher locomotor activity with each additional cocaine injection (*i.e.*, sensitization). However, there was no statistical difference between genotypes ($F_{(1,211)}$ = 0.30, p = 0.86).

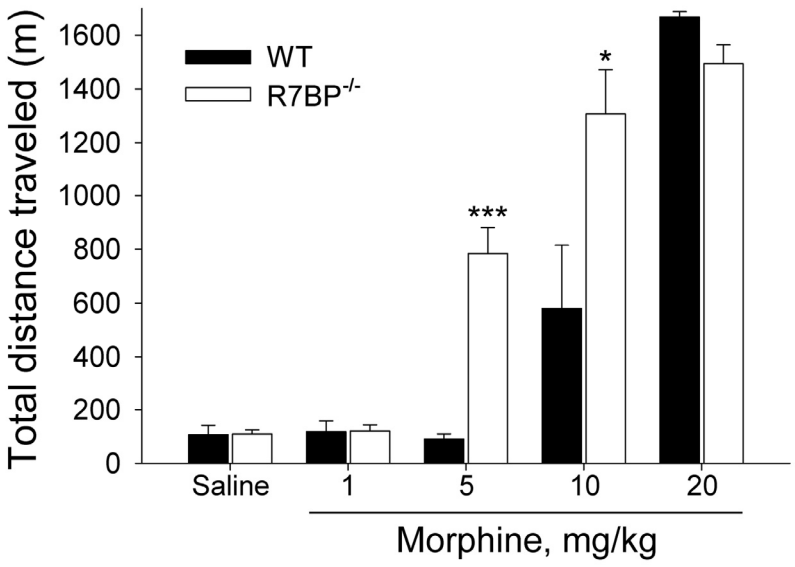

Figure 5.5: Increased sensitivity of R7BP$^{-/-}$ mice to locomotor stimulating effects of morphine. Mice of both genotypes (n = 9 for R7BP$^{-/-}$ and n = 5 for R7BP$^{+/+}$) were injected with increasing doses of morphine (1, 5, 10, 20 mg/kg) and their locomotor activities were measured for 3 hours following the administration. Total distance traveled in locomotor chambers was plotted as bar graphs. A two-way ANOVA (dose x genotype) revealed both a significant effect of dose ($F_{(4,60)} = 71.99$, $p < 0.001$), and a significant effect of genotype ($F_{(1,60)} = 14.37$, $p < 0.001$).

subsequent biochemical analysis, sections located only around the plane of viral injections were selected. As demonstrated in Figure 5.6A, unilateral injection of test mice with lentivirus targeting RGS7 resulted in approximately 35% down-regulation of RGS7 as compared to its expression in the contra-lateral side that received control virus (Figure 5.6A). Importantly, knockdown of RGS7 did not affect the expression of RGS9-2, R7BP (Figure 5.6A), or their complex formation as evidenced by co-immunoprecipitation experiments (Figure 5.6B). It is likely that the biochemical measures reflect an aggregate change in RGS7 concentration in the region. Based on the immunohistochemical data of the lentiviral mediated expression of R7BP (Figure 5.3C) we expect uneven changes in RGS7 concentration across the striatum where areas of high knockdown efficiency are intermingled with areas of intact RGS7 expression. Therefore, behavioral alterations caused by this genetic manipulation are likely to stem from the effects on the select striatal circuitries rather than global change in the function of the entire striatum.

When injected bilaterally into mouse striatum, virus targeting RGS7, but not control virus, led to a dramatic increase in the sensitivity of the mice to the locomotor-sensitizing action of cocaine (Figure 5.6C). At the same time, no difference in the baseline (saline-injected) locomotion was recorded between animal groups. A two-way ANOVA analysis revealed a significant effect of trial ($F_{(7,128)} = 13.48$, $p < 0.001$) as both groups demonstrated higher locomotor activity with each additional cocaine injection (*i.e.*, sensitization) and a significant effect of genotype ($F_{(1,125)} = 28.67$, $p < 0.001$). Evaluation of mice in the rotarod task revealed that knockdown of RGS7 did not negatively affect motor learning behavior (Figure 5.6D). The mean latency ± S.E.M. to fall off the rotarod across all trials were 175±6.5 (Control KD) and 194±5.8 (RGS7 KD). Overall, these results suggest that RGS7 expression level in the striatum substantially contribute to determining the sensitivity of the reinforcing effects of cocaine.

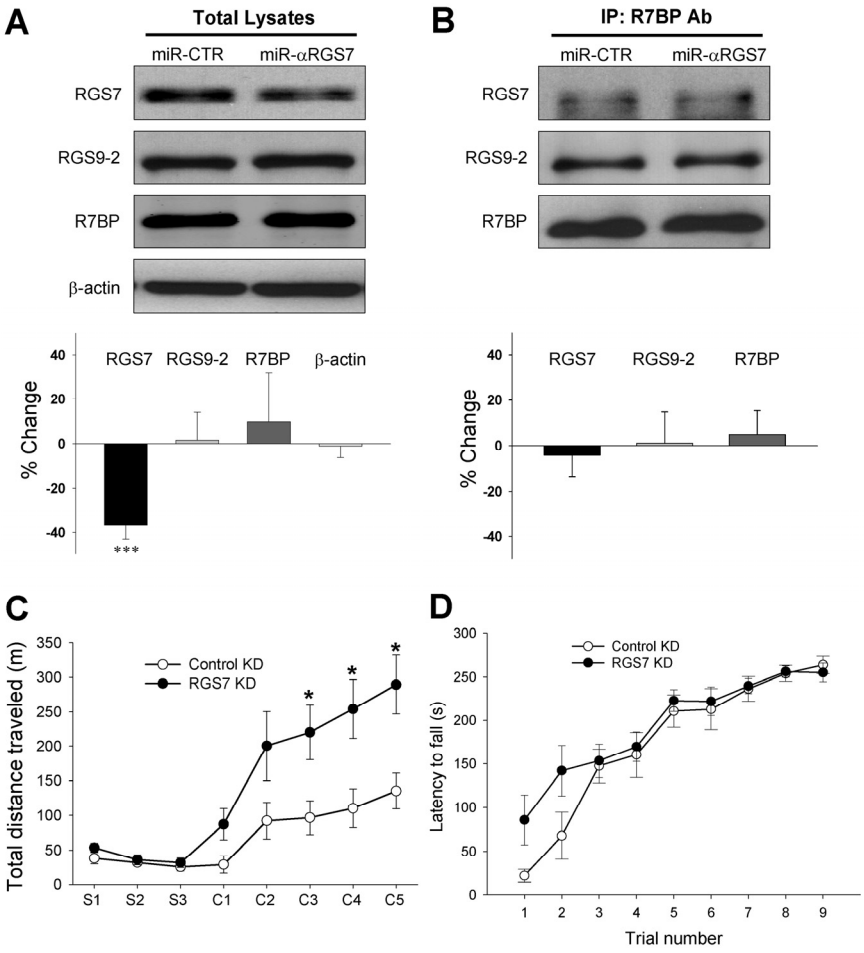

Figure 5.6: Knockdown of RGS7 in the striatum potentiates locomotor sensitization to cocaine. (**A**) Verification of lentivirus-mediated RGS7 knockdown in wild-type mice. Wild-type C57BL/6J mice at postnatal day 5 were unilaterally injected (600 nL per injection site) with either miR-CTR control knockdown lentivirus or miR-αRGS7 knockdown lentivirus into the striatum similarly as illustrated in Figure 5.3A. At post natal day 25, brains were sectioned at 300 μm thickness, and miR-αRGS7/miR-CTR lentivirus injected striatum was isolated. Tissue sections were solubilized with 1% Triton X-100 containing IP buffer, 10 μg of total extracted protein was separated on 12.5% PAGE, and subjected to Western blot analysis with the indicated antibodies. Shown is a representative maximal effect of RGS7 knockdown from one 300 μm section. Quantification of protein change shown below was performed from three maximal RGS7 knockdown sections per brain, with two mice analyzed. Image analysis was performed by densitometry quantification using ImageJ software package. Analysis of the data by Student's t-test, revealed a statistically significant difference between relative changes in RGS7 protein compared to β-actin (***, $p < 0.001$), and no difference ($p >> 0.05$) in relative changes between RGS9-2 and R7BP protein compared to β-actin. (**B**) Western blot analysis of proteins immunoprecipitation by 2 μg of anti-R7BP antibody from the total lysates shown in panel (A). Densitometry quantification of proteins present in immunoprecipitated fractions are presented below. (**C**) Knockdown of RGS7 potentiates sensitization to cocaine. Wild-type mice were bilaterally injected with either RGS7 knockdown (RGS7 KD) lentivirus (n = 10) or control knockdown (Control KD) lentivirus (n = 8) with 90 nL per injections site. At 8-weeks of age, animals were given daily injections of saline for 3 days (S1-3), followed by 5 daily injections of 10 mg/kg cocaine (C1-5). A two-way ANOVA (day by genotype) revealed a significant effect of day ($F_{(7,128)} = 13.48$, $p < 0.001$) as both groups demonstrated higher locomotor activity with each additional cocaine injection (i.e. sensitization). Injection of RGS7 KD viruse produced higher responses compared to the injection with control virus ($F_{(1,125)} = 28.67$, $p < 0.001$) and a higher degree of sensitization as indicated by a statistically significant interaction between day and virus ($F_{(7,128)} = 2.42$, $p = 0.023$). (**D**) RGS7 knockdown does not hamper motor learning performance as tested by rotarod test. A two-way ANOVA (trial by genotype) followed by Tukey's test revealed a significant improvement in rotarod performance with RGS7 knockdown virus within the first 2 trials ($p < 0.05$), but no significant difference between the two viruses for the remaining trials.

♦ ***Discussion***

In this study, we describe an underlining complexity governing the regulation of dopamine-mediated signaling in the striatum by macromolecular complexes of two members of G protein signaling regulators: RGS7 and RGS9-2. Previous studies have established an essential role of RGS9-2 as a negative regulator of D2 and μ-opioid receptor function by demonstrating that its elimination in mice leads to: (i) enhanced locomotor activity and reward behavior in response to drugs such as cocaine (27, 111), and morphine (28, 110), (ii) motor coordination/learning deficits (135), and (iii) an increased susceptibility to antipsychotic- (111) and L-DOPA- (136) induced tardive dyskinesia. Recent studies suggest that RGS9-2 does not function by itself but rather acts as a part of a macromolecular complex with its two subunits: Gβ5 and membrane anchor R7BP (see 213, 218, 219 for recent reviews). Association with both Gβ5 and R7BP is important for controlling proteolytic stability of RGS9-2 (50, 79) and hence determines its expression levels in the striatum (92). Binding to R7BP is also required for targeting of RGS9-2 to plasma membrane and postsynaptic density compartments of striatal neurons (92). In striatal neurons, R7BP is associated not only with RGS9-2 but also with a second RGS protein, RGS7. Furthermore, the extent of RGS7-R7BP coupling was found to be dictated by RGS9-2 concentration as both RGS proteins compete for R7BP binding (214).

By characterizing $R7BP^{-/-}$ mice in this study, we sought to establish the physiological role of R7BP and its constituent RGS complexes in regulation of behaviors controlled by striatal signaling. We utilized behavioral paradigms of motor coordination/learning and locomotor responses to opiate and dopamine receptor stimulation that have proven to be useful for delineating RGS9-2 functions in the past. We found that mice lacking R7BP exhibit deficits in motor coordination similar to that previously reported for $RGS9^{-/-}$ mice (135), consistent with the dramatic reduction in the levels of RGS9-2 observed upon the elimination of R7BP (92). Since lentivirus-mediated restoration of R7BP specifically in the striatum was accompanied by partial rescue of RGS9-2 expression and led to a considerable improvement of mouse performance in rotarod task, we conclude that normal motor coordination requires concerted contributions of striatal RGS9-2 and R7BP.

Interestingly, we find that deficits in motor coordination of $R7BP^{-/-}$ mice are not apparent upon initial trials but become pronounced when animals undergo several training sessions. Since cortico-striatal circuitry is becoming increasingly accepted as a substrate that mediates motor learning (220-222), these observations suggest that RGS9-2•R7BP complexes play an important

role in striatum-mediated motor learning. Similar, although more pronounced, deficits in striatal motor learning are observed upon elimination of NMDA receptor R1 subunit specifically in RGS9-2 expressing neurons (223) and upon perturbation of molecules known to modulate NMDAR function in the striatum such as Cdk5 (224) and PKA (225). Furthermore, motor coordination deficits are observed in several mouse models with altered dopamine signaling including knockout of the dopamine transporter (226), along with D1 (227) and D2 (228) receptor knockouts. Given that dopamine-mediated control of glutamate responses through NMDA receptors is altered in $RGS9^{-/-}$ mice (111) and that RGS9-2 has been found to be localized in the postsynaptic densities of spines (92) where it could physically interact with NMDA receptors via α-actinin 2 adapter (113), it seems plausible to suggest that RGS9-2•R7BP complexes are involved in modulation of dopamine signaling to the NMDAR that controls motor learning in the striatum.

Evaluation of $R7BP^{-/-}$ mice for their locomotor responses to opioids and cocaine have revealed striking differences that help dissect the underlying complexity of G protein signaling in the striatum. We found that while elimination of R7BP resulted in a predicted increase in the sensitivity of mice to the locomotor effects of morphine (28, 110), their responses to cocaine administration remained unaltered, contrary to what is expected based on the severe reduction in RGS9-2 levels in $R7BP^{-/-}$ mice (92) and reports that RGS9-2 acts as a negative regulator of the D2 receptor signaling (27). The insights provided by these observations are two-fold. First, they suggest that the increased sensitivity to opioids and psychostimulants previously reported for $RGS9^{-/-}$ mice likely involves simultaneous alteration of μ-opioid and D2 dopamine receptor signaling regulation that appears to be differentially controlled by distinct R7BP-RGS complexes in the striatum. Second, they indicate that regulation of dopamine signaling sensitivity is dictated not merely by RGS9-2 concentrations but rather involves three-way balancing between RGS9-2, RGS7 and R7BP. Indeed, consistent with this idea, we find that manipulation of RGS7 levels in the striatum leads to profound changes in the locomotor responses of mice to cocaine administration. We have recently reported that both RGS9-2 and RGS7 are equally abundant in the striatum, yet they are unequally coupled to R7BP (214). While a high percentage of RGS9-2 (~80%) is coupled to R7BP, only ~ 20% of RGS7 exists in such complexes. Further, we have found that a decrease in RGS9-2 concentration triggers remodeling of these complexes, which enhances RGS7 coupling to R7BP. The extreme case of such remodeling is observed in $RGS9^{-/-}$ mice where in the absence of RGS9-2, most of the striatal RGS7 is bound to R7BP, leading to a substantial change in its subcellular localization. Therefore, enhanced cocaine sensitivity reported

for RGS9$^{-/-}$ mice might involve alteration of RGS7 function and thus must be considered when interpreting molecular mechanisms underlying sensitivity to cocaine action.

How can an increase in RGS7-R7BP coupling and decrease in RGS7 levels both lead to the same outcome of increased locomotor stimulation by cocaine? Mechanistically, we think this can be explained by the fact that both RNAi manipulation and increased coupling to R7BP observed in RGS9$^{-/-}$ mice leads to the reduction of free RGS7. At this time, the signaling pathways regulated by RGS7 in the striatum are unknown and it appears possible that alteration of its function could affect the sensitivity of psychostimulant action by modulating GPCRs distinct from the ones controlled by RGS9-2. Furthermore, the effects of R7BP on the ability of R7 RGS proteins to regulate GPCR signaling are far from being understood, and it is possible that R7BP might regulate RGS9-2 and RGS7 function very differently. It is equally possible that R7BP exerts differential effects on the same RGS protein depending on the specific GPCR involved. Indeed, R7BP has been shown to stimulate the activity of RGS7 on Gi/o-coupled muscarinic M2 receptor (93, 99) but was also found to inhibit the regulation of the Gq-coupled muscarinic M3 receptor (82). Finally, GAP activities of RGS9-2 and RGS7 differ in their potencies towards individual members of the Gi/o class of G proteins (34), and changes in RGS protein recruitment to postsynaptic sites is expected to alter both the extent and selectivity of GPCR regulation in the region. Therefore, future studies will need to establish GPCR specificity of RGS7 and RGS9-2 action in the striatum as well as the contribution of R7BP in establishing this selectivity.

In summary, the results presented in this study for the first time implicates RGS7 in controlling the sensitivity of cocaine induced locomotor sensitization, describes the role of R7BP in controlling striatal motor functions, and provides evidence implicating interactions between two RGS proteins in control of dopamine signaling in the striatum.

Acknowledgements

We thank Dr. William Simonds (NIH/NIDDKD) for the generous gift of anti- RGS7 and R7BP antibodies. This work was supported by NIH grants DA021743 (KAM), DA026405 (KAM), F31 DA024944 (GRA), NS047399 (GJG), F31 NS047399 (SD), MH061933 (KW), DA011806 (KW), DA019666 (MJT), and a McKnight Land-Grant Award (K.A.M),

Thesis Synopsis

G protein-coupled receptor (GPCR) signaling pathways mediate the transmission of signals from the extracellular environment to the generation of cellular responses, a process that is critically important for neurons and neurotransmitter action. The ability to promptly respond to rapidly changing stimulation requires timely inactivation of G proteins, a process controlled by a family of specialized proteins known as regulators of G protein signaling (RGS). The R7 group of RGS proteins (R7 RGS) has received special attention due to their pivotal roles in the regulation of a range of crucial neuronal processes such as vision, motor control, reward behavior and nociception in mammals. Four proteins in this group: RGS6, RGS7, RGS9 and RGS11 share a common molecular organization of three modules: (i) the catalytic RGS domain, (ii) a GGL domain that recruits $G\beta_5$, an outlying member of the G protein beta subunit family, and (iii) a DEP/DHEX domain that mediates interactions with the membrane anchor protein R7BP (R7 family Binding Protein).

One member of the R7 RGS family, RGS9-2 has been previously implicated as an essential modulator of signaling through neuronal dopamine and opioid G protein coupled receptors. These studies have shown that the abundance of RGS9-2 alters the sensitivity of these signaling pathways, which play a critical role in controlling the locomotor and reward systems in the striatal region of the brain. RGS9-2 is specifically expressed in striatal neurons where it forms complexes with R7BP, which ultimately affects several critical properties of RGS9-2. First, it is this interaction with R7BP which is necessary for determining the subcellular targeting of RGS9-2, as in native neurons these complexes are found on the plasma membrane and in the specialized neuronal compartment of excitatory synapses, the postsynaptic density. Upon the elimination of R7BP this localization patterning of RGS9-2 is lost. Secondly, R7BP plays an important role in determining the proteolytic stability of RGS9-2. We have found that manipulation of R7BP expression levels both in striatal cultures and *in vivo*, correlates with a respective change in RGS9-2 expression. R7BP mediated alteration in RGS9-2 post-translational stability was implicated as the mechanism of action, as measurements of RGS9-2 degradation kinetics in cells indicates that R7BP markedly reduces the rate of RGS9-2 proteolysis. Analysis of the molecular determinants that mediate R7BP•RGS9-2 binding to result in this proteolytic protection mechanism, have identified that the binding site for R7BP in RGS proteins is formed by pairing of the DEP domain with the R7H domain (a domain of previously unknown function)

which interact with the four putative alpha helices of R7BP's core. Further, we found that RGS9-2 possesses specific degradation determinants not found in other R7 RGS proteins, which target it for constitutive destruction by lysosomal cysteine proteases, and that shielding of these determinants by R7BP controls RGS9-2 expression. These findings provide a mechanism for the selective regulation of RGS9-2 expression levels in striatal neurons amongst other R7 RGS proteins, allowing for the potential modulation of specific GPCR pathways controlled by RGS9-2. This mechanism is perhaps best observed during ontogenetic development, as changes in R7BP mRNA ultimately determine the expression of RGS9-2•Gβ5•R7BP complexes at postsynaptic sites in unison with increased signaling demands at mature synapses.

Since RGS9-2 is selectively dependent on R7BP for its localization and proteolytic stability, and other striatal R7 RGS proteins appear to be unaffected by manipulations in R7BP expression, we decided to further characterize how these R7 RGS containing complexes are organized. We found that under normal conditions two equally abundant striatal R7 RGS proteins, RGS9-2 and RGS7, are unequally coupled to the R7BP subunit which is present in complex predominantly with RGS9-2 rather than with RGS7. However, upon changes in neuronal activity the subunit composition of these complexes in the striatum undergoes rapid and extensive remodeling. Changes in the neuronal excitability or oxygenation status resulting in extracellular calcium entry, uncouples RGS9-2 from R7BP, triggering its selective degradation. Concurrently, released R7BP binds to mainly intracellular RGS7 and recruits it to the plasma membrane and the postsynaptic density. These observations introduce activity dependent remodeling of R7 RGS complexes as a new molecular plasticity mechanism in striatal neurons and suggest a general model for achieving rapid posttranslational subunit rearrangement in multi-subunit complexes.

This remodeling process is best observed upon the genetic elimination of RGS9, which drives all available R7BP towards complex formation with RGS7. Thus, by eliminating RGS9, not only is RGS9 controlled GPCR signaling pathways affected, but those controlled by RGS7 as well. Considering reports using RGS9 knockout mice that have implicated the role of RGS9-2 in controlling G protein-coupled dopamine and opioid receptors that mediate motor and reward behavior, the question arises as to the role of modulation of RGS7 function in controlling these behaviors. We addressed this question by analyzing R7BP knockout mice against the striatal mediated behaviors observed in RGS9 knockouts, namely motor coordination deficits, increased sensitivity to μ-opioid receptor stimulation, and enhanced locomotor affects upon the delivery of psychostimulants such as cocaine. Since the function of RGS9-2 is controlled by its association

with R7BP, we would predict that the elimination of R7BP would lead to similar alterations in striatal physiology for RGS9 controlled pathways. While at the same time, RGS7 would be largely unaffected by the elimination of R7BP, thus RGS7 controlled pathways would predictably remain unaltered. Using this rationale, we report that elimination of R7BP in mice results in motor coordination deficits and greater locomotor response to morphine administration consistent with the essential role of RGS9 in controlling these behaviors and the critical role played by R7BP in maintaining RGS9-2 expression in the striatum. However, in contrast to previously reported observations with RGS9-2 knockouts, mice lacking R7BP do not exhibit higher sensitivity to locomotor-stimulating effects of cocaine, suggesting a role for RGS7 in controlling dopamine sensitivity. Using a striatum-specific knockdown approach, we demonstrate that the sensitivity of motor stimulation to cocaine is indeed dependent on RGS7 function. These results indicate that dopamine signaling in the striatum is controlled by concerted interplay between two RGS proteins, RGS7 and RGS9-2, which are balanced by a common subunit, R7BP. Thus, the molecular mechanisms controlling the extent of RGS9-2 coupling to R7BP can have a two-fold effect on R7 RGS proteins function: 1) Determining the expression level of RGS9-2 and subsequent control of RGS9-2 controlled pathways, and 2) Determining the extent of RGS7•R7BP coupling and the extent of RGS7 trafficking to plasma membrane and post-synaptic density sites.

To fully understand these observations, the future directions of this work requires a greater understanding of the specificity of the GPCR pathways that R7 RGS proteins control, and the role of R7BP in determining this specificity. It is clear however, that this study reveals an underlining complexity that needs to be considered when manipulating the protein expression level of one member of macro-molecular complexes. The homologous protein family and their respective complex components as a whole can be subsequently affected, leading to alterations in their function as well as that of the intended target. Therefore, the work presented in this dissertation serves as a reminder to the importance of why interpretation of genetic knockout data needs to be considered in this context.

References

1. Hepler, J.R. and A.G. Gilman, G proteins. *Trends in Biochemical Sciences*, 1992. **17**: p. 383-387.
2. Neer, E.J., G proteins: critical control points for transmembrane signals. *Protein Sci*, 1994. **3**(1): p. 3-14.
3. Cabrera-Vera, T.M., J. Vanhauwe, T.O. Thomas, M. Medkova, A. Preininger, M.R. Mazzoni and H.E. Hamm, Insights into G protein structure, function, and regulation. *Endocr Rev*, 2003. **24**(6): p. 765-81.
4. Offermanns, S., G-proteins as transducers in transmembrane signalling. *Prog Biophys Mol Biol*, 2003. **83**(2): p. 101-30.
5. Gainetdinov, R.R., R.T. Premont, L.M. Bohn, R.J. Lefkowitz and M.G. Caron, Desensitization of G protein-coupled receptors and neuronal functions. *Annu Rev Neurosci*, 2004. **27**: p. 107-44.
6. Clapham, D.E. and E.J. Neer, G protein *gamma subunits. *Annual Review of Pharmacology and Toxicology*, 1997. **37**: p. 167-203.
7. Bourne, H.R. and L. Stryer, G proteins: The target sets the tempo. 1992. **358**: p. 541-543.
8. Berman, D.M. and A.G. Gilman, Mammalian RGS proteins: Barbarians at the gate. *Journal of Biological Chemistry*, 1998. **273**(3): p. 1269-1272.
9. Burchett, S.A., Regulators of G protein signaling: A bestiary of modular protein binding domains. *Journal of Neurochemistry*, 2000. **75**(4): p. 1335-1351.
10. Ross, E.M. and T.M. Wilkie, GTPase-activating proteins for heterotrimeric G proteins: Regulators of G protein signaling (RGS) and RGS-like proteins. *Annual Review of Biochemistry*, 2000. **69**: p. 795-827.
11. Sun, X., K.M. Kaltenbronn, T.H. Steinberg and K.J. Blumer, RGS2 is a mediator of nitric oxide action on blood pressure and vasoconstrictor signaling. *Mol Pharmacol*, 2005. **67**(3): p. 631-9.
12. Rahman, Z., J. Schwarz, S.J. Gold, V. Zachariou, M.N. Wein, K.H. Choi, A. Kovoor, C.K. Chen, R.J. DiLeone, S.C. Schwarz, D.E. Selley, L.J. Sim-Selley, M. Barrot, R.R. Luedtke, D. Self, R.L. Neve, H.A. Lester, M.I. Simon and E.J. Nestler, RGS9 modulates dopamine signaling in the basal ganglia. *Neuron*, 2003. **38**(6): p. 941-52.
13. Chen, C.K., M.E. Burns, W. He, T.G. Wensel, D.A. Baylor and M.I. Simon, Slowed recovery of rod photoresponse in mice lacking the GTPase accelerating protein RGS9-1. 2000. **403**(6769): p. 557-560.
14. Xie, Z., T.R. Geiger, E.N. Johnson, J.K. Nyborg and K.M. Druey, RGS13 acts as a nuclear repressor of CREB. *Mol Cell*, 2008. **31**(5): p. 660-70.
15. Cifelli, C., R.A. Rose, H. Zhang, J. Voigtlaender-Bolz, S.S. Bolz, P.H. Backx and S.P. Heximer, RGS4 regulates parasympathetic signaling and heart rate control in the sinoatrial node. *Circ Res*, 2008. **103**(5): p. 527-35.
16. Iankova, I., C. Chavey, C. Clape, C. Colomer, N.C. Guerineau, N. Grillet, J.F. Brunet, J.S. Annicotte and L. Fajas, Regulator of G protein signaling-4 controls fatty acid and glucose homeostasis. *Endocrinology*, 2008. **149**(11): p. 5706-12.
17. Cho, H., C. Park, I.Y. Hwang, S.B. Han, D. Schimel, D. Despres and J.H. Kehrl, Rgs5 targeting leads to chronic low blood pressure and a lean body habitus. *Mol Cell Biol*, 2008. **28**(8): p. 2590-7.
18. Martin-McCaffrey, L., F.S. Willard, A.J. Oliveira-dos-Santos, D.R. Natale, B.E. Snow, R.J. Kimple, A. Pajak, A.J. Watson, L. Dagnino, J.M. Penninger, D.P. Siderovski and S.J. D'Souza, RGS14 is a mitotic spindle protein essential from the first division of the mammalian zygote. *Dev Cell*, 2004. **7**(5): p. 763-9.

19. Huang, X., Y. Fu, R.A. Charbeneau, T.L. Saunders, D.K. Taylor, K.D. Hankenson, M.W. Russell, L.G. D'Alecy and R.R. Neubig, Pleiotropic phenotype of a genomic knock-in of an RGS-insensitive G184S Gnai2 allele. *Mol Cell Biol*, 2006. **26**(18): p. 6870-9.
20. Krispel, C.M., D. Chen, N. Melling, Y.J. Chen, K.A. Martemyanov, N. Quillinan, V.Y. Arshavsky, T.G. Wensel, C.K. Chen and M.E. Burns, RGS expression rate-limits recovery of rod photoresponses. *Neuron*, 2006. **51**(4): p. 409-16.
21. Wettschureck, N. and S. Offermanns, Mammalian G proteins and their cell type specific functions. *Physiol Rev*, 2005. **85**(4): p. 1159-204.
22. Farfel, Z., H.R. Bourne and T. Iiri, The expanding spectrum of G protein diseases. *New England Journal of Medicine*, 1999. **340**(13): p. 1012-1020.
23. Burchett, S.A., Psychostimulants, madness, memory... and RGS proteins? *Neuromolecular Med*, 2005. **7**(1-2): p. 101-27.
24. Hooks, S.B., K. Martemyanov and V. Zachariou, A role of RGS proteins in drug addiction. *Biochem Pharmacol*, 2008. **75**(1): p. 76-84.
25. Burns, M.E. and V.Y. Arshavsky, Beyond counting photons: trials and trends in vertebrate visual transduction. *Neuron*, 2005. **48**(3): p. 387-401.
26. Koelle, M.R. and H.R. Horvitz, EGL-10 regulates G protein signaling in the C. elegans nervous system and shares a conserved domain with many mammalian proteins. *Cell*, 1996. **84**(1): p. 115-25.
27. Rahman, Z., J. Schwarz, S.J. Gold, V. Zachariou, M.N. Wein, K.H. Choi, A. Kovoor, C.K. Chen, R.J. DiLeone, S.C. Schwarz, D.E. Selley, L.J. Sim-Selley, M. Barrot, R.R. Luedtke, D. Self, R.L. Neve, H.A. Lester, M.I. Simon and E.J. Nestler, RGS9 modulates dopamine signaling in the basal ganglia. 2003. **38**(6): p. 941-952.
28. Zachariou, V., D. Georgescu, N. Sanchez, Z. Rahman, R. DiLeone, O. Berton, R.L. Neve, L.J. Sim-Selley, D.E. Selley, S.J. Gold and E.J. Nestler, Essential role for RGS9 in opiate action. 2003. **100**(23): p. 13656-13661.
29. Garzon, J., A. Lopez-Fando and P. Sanchez-Blazquez, The R7 subfamily of RGS proteins assists tachyphylaxis and acute tolerance at mu-opioid receptors. *Neuropsychopharmacology*, 2003. **28**(11): p. 1983-90.
30. Gold, S.J., Y.G. Ni, H.G. Dohlman and E.J. Nestler, Regulators of G-protein signaling (RGS) proteins: Region- specific expression of nine subtypes in rat brain. *Journal of Neuroscience*, 1997. **17**(20): p. 8024-8037.
31. Rose, J.J., J.B. Taylor, J. Shi, M.I. Cockett, P.G. Jones and J.R. Hepler, RGS7 is palmitoylated and exists as biochemically distinct forms. *Journal of Neurochemistry*, 2000. **75**(5): p. 2103-2112.
32. He, W., L.S. Lu, X. Zhang, H.M. El Hodiri, C.K. Chen, K.C. Slep, M.I. Simon, M. Jamrich and T.G. Wensel, Modules in the photoreceptor RGS9-1.G*5L GTPase-accelerating protein complex control effector coupling, GTPase acceleration, protein folding, and stability. *Journal of Biological Chemistry*, 2000. **275**(47): p. 37093-37100.
33. Skiba, N.P., K.A. Martemyanov, A. Elfenbein, J.A. Hopp, A. Bohm, W.F. Simonds and V.Y. Arshavsky, RGS9-G*5 substrate selectivity in photoreceptors - Opposing effects of constituent domains yield high affinity of RGS interaction with the G protein-effector complex. *Journal of Biological Chemistry*, 2001. **276**(40): p. 37365-37372.
34. Hooks, S.B., G.L. Waldo, J. Corbitt, E.T. Bodor, A.M. Krumins and T.K. Harden, RGS6, RGS7, RGS9, and RGS11 stimulate GTPase activity of Gi family G-proteins with differential selectivity and maximal activity. *Journal of Biological Chemistry*, 2003: p. M211382200.
35. Witherow, D.S., Q. Wang, K. Levay, J.L. Cabrera, J. Chen, G.B. Willars and V.Z. Slepak, Complexes of the G protein subunit G*5 with the regulators of G protein

signaling RGS7 and RGS9 - Characterization in native tissues and in transfected cells. *Journal of Biological Chemistry*, 2000. **275**(32): p. 24872-24880.
36. Wall, M.A., D.E. Coleman, E. Lee, J.A. IÞiguez-Lluhi, B.A. Posner, A.G. Gilman and S.R. Sprang, The structure of the G protein heterotrimer Gi*1*1gamma2. 1995. **83**: p. 1047-1058.
37. McEntaffer, R.L., M. Natochin and N.O. Artemyev, Modulation of transducin GTPase activity by chimeric RGS16 and RGS9 regulators of G protein signaling and the effect or molecule. 1999. **38**(16): p. 4931-4937.
38. Snow, B.E., A.M. Krumins, G.M. Brothers, S.F. Lee, M.A. Wall, S. Chung, J. Mangion, S. Arya, A.G. Gilman and D.P. Siderovski, A G protein gamma subunit-like domain shared between RGS11 and other RGS proteins specifies binding to G*5 subunits. 1998. **95**(22): p. 13307-13312.
39. Posner, B.A., A.G. Gilman and B.A. Harris, Regulators of g protein signaling 6 and 7 - Purification of complexes with G*5 and assessment of their effects on G protein-mediated signaling pathways. *Journal of Biological Chemistry*, 1999. **274**(43): p. 31087-31093.
40. Martemyanov, K.A. and V.Y. Arshavsky, Kinetic approaches to study the function of RGS9 isoforms. *Methods Enzymol*, 2004. **390**: p. 196-209.
41. Soundararajan, M., F.S. Willard, A.J. Kimple, A.P. Turnbull, L.J. Ball, G.A. Schoch, C. Gileadi, O.Y. Fedorov, E.F. Dowler, V.A. Higman, S.Q. Hutsell, M. Sundstrom, D.A. Doyle and D.P. Siderovski, Structural diversity in the RGS domain and its interaction with heterotrimeric G protein alpha-subunits. *Proc Natl Acad Sci U S A*, 2008. **105**(17): p. 6457-62.
42. Slep, K.C., M.A. Kercher, W. He, C.W. Cowan, T.G. Wensel and P.B. Sigler, Structural determinants for regulation of phosphodiesterase by a G protein at 2.0 □. 2001. **409**(6823): p. 1071-1077.
43. De Alba, E., L. De Vries, M.G. Farquhar and N. Tjandra, Solution structure of human GAIP (G* interacting protein): A regulator of G protein signaling. *Journal of Molecular Biology*, 1999. **291**(4): p. 927-939.
44. Moy, F.J., P.K. Chanda, M.I. Cockett, W. Edris, P.G. Jones, K. Mason, S. Semus and R. Powers, NMR structure of free RGS4 reveals an induced conformational change upon binding Galpha. *Biochemistry*, 2000. **39**(24): p. 7063-73.
45. Chen, Z., C.D. Wells, P.C. Sternweis and S.R. Sprang, Structure of the rgRGS domain of p115RhoGEF. *Nature Structural Biology*, 2001. **8**(9): p. 805-809.
46. Cabrera, J.L., F. De Freitas, D.K. Satpaev and V.Z. Slepak, Identification of the G*5-RGS7 protein complex in the retina. *Biochemical and Biophysical Research Communications*, 1998. **249**(3): p. 898-902.
47. Makino, E.R., J.W. Handy, T.S. Li and V.Y. Arshavsky, The GTPase activating factor for transducin in rod photoreceptors is the complex between RGS9 and type 5 G protein * subunit. *Proceedings of the National Academy of Sciences of the United States of America*, 1999. **96**(5): p. 1947-1952.
48. Cheever, M.L., J.T. Snyder, S. Gershburg, D.P. Siderovski, T.K. Harden and J. Sondek, Crystal structure of the multifunctional Gbeta5-RGS9 complex. *Nat Struct Mol Biol*, 2008. **15**(2): p. 155-62.
49. Ponting, C.P. and P. Bork, Pleckstrin's repeat performance: a novel domain in G-protein signaling?, in *Trends in Biochemical Sciences*. 1996. p. 245-246.
50. Anderson, G.R., A. Semenov, J.H. Song and K.A. Martemyanov, The membrane anchor R7BP controls the proteolytic stability of the striatal specific RGS protein, RGS9-2. *J Biol Chem*, 2007. **282**(7): p. 4772-81.

51. Chatterjee, T.K., Z.Y. Liu and R.A. Fisher, Human RGS6 gene structure, complex alternative splicing, and role of N terminus and G protein gamma-subunit-like (GGL) domain in subcellular localization of RGS6 splice variants. *Journal of Biological Chemistry*, 2003. **278**(32): p. 30261-30271.
52. Zhang, K., K.A. Howes, W. He, J.D. Bronson, M.J. Pettenati, C.K. Chen, K. Palczewski, T.G. Wensel and W. Baehr, Structure, alternative splicing, and expression of the human RGS9 gene. 1999. **240**(1): p. 23-34.
53. Granneman, J.G., Y. Zhai, Z. Zhu, M.J. Bannon, S.A. Burchett, C.J. Schmidt, R. Andrade and J. Cooper, Molecular Characterization of Human and Rat RGS 9L, a Novel Splice Variant Enriched in Dopamine Target Regions, and Chromosomal Localization of the RGS 9 Gene. *Molecular Pharmacology*, 1998. **54**: p. 687-694.
54. Rahman, Z., S.J. Gold, M.N. Potenza, C.W. Cowan, Y.G. Ni, W. He, T.G. Wensel and E.J. Nestler, Cloning and characterization of RGS9-2: A striatal-enriched alternatively spliced product of the RGS9 gene. *Journal of Neuroscience*, 1999. **19**(6): p. 2016-2026.
55. Giudice, A., J.A. Gould, K.B. Freeman, S. Rastan, P. Hertzog, I. Kola and R.C. Iannello, Identification and characterization of alternatively spliced murine Rgs11 isoforms: genomic structure and gene analysis. *Cytogenet Cell Genet*, 2001. **94**(3-4): p. 216-24.
56. Chatterjee, T.K. and R.A. Fisher, Mild heat and proteotoxic stress promote unique subcellular trafficking and nucleolar accumulation of RGS6 and other RGS proteins - Role of the RGS domain in stress-induced trafficking of RGS proteins. *Journal of Biological Chemistry*, 2003. **278**(32): p. 30272-30282.
57. Thomas, E.A., P.E. Danielson and J.G. Sutcliffe, RGS9: A regulator of G-protein signalling with specific expression in rat and mouse striatum. *Journal of Neuroscience Research*, 1998. **52**(1): p. 118-124.
58. Arshavsky, V.Y., C.L. Dumke, Y. Zhu, N.O. Artemyev, N.P. Skiba, H.E. Hamm and M.D. Bownds, Regulation of transducin GTPase activity in bovine rod outer segments. 1994. **269**: p. 19882-19887.
59. Angleson, J.K. and T.G. Wensel, Enhancement of rod outer segment GTPase accelerating protein activity by the inhibitory subunit of cGMP phosphodiesterase. 1994. **269**: p. 16290-16296.
60. Otto-Bruc, A., B. Antonny and T.M. Vuong, Modulation of the GTPase activity of transducin. Kinetic studies of reconstituted systems. 1994. **33**: p. 15215-15222.
61. Skiba, N.P., J.A. Hopp and V.Y. Arshavsky, The effector enzyme regulates the duration of G protein signaling in vertebrate photoreceptors by increasing the affinity between transducin and RGS protein. *Journal of Biological Chemistry*, 2000. **275**(42): p. 32716-32720.
62. Martemyanov, K.A., J.A. Hopp and V.Y. Arshavsky, Specificity of G protein-RGS protein recognition is regulated by affinity adapters. 2003. **38**(6): p. 857-862.
63. Watson, A.J., A. Katz and M.I. Simon, A fifth member of the mammalian G-protein *-subunit family. Expression in brain and activation of the *2 isotype of phospholipase C. 1994. **269**: p. 22150-22156.
64. Zhang, J.H. and W.F. Simonds, Copurification of brain G-protein *5 with RGS6 and RGS7. *Journal of Neuroscience*, 2000. **20**(3): p. RC59-NIL13.
65. Yoshikawa, D.M., M. Hatwar and A.V. Smrcka, G protein *5 subunit interactions with * subunits and effectors. 2000. **39**(37): p. 11340-11347.
66. Lindorfer, M.A., C.S. Myung, Y. Savino, H. Yasuda, R. Khazan and J.C. Garrison, Differential activity of the G protein *5gamma2 subunit at receptors and effectors. *Journal of Biological Chemistry*, 1998. **273**(51): p. 34429-34436.

67. Mirshahi, T., V. Mittal, H. Zhang, M.E. Linder and D.E. Logothetis, Distinct sites on G protein *gamma subunits regulate different effector functions. *Journal of Biological Chemistry*, 2002. **277**(39): p. 36345-36350.
68. Zhou, J.Y., D.P. Siderovski and R.J. Miller, Selective regulation of N-type Ca channels by different combinations of G-protein */gamma subunits and RGS proteins. *Journal of Neuroscience*, 2000. **20**(19): p. 7143-7148.
69. Maier, U., A. Babich, N. Macrez, D. Leopoldt, P. Gierschik, D. Illenberger and B. Nurnberg, Gbeta 5gamma 2 is a highly selective activator of phospholipid-dependent enzymes. *J Biol Chem*, 2000. **275**(18): p. 13746-54.
70. Fletcher, J.E., M.A. Lindorfer, J.M. DeFilippo, H. Yasuda, M. Guilmard and J.C. Garrison, The G protein beta5 subunit interacts selectively with the Gq alpha subunit. *J Biol Chem*, 1998. **273**(1): p. 636-44.
71. Watson, A.J., A.M. Aragay, V.Z. Slepak and M.I. Simon, A novel form of the G protein * subunit G*5 is specifically expressed in the vertebrate retina. 1996. **271**: p. 28154-28160.
72. Jones, M.B. and J.C. Garrison, Instability of the G-protein *5 Subunit in detergent. *Analytical Biochemistry*, 1999. **268**(1): p. 126-133.
73. Sondek, J. and D.P. Siderovski, Ggamma-like (GGL) domains: new frontiers in G-protein signaling and beta-propeller scaffolding. *Biochemical Pharmacology*, 2001. **61**(11): p. 1329-1337.
74. Snow, B.E., L. Betts, J. Mangion, J. Sondek and D.P. Siderovski, Fidelity of G protein *-subunit association by the G protein gamma-subunit-like domains of RGS6, RGS7, and RGS11. *Proceedings of the National Academy of Sciences of the United States of America*, 1999. **96**(11): p. 6489-6494.
75. Yost, E.A., S.M. Mervine, J.L. Sabo, T.R. Hynes and C.H. Berlot, Live cell analysis of G protein beta5 complex formation, function, and targeting. *Mol Pharmacol*, 2007. **72**(4): p. 812-25.
76. Martemyanov, K.A., P.J. Yoo, N.P. Skiba and V.Y. Arshavsky, R7BP, a novel neuronal protein interacting with RGS proteins of the R7 family. *J Biol Chem*, 2005. **280**(7): p. 5133-6.
77. Hadcock, J.R., M. Ros, D.C. Watkins and C.C. Malbon, Cross-regulation between G-protein-mediated pathways. Stimulation of adenylyl cyclase increases expression of the inhibitory G-protein, Gi*2. 1990. **265**: p. 14784-14790.
78. Kovoor, A., C.K. Chen, W. He, T.G. Wensel, M.I. Simon and H.A. Lester, Co-expression of G*5 enhances the function of two Ggamma subunit-like domain-containing regulators of G protein signaling proteins. *Journal of Biological Chemistry*, 2000. **275**(5): p. 3397-3402.
79. Chen, C.K., P. Eversole-Cire, H.K. Zhang, V. Mancino, Y.J. Chen, W. He, T.G. Wensel and M.I. Simon, Instability of GGL domain-containing RGS proteins in mice lacking the G protein *-subunit G*5. *Proceedings of the National Academy of Sciences of the United States of America*, 2003. **100**(11): p. 6604-6609.
80. Schwindinger, W.F., K.E. Giger, K.S. Betz, A.M. Stauffer, E.M. Sunderlin, L.J. Sim-Selley, D.E. Selley, S.K. Bronson and J.D. Robishaw, Mice with deficiency of G protein gamma3 are lean and have seizures. *Mol Cell Biol*, 2004. **24**(17): p. 7758-68.
81. Lobanova, E.S., S. Finkelstein, R. Herrmann, Y.M. Chen, C. Kessler, N.A. Michaud, L.H. Trieu, K.J. Strissel, M.E. Burns and V.Y. Arshavsky, Transducin gamma-subunit sets expression levels of alpha- and beta-subunits and is crucial for rod viability. *J Neurosci*, 2008. **28**(13): p. 3510-20.

82. Narayanan, V., S.L. Sandiford, Q. Wang, T. Keren-Raifman, K. Levay and V.Z. Slepak, Intramolecular interaction between the DEP domain of RGS7 and the Gbeta5 subunit. *Biochemistry*, 2007. **46**(23): p. 6859-70.
83. Levay, K., J.L. Cabrera, D.K. Satpaev and V.Z. Slepak, G*5 prevents the RGS7-G*o interaction through binding to a distinct Ggamma-like domain found in RGS7 and other RGS proteins. *Proceedings of the National Academy of Sciences of the United States of America*, 1999. **96**(5): p. 2503-2507.
84. Karan, S., H. Zhang, S. Li, J.M. Frederick and W. Baehr, A model for transport of membrane-associated phototransduction polypeptides in rod and cone photoreceptor inner segments. *Vision Res*, 2008. **48**(3): p. 442-52.
85. Deretic, D., A role for rhodopsin in a signal transduction cascade that regulates membrane trafficking and photoreceptor polarity. *Vision Res*, 2006. **46**(27): p. 4427-33.
86. Calvert, P.D., K.J. Strissel, W.E. Schiesser, E.N. Pugh, Jr. and V.Y. Arshavsky, Light-driven translocation of signaling proteins in vertebrate photoreceptors. *Trends Cell Biol*, 2006. **16**(11): p. 560-8.
87. Arshavsky, V.Y., T.D. Lamb and E.N. Pugh, Jr., G proteins and phototransduction. 2002. **64**: p. 153-187.
88. He, W., C.W. Cowan and T.G. Wensel, RGS9, a GTPase accelerator for phototransduction. 1998. **20**(1): p. 95-102.
89. Martemyanov, K.A., P.V. Lishko, N. Calero, G. Keresztes, M. Sokolov, K.J. Strissel, I.B. Leskov, J.A. Hopp, A.V. Kolesnikov, C.K. Chen, J. Lem, S. Heller, M.E. Burns and V.Y. Arshavsky, The DEP domain determines subcellular targeting of the GTPase activating protein RGS9 in vivo. *Journal of Neuroscience*, 2003. **23**(32): p. 10175-10181.
90. Lishko, P.V., K.A. Martemyanov, J.A. Hopp and V.Y. Arshavsky, Specific binding of RGS9-G*5L to protein anchor in photoreceptor membranes greatly enhances its catalytic activity. *Journal of Biological Chemistry*, 2002. **277**(27): p. 24376-24381.
91. Hu, G. and T.G. Wensel, R9AP, a membrane anchor for the photoreceptor GTPase accelerating protein,, RGS9-1. *Proceedings of the National Academy of Sciences of the United States of America*, 2002. **99**(15): p. 9755-9760.
92. Anderson, G.R., R. Lujan, A. Semenov, M. Pravetoni, E.N. Posokhova, J.H. Song, V. Uversky, C.K. Chen, K. Wickman and K.A. Martemyanov, Expression and localization of RGS9-2/G 5/R7BP complex in vivo is set by dynamic control of its constitutive degradation by cellular cysteine proteases. *J Neurosci*, 2007. **27**(51): p. 14117-27.
93. Drenan, R.M., C.A. Doupnik, M.P. Boyle, L.J. Muglia, J.E. Huettner, M.E. Linder and K.J. Blumer, Palmitoylation regulates plasma membrane-nuclear shuttling of R7BP, a novel membrane anchor for the RGS7 family. *J Cell Biol*, 2005. **169**(4): p. 623-33.
94. Keresztes, G., H. Mutai, H. Hibino, A.J. Hudspeth and S. Heller, Expression patterns of the RGS9-1 anchoring protein R9AP in the chicken and mouse suggest multiple roles in the nervous system. 2003. **24**(3): p. 687-695.
95. Harbury, P.A., Springs and zippers: coiled coils in SNARE-mediated membrane fusion. 1998. **6**(12): p. 1487-1491.
96. Chen, Y.A. and R.H. Scheller, SNARE-mediated membrane fusion. *Nature Reviews Molecular Cell Biology*, 2001. **2**(2): p. 98-106.
97. Burchett, S.A., P. Flanary, C. Aston, L. Jiang, K.H. Young, P. Uetz, S. Fields and H.G. Dohlman, Regulation of stress response signaling by the N-terminal dishevelled/EGL-10/pleckstrin domain of Sst2, a regulator of G protein signaling in Saccharomyces cerevisiae. 2002. **277**(25): p. 22156-22167.
98. Song, J.H., J.J. Waataja and K.A. Martemyanov, Subcellular targeting of RGS9-2 is controlled by multiple molecular determinants on its membrane anchor, R7BP. *J Biol Chem*, 2006. **281**(22): p. 15361-9.

99. Drenan, R.M., C.A. Doupnik, M. Jayaraman, A.L. Buchwalter, K.M. Kaltenbronn, J.E. Huettner, M.E. Linder and K.J. Blumer, R7BP augments the function of RGS7*Gbeta5 complexes by a plasma membrane-targeting mechanism. *J Biol Chem*, 2006. **281**(38): p. 28222-31.
100. Grabowska, D., M. Jayaraman, K.M. Kaltenbronn, S.L. Sandiford, Q. Wang, S. Jenkins, V.Z. Slepak, Y. Smith and K.J. Blumer, Postnatal induction and localization of R7BP, a membrane-anchoring protein for regulator of G protein signaling 7 family-Gbeta5 complexes in brain. *Neuroscience*, 2008. **151**(4): p. 969-82.
101. Bouhamdan, M., S.K. Michelhaugh, I. Calin-Jageman, S. Ahern-Djamali and M.J. Bannon, Brain-specific RGS9-2 is localized to the nucleus via its unique proline-rich domain. *Biochim Biophys Acta*, 2004. **1691**(2-3): p. 141-50.
102. Zhang, J.H., V.A. Barr, Y.Y. Mo, A.M. Rojkova, S.H. Liu and W.F. Simonds, Nuclear localization of G protein *5 and regulator of G protein signaling 7 in neurons and brain. *Journal of Biological Chemistry*, 2001. **276**(13): p. 10284-10289.
103. Hu, G., Z. Zhang and T.G. Wensel, Activation of RGS9-1GTPase Acceleration by Its Membrane Anchor, R9AP. 2003. **278**(16): p. 14550-14554.
104. Baker, S.A., K.A. Martemyanov, A.S. Shavkunov and V.Y. Arshavsky, Kinetic mechanism of RGS9-1 potentiation by R9AP. *Biochemistry*, 2006. **45**(35): p. 10690-7.
105. Baker, S.A., M. Haeri, P. Yoo, S.M. Gospe, 3rd, N.P. Skiba, B.E. Knox and V.Y. Arshavsky, The outer segment serves as a default destination for the trafficking of membrane proteins in photoreceptors. *J Cell Biol*, 2008. **183**(3): p. 485-98.
106. Cao, Y., H. Song, H. Okawa, A.P. Sampath, M. Sokolov and K.A. Martemyanov, Targeting of RGS7/Gbeta5 to the dendritic tips of ON-bipolar cells is independent of its association with membrane anchor R7BP. *J Neurosci*, 2008. **28**(41): p. 10443-9.
107. Keresztes, G., K.A. Martemyanov, C.M. Krispel, H. Mutai, P.J. Yoo, S.F. Maison, M.E. Burns, V.Y. Arshavsky and S. Heller, Absence of the RGS9{middle dot}G{beta}5 GTPase-activating Complex in Photoreceptors of the R9AP Knockout Mouse. 2004. **279**(3): p. 1581-1584.
108. Martemyanov, K.A., C.M. Krispel, P.V. Lishko, M.E. Burns and V.Y. Arshavsky, Functional comparison of RGS9 splice isoforms in a living cell. *Proc Natl Acad Sci U S A*, 2008. **105**(52): p. 20988-93.
109. Garzon, J., M. Rodriguez-Munoz, A. Lopez-Fando and P. Sanchez-Blazquez, Activation of mu-opioid receptors transfers control of Galpha subunits to the regulator of G-protein signaling RGS9-2: role in receptor desensitization. *J Biol Chem*, 2005. **280**(10): p. 8951-60.
110. Psifogeorgou, K., P. Papakosta, S.J. Russo, R.L. Neve, D. Kardassis, S.J. Gold and V. Zachariou, RGS9-2 is a negative modulator of mu-opioid receptor function. *J Neurochem*, 2007. **103**(2): p. 617-25.
111. Kovoor, A., P. Seyffarth, J. Ebert, S. Barghshoon, C.K. Chen, S. Schwarz, J.D. Axelrod, B.N. Cheyette, M.I. Simon, H.A. Lester and J. Schwarz, D2 dopamine receptors colocalize regulator of G-protein signaling 9-2 (RGS9-2) via the RGS9 DEP domain, and RGS9 knock-out mice develop dyskinesias associated with dopamine pathways. *J Neurosci*, 2005. **25**(8): p. 2157-65.
112. Sandiford, S. and V. Slepak, G5-RGS7 selectively inhibits muscarinic M3 receptor signaling via the interaction between the third intracellular loop of the receptor and the DEP domain of RGS7. *Biochemistry*, 2009.
113. Bouhamdan, M., H.D. Yan, X.H. Yan, M.J. Bannon and R. Andrade, Brain-specific regulator of G-protein signaling 9-2 selectively interacts with alpha-actinin-2 to regulate calcium-dependent inactivation of NMDA receptors. *J Neurosci*, 2006. **26**(9): p. 2522-30.

114. Benzing, T., M. K*ttgen, M. Johnson, B. Schermer, H. Zentgraf, G. Walz and E. Kim, Interaction of 14-3-3 protein with regulator of G protein signaling 7 is dynamically regulated by tumor necrosis factor-à. *Journal of Biological Chemistry*, 2002. **277**(36): p. 32954-32962.
115. Liu, Z. and R.A. Fisher, RGS6 interacts with DMAP1 and DNMT1 and inhibits DMAP1 transcriptional repressor activity. *J Biol Chem*, 2004. **279**(14): p. 14120-8.
116. Liu, Z.Y., T.K. Chatterjee and R.A. Fisher, RGS6 interacts with SCG10 and promotes neuronal differentiation - Role of the G gamma subunit-like (GGL) domain of RGS6. *Journal of Biological Chemistry*, 2002. **277**(40): p. 37832-37839.
117. Hunt, R.A., W. Edris, P.K. Chanda, B. Nieuwenhuijsen and K.H. Young, Snapin interacts with the N-terminus of regulator of G protein signaling 7. *Biochemical and Biophysical Research Communications*, 2003. **303**(2): p. 594-599.
118. Kim, E., T. Arnould, L. Sellin, T. Benzing, N. Comella, O. Kocher, L. Tsiokas, V.P. Sukhatme and G. Walz, Interaction between RGS7 and polycystin. *Proceedings of the National Academy of Sciences of the United States of America*, 1999. **96**(11): p. 6371-6376.
119. Charlton, J.J., P.B. Allen, K. Psifogeorgou, S. Chakravarty, I. Gomes, R.L. Neve, L.A. Devi, P. Greengard, E.J. Nestler and V. Zachariou, Multiple actions of spinophilin regulate mu opioid receptor function. *Neuron*, 2008. **58**(2): p. 238-47.
120. Seno, K., A. Kishigami, S. Ihara, T. Maeda, V.A. Bondarenko, Y. Nishizawa, J. Usukura, A. Yamazaki and F. Hayashi, A possible role of RGS9 in phototransduction - A bridge between the cGMP-phosphodiesterase system and the guanylyl cyclase system. *Journal of Biological Chemistry*, 1998. **273**(35): p. 22169-22172.
121. Ballon, D.R., P.L. Flanary, D.P. Gladue, J.B. Konopka, H.G. Dohlman and J. Thorner, DEP-domain-mediated regulation of GPCR signaling responses. *Cell*, 2006. **126**(6): p. 1079-93.
122. Chen, J.G., F.S. Willard, J. Huang, J.S. Liang, S.A. Chasse, A.M. Jones and D.P. Siderovski, A seven-transmembrane RGS protein that modulates plant cell proliferation. 2003. **301**(5640): p. 1728-1731.
123. Rojkova, A.M., G.E. Woodard, T.C. Huang, C.A. Combs, J.H. Zhang and W.F. Simonds, Ggamma subunit-selective G protein beta 5 mutant defines regulators of G protein signaling protein binding requirement for nuclear localization. *J Biol Chem*, 2003. **278**(14): p. 12507-12.
124. Luo, D.G., T. Xue and K.W. Yau, How vision begins: an odyssey. *Proc Natl Acad Sci U S A*, 2008. **105**(29): p. 9855-62.
125. Pugh, E.N., Jr., RGS expression level precisely regulates the duration of rod photoresponses. *Neuron*, 2006. **51**(4): p. 391-3.
126. Lyubarsky, A.L., F. Naarendorp, X. Zhang, T. Wensel, M.I. Simon and E.N. Pugh, Jr., RGS9-1 is required for normal inactivation of mouse cone phototransduction. 2001. **7**: p. 71-78.
127. Krispel, C.M., C.K. Chen, M.I. Simon and M.E. Burns, Prolonged photoresponses and defective adaptation in rods of G*5-/- mice. *Journal of Neuroscience*, 2003. **23**(18): p. 6965-6971.
128. Nishiguchi, K.M., M.A. Sandberg, A.C. Kooijman, K.A. Martemyanov, J.W. Pott, S.A. Hagstrom, V.Y. Arshavsky, E.L. Berson and T.P. Dryja, Defects in RGS9 or its anchor protein R9AP in patients with slow photoreceptor deactivation. 2004. **427**(6969): p. 75-78.
129. Cheng, J.Y., C.D. Luu, V.H. Yong, R. Mathur, T. Aung and E.N. Vithana, Bradyopsia in an Asian man. *Arch Ophthalmol*, 2007. **125**(8): p. 1138-40.

130. Hartong, D.T., J.W. Pott and A.C. Kooijman, Six patients with bradyopsia (slow vision): clinical features and course of the disease. *Ophthalmology*, 2007. **114**(12): p. 2323-31.
131. Garzon, J., M. Rodriguez-Diaz, A. Lopez-Fando and P. Sanchez-Blazquez, RGS9 proteins facilitate acute tolerance to mu-opioid effects. *Eur J Neurosci*, 2001. **13**(4): p. 801-11.
132. Kim, K.J., K. Moriyama, K.R. Han, M. Sharma, X. Han, G.X. Xie and P.P. Palmer, Differential expression of the regulator of G protein signaling RGS9 protein in nociceptive pathways of different age rats. *Brain Res Dev Brain Res*, 2005. **160**(1): p. 28-39.
133. Zachariou, V., D. Georgescu, N. Sanchez, Z. Rahman, R. DiLeone, O. Berton, R.L. Neve, L.J. Sim-Selley, D.E. Selley, S.J. Gold and E.J. Nestler, Essential role for RGS9 in opiate action. *Proc Natl Acad Sci U S A*, 2003. **100**(23): p. 13656-61.
134. Seeman, P., F. Ko, E. Jack, R. Greenstein and B. Dean, Consistent with dopamine supersensitivity, RGS9 expression is diminished in the amphetamine-treated animal model of schizophrenia and in postmortem schizophrenia brain. *Synapse*, 2007. **61**(5): p. 303-9.
135. Blundell, J., C.V. Hoang, B. Potts, S.J. Gold and C.M. Powell, Motor coordination deficits in mice lacking RGS9. *Brain Res*, 2008. **1190**: p. 78-85.
136. Gold, S.J., C.V. Hoang, B.W. Potts, G. Porras, E. Pioli, K.W. Kim, A. Nadjar, C. Qin, G.J. LaHoste, Q. Li, B.H. Bioulac, J.L. Waugh, E. Gurevich, R.L. Neve and E. Bezard, RGS9-2 negatively modulates L-3,4-dihydroxyphenylalanine-induced dyskinesia in experimental Parkinson's disease. *J Neurosci*, 2007. **27**(52): p. 14338-48.
137. Cabrera-Vera, T.M., S. Hernandez, L.R. Earls, M. Medkova, A.K. Sundgren-Andersson, D.J. Surmeier and H.E. Hamm, RGS9-2 modulates D2 dopamine receptor-mediated Ca2+ channel inhibition in rat striatal cholinergic interneurons. *Proc Natl Acad Sci U S A*, 2004. **101**(46): p. 16339-44.
138. Tekumalla, P.K., F. Calon, Z. Rahman, S. Birdi, A.H. Rajput, O. Hornykiewicz, T. Di Paolo, P.J. Bedard and E.J. Nestler, Elevated levels of DeltaFosB and RGS9 in striatum in Parkinson's disease. *Biol Psychiatry*, 2001. **50**(10): p. 813-6.
139. Burchett, S.A., M.L. Volk, M.J. Bannon and J.G. Granneman, Regulators of G protein signaling: rapid changes in mRNA abundance in response to amphetamine. *J Neurochem*, 1998. **70**(5): p. 2216-9.
140. Burns, M.E. and T.G. Wensel, From molecules to behavior: New clues for RGS function in the striatum. 2003. **38**(6): p. 853-856.
141. Sanchez-Blazquez, P., M. Rodriguez-Diaz, A. Lopez-Fando, M. Rodriguez-Munoz and J. Garzon, The GBeta5 subunit that associates with the R7 subfamily of RGS proteins regulates mu-opioid effects. *Neuropharmacology*, 2003. **45**(1): p. 82-95.
142. Jedema, H.P., S.J. Gold, G. Gonzalez-Burgos, A.F. Sved, B.J. Tobe, T. Wensel and A.A. Grace, Chronic cold exposure increases RGS7 expression and decreases alpha(2)-autoreceptor-mediated inhibition of noradrenergic locus coeruleus neurons. *Eur J Neurosci*, 2008. **27**(9): p. 2433-43.
143. Singh, R.K., J. Shi, B.W. Zemaitaitis and N.A. Muma, Olanzapine increases RGS7 protein expression via stimulation of the Janus tyrosine kinase-signal transducer and activator of transcription signaling cascade. *J Pharmacol Exp Ther*, 2007. **322**(1): p. 133-40.
144. Shelat, P.B., A.P. Coulibaly, Q. Wang, A.Y. Sun, G.Y. Sun and A. Simonyi, Ischemia-induced increase in RGS7 mRNA expression in gerbil hippocampus. *Neurosci Lett*, 2006. **403**(1-2): p. 157-61.

145. Lopez-Fando, A., M. Rodriguez-Munoz, P. Sanchez-Blazquez and J. Garzon, Expression of neural RGS-R7 and Gbeta5 Proteins in Response to Acute and Chronic Morphine. *Neuropsychopharmacology*, 2005. **30**(1): p. 99-110.
146. Witherow, D.S., S.C. Tovey, Q. Wang, G.B. Willars and V.Z. Slepak, G beta 5.RGS7 inhibits G alpha q-mediated signaling via a direct protein-protein interaction. *J Biol Chem*, 2003. **278**(23): p. 21307-13.
147. Shuey, D.J., M. Betty, P.G. Jones, X.Z. Khawaja and M.I. Cockett, RGS7 attenuates signal transduction through the G*q family of heterotrimeric G proteins in mammalian cells. *Journal of Neurochemistry*, 1998. **70**(5): p. 1964-1972.
148. Rao, A., R. Dallman, S. Henderson and C.K. Chen, Gbeta5 is required for normal light responses and morphology of retinal ON-bipolar cells. *J Neurosci*, 2007. **27**(51): p. 14199-204.
149. Hollinger, S. and J.R. Hepler, Cellular regulation of RGS proteins: Modulators and integrators of G protein signaling. *Pharmacological Reviews*, 2002. **54**(3): p. 527-559.
150. Siderovski, D.P. and F.S. Willard, The GAPs, GEFs, and GDIs of heterotrimeric G-protein alpha subunits. *Int J Biol Sci*, 2005. **1**(2): p. 51-66.
151. Heximer, S.P., R.H. Knutsen, X. Sun, K.M. Kaltenbronn, M.H. Rhee, N. Peng, A. Oliveira-dos-Santos, J.M. Penninger, A.J. Muslin, T.H. Steinberg, J.M. Wyss, R.P. Mecham and K.J. Blumer, Hypertension and prolonged vasoconstrictor signaling in RGS2-deficient mice. *J Clin Invest*, 2003. **111**(8): p. 1259.
152. Witherow, D.S. and V.Z. Slepak, A novel kind of G protein heterodimer: the G beta5-RGS complex. *Receptors Channels*, 2003. **9**(3): p. 205-12.
153. Song, J.H., J.J. Waataja and K.A. Martemyanov, Subcellular targeting of RGS9-2 is controlled by multiple molecular determinants on its membrane anchor, R7BP. *J Biol Chem*, 2006.
154. Lefebvre, B., P. Formstecher and P. Lefebvre, Improvement of the gene splicing overlap (SOE) method. *Biotechniques*, 1995. **19**(2): p. 186-188.
155. Ivkovic, S. and M.E. Ehrlich, Expression of the striatal DARPP-32/ARPP-21 phenotype in GABAergic neurons requires neurotrophins in vivo and in vitro. *J Neurosci*, 1999. **19**(13): p. 5409-19.
156. Coleman, J.E., M.J. Huentelman, S. Kasparov, B.L. Metcalfe, J.F. Paton, M.J. Katovich, S.L. Semple-Rowland and M.K. Raizada, Efficient large-scale production and concentration of HIV-1-based lentiviral vectors for use in vivo. *Physiol Genomics*, 2003. **12**(3): p. 221-8.
157. Cullen, B.R., Derivation and function of small interfering RNAs and microRNAs. *Virus Res*, 2004. **102**(1): p. 3-9.
158. Berghuis, A.M., E. Lee, A.S. Raw, A.G. Gilman and S.R. Sprang, Structure of the GDP-Pi complex of Gly203-->Gi*1: A mimic of the ternary product complex of G*-catalyzed GTP hydrolysis. 1996. **4**: p. 1277-1290.
159. Svenningsson, P., A. Nishi, G. Fisone, J.A. Girault, A.C. Nairn and P. Greengard, DARPP-32: an integrator of neurotransmission. *Annu Rev Pharmacol Toxicol*, 2004. **44**: p. 269-96.
160. Lupas, A., M. Van Dyke and J. Stock, Predicting coiled coils from protein sequences. *Science*, 1991. **252**(5010): p. 1162-4.
161. Sharifi, J.L., D.L. Brady and J.I. Koenig, Estrogen modulates RGS9 expression in the nucleus accumbens. *Neuroreport*, 2004. **15**(15): p. 2433-6.
162. Lujan, R., Z. Nusser, J.D. Roberts, R. Shigemoto and P. Somogyi, Perisynaptic location of metabotropic glutamate receptors mGluR1 and mGluR5 on dendrites and dendritic spines in the rat hippocampus. *Eur J Neurosci*, 1996. **8**(7): p. 1488-500.

163. Peng, K., S. Vucetic, P. Radivojac, C.J. Brown, A.K. Dunker and Z. Obradovic, Optimizing long intrinsic disorder predictors with protein evolutionary information. *J Bioinform Comput Biol*, 2005. **3**(1): p. 35-60.
164. Obradovic, Z., K. Peng, S. Vucetic, P. Radivojac and A.K. Dunker, Exploiting heterogeneous sequence properties improves prediction of protein disorder. *Proteins*, 2005. **61 Suppl 7**: p. 176-82.
165. Ehrlich, M.E., N.L. Rosen, T. Kurihara, I.A. Shalaby and P. Greengard, DARPP-32 development in the caudate nucleus is independent of afferent input from the substantia nigra. *Brain Res Dev Brain Res*, 1990. **54**(2): p. 257-63.
166. Lujan, R., *Electron Microscopic Studies of Receptor Localization*, in *Methods in Molecular Biology*, G.B.a.C. Willars, R.A.J., Editor. 2004, Humana Press: Totowa, NJ. p. 123-136.
167. Dyson, H.J. and P.E. Wright, Intrinsically unstructured proteins and their functions. *Nat Rev Mol Cell Biol*, 2005. **6**(3): p. 197-208.
168. Uversky, V.N., C.J. Oldfield and A.K. Dunker, Showing your ID: intrinsic disorder as an ID for recognition, regulation and cell signaling. *J Mol Recognit*, 2005. **18**(5): p. 343-84.
169. Dice, J.F., Peptide sequences that target cytosolic proteins for lysosomal proteolysis. *Trends Biochem Sci*, 1990. **15**(8): p. 305-9.
170. Song, J.H., H. Song, T.G. Wensel, M. Sokolov and K.A. Martemyanov, Localization and differential interaction of R7 RGS proteins with their membrane anchors R7BP and R9AP in neurons of vertebrate retina. *Mol Cell Neurosci*, 2007. **35**(2): p. 311-9.
171. Radivojac, P., L.M. Iakoucheva, C.J. Oldfield, Z. Obradovic, V.N. Uversky and A.K. Dunker, Intrinsic disorder and functional proteomics. *Biophys J*, 2007. **92**(5): p. 1439-56.
172. Dice, J.F., Selective degradation of cytosolic proteins by lysosomes. *Ann N Y Acad Sci*, 1992. **674**: p. 58-64.
173. Massey, A.C., C. Zhang and A.M. Cuervo, Chaperone-mediated autophagy in aging and disease. *Curr Top Dev Biol*, 2006. **73**: p. 205-35.
174. Bourhis, J.M., B. Canard and S. Longhi, Predicting protein disorder and induced folding: from theoretical principles to practical applications. *Curr Protein Pept Sci*, 2007. **8**(2): p. 135-49.
175. Urbe, S., Ubiquitin and endocytic protein sorting. *Essays Biochem*, 2005. **41**: p. 81-98.
176. Mukhopadhyay, D. and H. Riezman, Proteasome-independent functions of ubiquitin in endocytosis and signaling. *Science*, 2007. **315**(5809): p. 201-5.
177. Sans, N., R.S. Petralia, Y.X. Wang, J. Blahos, 2nd, J.W. Hell and R.J. Wenthold, A developmental change in NMDA receptor-associated proteins at hippocampal synapses. *J Neurosci*, 2000. **20**(3): p. 1260-71.
178. Lim, S., S. Naisbitt, J. Yoon, J.I. Hwang, P.G. Suh, M. Sheng and E. Kim, Characterization of the Shank family of synaptic proteins. Multiple genes, alternative splicing, and differential expression in brain and development. *J Biol Chem*, 1999. **274**(41): p. 29510-8.
179. Hess, H.A., J.C. Roper, S.W. Grill and M.R. Koelle, RGS-7 completes a receptor-independent heterotrimeric G protein cycle to asymmetrically regulate mitotic spindle positioning in C. elegans. *Cell*, 2004. **119**(2): p. 209-18.
180. Saitoh, O., Y. Kubo, Y. Miyatani, T. Asano and H. Nakata, RGS8 accelerates G-protein-mediated modulation of K+ currents. 1997. **390**(6659): p. 525-529.
181. Hamzah, J., M. Jugold, F. Kiessling, P. Rigby, M. Manzur, H.H. Marti, T. Rabie, S. Kaden, H.J. Grone, G.J. Hammerling, B. Arnold and R. Ganss, Vascular normalization in Rgs5-deficient tumours promotes immune destruction. *Nature*, 2008. **453**(7193): p. 410-4.

182. Tang, M., G. Wang, P. Lu, R.H. Karas, M. Aronovitz, S.P. Heximer, K.M. Kaltenbronn, K.J. Blumer, D.P. Siderovski, Y. Zhu and M.E. Mendelsohn, Regulator of G-protein signaling-2 mediates vascular smooth muscle relaxation and blood pressure. *Nature Medicine*, 2003. **9**(12): p. 1506-1512.
183. Zheng, B., L. De Vries and M.G. Farquhar, Divergence of RGS proteins: evidence for the existence of six mammalian RGS subfamilies. *Trends in Biochemical Sciences*, 1999. **24**(11): p. 411-414.
184. Cowan, C.W., W. He and T.G. Wensel, RGS proteins: lessons from the RGS9 subfamily. 2000. **65**: p. 341-359.
185. Jones, M.B., D.P. Siderovski and S.B. Hooks, The G{beta}{gamma} DIMER as a NOVEL SOURCE of SELECTIVITY in G-Protein Signaling: GGL-ing AT CONVENTION. *Mol Interv*, 2004. **4**(4): p. 200-214.
186. Gold, S.J., Y.G. Ni, H.G. Dohlman and E.J. Nestler, Regulators of G-protein signaling (RGS) proteins: region-specific expression of nine subtypes in rat brain. *J Neurosci*, 1997. **17**(20): p. 8024-37.
187. Nekrasova, E.R., D.M. Berman, R.R. Rustandi, H.E. Hamm, A.G. Gilman and V.Y. Arshavsky, Activation of transducin guanosine triphosphatase by two proteins of the RGS family. 1997. **36**(25): p. 7638-7643.
188. Lee, E., M.E. Linder and A.G. Gilman, Expression of G-protein * subunits in Escherichia coli. 1994. **237**: p. 146-164.
189. Ting, T.D., S.B. Goldin and Y.-K. Ho, Purification and characterization of bovine transducin and its subunits. 1993. p. 180-195.
190. Lessard, J., J.I. Wu, J.A. Ranish, M. Wan, M.M. Winslow, B.T. Staahl, H. Wu, R. Aebersold, I.A. Graef and G.R. Crabtree, An essential switch in subunit composition of a chromatin remodeling complex during neural development. *Neuron*, 2007. **55**(2): p. 201-15.
191. Grumont, R.J. and S. Gerondakis, The subunit composition of NF-kappa B complexes changes during B-cell development. *Cell Growth Differ*, 1994. **5**(12): p. 1321-31.
192. Hanna, J. and D. Finley, A proteasome for all occasions. *FEBS Lett*, 2007. **581**(15): p. 2854-61.
193. Paoletti, P. and J. Neyton, NMDA receptor subunits: function and pharmacology. *Curr Opin Pharmacol*, 2007. **7**(1): p. 39-47.
194. Sprengel, R., Role of AMPA receptors in synaptic plasticity. *Cell Tissue Res*, 2006. **326**(2): p. 447-55.
195. Schmid, A., S. Hallermann, R.J. Kittel, O. Khorramshahi, A.M. Frolich, C. Quentin, T.M. Rasse, S. Mertel, M. Heckmann and S.J. Sigrist, Activity-dependent site-specific changes of glutamate receptor composition in vivo. *Nat Neurosci*, 2008. **11**(6): p. 659-66.
196. Verma, S., Y. Xiong, M.U. Mayer and T.C. Squier, Remodeling of the bacterial RNA polymerase supramolecular complex in response to environmental conditions. *Biochemistry*, 2007. **46**(11): p. 3023-35.
197. Dirnagl, U., C. Iadecola and M.A. Moskowitz, Pathobiology of ischaemic stroke: an integrated view. *Trends Neurosci*, 1999. **22**(9): p. 391-7.
198. Yao, H. and G.G. Haddad, Calcium and pH homeostasis in neurons during hypoxia and ischemia. *Cell Calcium*, 2004. **36**(3-4): p. 247-55.
199. Bright, R. and D. Mochly-Rosen, The role of protein kinase C in cerebral ischemic and reperfusion injury. *Stroke*, 2005. **36**(12): p. 2781-90.
200. Sheng, M. and C.C. Hoogenraad, The postsynaptic architecture of excitatory synapses: a more quantitative view. *Annu Rev Biochem*, 2007. **76**: p. 823-47.
201. Citri, A. and R.C. Malenka, Synaptic plasticity: multiple forms, functions, and mechanisms. *Neuropsychopharmacology*, 2008. **33**(1): p. 18-41.

202. Calabresi, P., D. Centonze, A. Pisani, L. Cupini and G. Bernardi, Synaptic plasticity in the ischaemic brain. *Lancet Neurol*, 2003. **2**(10): p. 622-9.
203. Meller, R., S.J. Thompson, T.A. Lusardi, A.N. Ordonez, M.D. Ashley, V. Jessick, W. Wang, D.J. Torrey, D.C. Henshall, P.R. Gafken, J.A. Saugstad, Z.G. Xiong and R.P. Simon, Ubiquitin proteasome-mediated synaptic reorganization: a novel mechanism underlying rapid ischemic tolerance. *J Neurosci*, 2008. **28**(1): p. 50-9.
204. Adhami, F., A. Schloemer and C.Y. Kuan, The roles of autophagy in cerebral ischemia. *Autophagy*, 2007. **3**(1): p. 42-4.
205. Seeman, P., J. Schwarz, J.F. Chen, H. Szechtman, M. Perreault, G.S. McKnight, J.C. Roder, R. Quirion, P. Boksa, L.K. Srivastava, K. Yanai, D. Weinshenker and T. Sumiyoshi, Psychosis pathways converge via D2high dopamine receptors. *Synapse*, 2006. **60**(4): p. 319-46.
206. Pierce, R.C. and V. Kumaresan, The mesolimbic dopamine system: the final common pathway for the reinforcing effect of drugs of abuse? *Neurosci Biobehav Rev*, 2006. **30**(2): p. 215-38.
207. Groenewegen, H.J., The basal ganglia and motor control. *Neural Plast*, 2003. **10**(1-2): p. 107-20.
208. Kreitzer, A.C., Physiology and pharmacology of striatal neurons. *Annu Rev Neurosci*, 2009. **32**: p. 127-47.
209. Nicola, S.M., J. Surmeier and R.C. Malenka, Dopaminergic modulation of neuronal excitability in the striatum and nucleus accumbens. *Annu Rev Neurosci*, 2000. **23**: p. 185-215.
210. Kreitzer, A.C. and R.C. Malenka, Striatal plasticity and basal ganglia circuit function. *Neuron*, 2008. **60**(4): p. 543-54.
211. DeLong, M.R. and T. Wichmann, Circuits and circuit disorders of the basal ganglia. *Arch Neurol*, 2007. **64**(1): p. 20-4.
212. Hyman, S.E., R.C. Malenka and E.J. Nestler, Neural mechanisms of addiction: the role of reward-related learning and memory. *Annu Rev Neurosci*, 2006. **29**: p. 565-98.
213. Traynor, J.R., D. Terzi, B.J. Caldarone and V. Zachariou, RGS9-2: probing an intracellular modulator of behavior as a drug target. *Trends Pharmacol Sci*, 2009. **30**(3): p. 105-11.
214. Anderson, G.R., R. Lujan and K.A. Martemyanov, Changes in striatal signaling induce remodeling of RGS complexes containing Gbeta5 and R7BP subunits. *Mol Cell Biol*, 2009. **29**(11): p. 3033-44.
215. Pravetoni, M. and K. Wickman, Behavioral characterization of mice lacking GIRK/Kir3 channel subunits. *Genes Brain Behav*, 2008. **7**(5): p. 523-31.
216. Paxinos, G., G. Halliday, C. Watson, Y. Koutcherov and H.Q. Wang, *Atlas of the Developing Mouse Brain*. 2007, Amsterdam, Netherlands.: Elsevier.
217. Nestler, E.J., Is there a common molecular pathway for addiction? *Nat Neurosci*, 2005. **8**(11): p. 1445-9.
218. Anderson, G.R., E. Posokhova and K.A. Martemyanov, The R7 RGS protein family: multi-subunit regulators of neuronal G protein signaling. *Cell Biochem Biophys*, 2009. **54**(1-3): p. 33-46.
219. Jayaraman, M., H. Zhou, L. Jia, M.D. Cain and K.J. Blumer, R9AP and R7BP: traffic cops for the RGS7 family in phototransduction and neuronal GPCR signaling. *Trends Pharmacol Sci*, 2009. **30**(1): p. 17-24.
220. Costa, R.M., D. Cohen and M.A. Nicolelis, Differential corticostriatal plasticity during fast and slow motor skill learning in mice. *Curr Biol*, 2004. **14**(13): p. 1124-34.

221. Pisani, A., D. Centonze, G. Bernardi and P. Calabresi, Striatal synaptic plasticity: implications for motor learning and Parkinson's disease. *Mov Disord*, 2005. **20**(4): p. 395-402.
222. Packard, M.G. and B.J. Knowlton, Learning and memory functions of the Basal Ganglia. *Annu Rev Neurosci*, 2002. **25**: p. 563-93.
223. Dang, M.T., F. Yokoi, H.H. Yin, D.M. Lovinger, Y. Wang and Y. Li, Disrupted motor learning and long-term synaptic plasticity in mice lacking NMDAR1 in the striatum. *Proc Natl Acad Sci U S A*, 2006. **103**(41): p. 15254-9.
224. Meyer, D.A., E. Richer, S.A. Benkovic, K. Hayashi, J.W. Kansy, C.F. Hale, L.Y. Moy, Y. Kim, J.P. O'Callaghan, L.H. Tsai, P. Greengard, A.C. Nairn, C.W. Cowan, D.B. Miller, P. Antich and J.A. Bibb, Striatal dysregulation of Cdk5 alters locomotor responses to cocaine, motor learning, and dendritic morphology. *Proc Natl Acad Sci U S A*, 2008. **105**(47): p. 18561-6.
225. Brandon, E.P., S.F. Logue, M.R. Adams, M. Qi, S.P. Sullivan, A.M. Matsumoto, D.M. Dorsa, J.M. Wehner, G.S. McKnight and R.L. Idzerda, Defective motor behavior and neural gene expression in RIIbeta-protein kinase A mutant mice. *J Neurosci*, 1998. **18**(10): p. 3639-49.
226. Fernagut, P.O., S. Chalon, E. Diguet, D. Guilloteau, F. Tison and M. Jaber, Motor behaviour deficits and their histopathological and functional correlates in the nigrostriatal system of dopamine transporter knockout mice. *Neuroscience*, 2003. **116**(4): p. 1123-30.
227. Short, J.L., C. Ledent, J. Drago and A.J. Lawrence, Receptor crosstalk: characterization of mice deficient in dopamine D1 and adenosine A2A receptors. *Neuropsychopharmacology*, 2006. **31**(3): p. 525-34.
228. Fowler, S.C., T.J. Zarcone, E. Vorontsova and R. Chen, Motor and associative deficits in D2 dopamine receptor knockout mice. *Int J Dev Neurosci*, 2002. **20**(3-5): p. 309-21.